ELECTRICAL COMMUNICATION

Technical Journal of the
International Telephone and Telegraph Corporation
and Associate Companies

•

ELECTROMECHANICAL DISTRIBUTOR FOR SORTING MAIL

MANUFACTURE OF A HIGH-FREQUENCY TRANSMITTING TUBE

LINEAR ELECTRON ACCELERATOR TO ONE MILLION VOLTS

CRYSTAL TRIODES

CROSS-TALK CONSIDERATIONS IN TIME-DIVISION MULTIPLEX SYSTEMS

SPACE-CHARGE WAVES IN CYLINDRICAL WAVEGUIDES WITH MANY BEAMS

PERIODIC-WAVEGUIDE TRAVELING-WAVE AMPLIFIER FOR MEDIUM POWERS

EFFECT OF HYDROSTATIC PRESSURE ON TRAVELING-WAVE DEVICES

MAGNETO-OPTICS OF AN ELECTRON GAS WITH GUIDED MICROWAVES

GROWTH AND AMPLIFICATION

Volume 28 **SEPTEMBER, 1951** **Number 3**

ELECTRICAL COMMUNICATION

Technical Journal of the
INTERNATIONAL TELEPHONE AND TELEGRAPH CORPORATION
and Associate Companies

H. P. WESTMAN, Editor
F. J. MANN, Managing Editor J. E. SCHLAIKJER, Assistant Editor

EDITORIAL BOARD

P. F. Bourget, H. Busignies, H. H. Buttner, E. M. Deloraine, W. Hatton, B. C. Holding, J. S. Jammer, E. Labin, A. W. Montgomery, E. D. Phinney, E. G. Ports, Haraden Pratt, G. Rabuteau, T. R. Scott, C. E. Strong, A. E. Thompson, E. N. Wendell, H. B. Wood

Published Quarterly by the
INTERNATIONAL TELEPHONE AND TELEGRAPH CORPORATION
67 BROAD STREET, NEW YORK 4, NEW YORK, U.S.A.

Sosthenes Behn, Chairman William H. Harrison, President
Charles D. Hilles, Jr., Vice President and Secretary

Subscription, $2.00 per year; single copies, 50 cents

Electrical Communication is indexed in Industrial Arts Index

Copyrighted 1951 by International Telephone and Telegraph Corporation

Volume 28 SEPTEMBER, 1951 Number 3

CONTENTS

ELECTROMECHANICAL DISTRIBUTOR FOR SORTING MAIL 163
By S. Scheuer, C. B. Neyt, and L. J. G. Nijs

MANUFACTURE OF A HIGH-FREQUENCY TRANSMITTING TUBE 171

LINEAR ELECTRON ACCELERATOR TO ONE MILLION VOLTS 186
By A. T. Starr, G. King, and L. Lewin

CRYSTAL TRIODES 195
By T. R. Scott

CROSS-TALK CONSIDERATIONS IN TIME-DIVISION MULTIPLEX SYSTEMS 209
By Sidney Moskowitz, Liscum Diven, and Louis Feit

THEORY OF SPACE-CHARGE WAVES IN CYLINDRICAL WAVEGUIDES WITH MANY BEAMS ... 217
By Philip Parzen

PERIODIC-WAVEGUIDE TRAVELING-WAVE AMPLIFIER FOR MEDIUM POWERS 220
By G. C. Dewey, Philip Parzen, and T. J. Marchese

EFFECT OF HYDROSTATIC PRESSURE IN AN ELECTRON BEAM ON THE OPERATION OF TRAVELING-WAVE DEVICES 228
By Philip Parzen and Ladislas Goldstein

MAGNETO-OPTICS OF AN ELECTRON GAS WITH GUIDED MICROWAVES 233
By Ladislas Goldstein, M. A. Lampert, and J. F. Heney

GROWTH AND AMPLIFICATION 235
By Henry Busignies

RECENT TELECOMMUNICATION DEVELOPMENTS

TELEVISION PICTURE MONITOR 219
SELENIUM RECTIFIER FOR PROTECTING ELECTRIC CONTACTS 236
ROYAL AIR FORCE RADIO INSTALLATION AT NAIROBI 236

CONTRIBUTORS TO THIS ISSUE 237

Radio communication between the people of one nation and those of another provides a bridge over which understanding, friendship, and peaceful common interests may flow. This transmitting plant at Brentwood, Long Island, New York, of Mackay Radio and Telegraph Company, radio associate of American Cable and Radio Corporation, is an important link in the worldwide communication system of the International Telephone and Telegraph Corporation.

Electromechanical Distributor for Sorting Mail

By S. SCHEUER,
On Staff of Prime Minister of Belgium; Antwerp, Belgium

C. B. NEYT, and L. J. G. NIJS
Bell Telephone Manufacturing Company; Antwerp, Belgium

MANUAL SORTING of mail in a post office is a time-consuming and expensive process. Although no machine has yet been developed that can read the address inscribed on a letter and then route it to its destination, many benefits can be obtained by mechanizing the present sorting operation. A machine was developed in which the only human interpretation necessary is the reading of the address on each piece of mail and the operating of a keyboard to route the letter to the proper destination case. An endless chain of 626 boxes pass successively by each of 300 destination cases and place each piece of mail in its appropriate case. With four operators, mail can be sorted at the rate of 280 letters per minute and be distributed among the 300 cases. By logical extension, the principles will permit the assembly of a machine to distribute mail or similar matter at any rate and to any required number of destination cases.

• • •

The watchword of the postal service has always been, and remains, *speed:* every possible effort must be made to avoid unnecessary loss of time between the moment of dispatch of a letter and its safe delivery. Transportation has continually become faster but sorting mail as to destination is still a slow manual process that subjects workers to its particular vocational health hazards of communicable diseases, impaired blood circulation, and foot troubles.

From the earliest times, sorting has been done manually and is still carried out in that manner almost everywhere. But, while the speed of the carriers transporting the mail continues to increase along with the volume of mail, the sorting process has failed to keep step and is now consuming a disproportionate amount of the time between dispatch and delivery of a letter.

Realizing that the probable solution of the problem lay in the direction of mechanizing the sorting process as far as possible, the officers of the Belgian Postal Administration requested that the engineers of Bell Telephone Manufacturing Company make a survey of the problem. The Administration required that the machine have a capacity of 300 sorting cases with a speed per

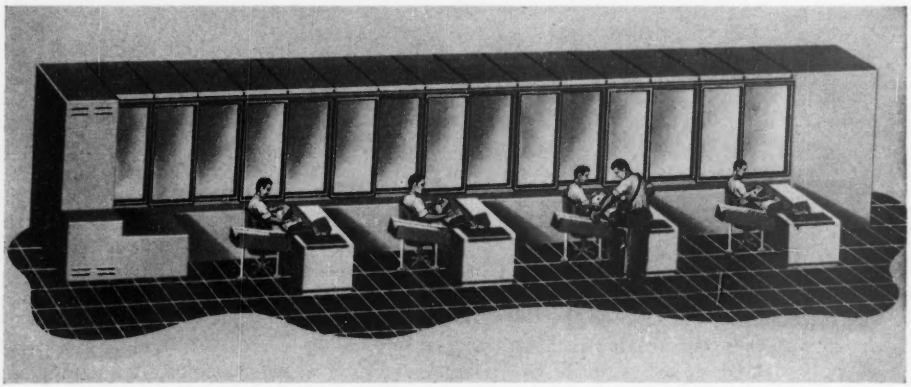

Figure 1—Artist's drawing of the 4-position sorting machine as it would appear installed in a cabinet.

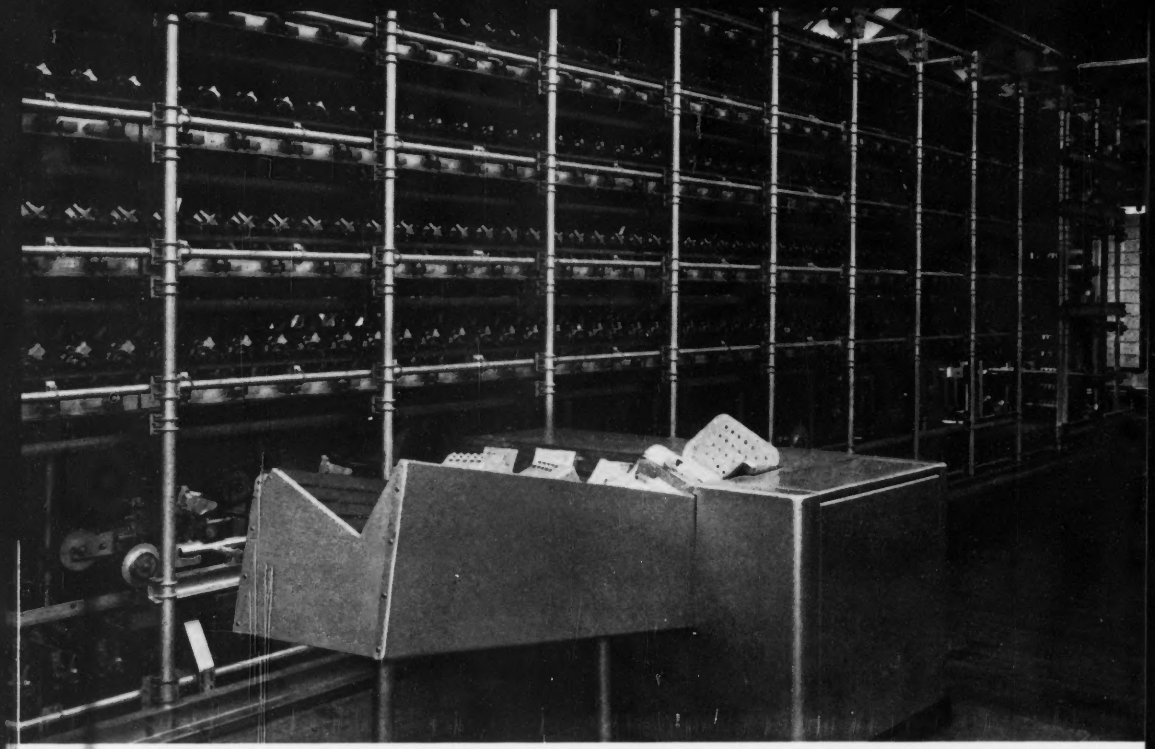

Figure 2—View of an operating position. Frame of the machine with the chain of transport boxes is in the background.

operator of 70 documents per minute, so that with four operators a maximum of 280 letters could be handled per minute.

The machine that was built as a result of the foregoing is of the electromechanical type, operating on principles inspired by automatic telephone practice.

1. General Description

A general view of the sorting machine is shown in Figure 1. The sorting mechanism is built on a large frame containing the endless-belt carrier; the 300 sorting cases that receive the mail are at the rear of the frame. The four operating desks extend at right angles from the frame. The incoming mail is stacked on edge on the inclined loading ramp at the right of the operator. Each letter is brought in front of the operator where it pauses for an instant while he punches on a key-set a 3-number code corresponding to the destination case to which the letter is to be directed. The letter then resumes its motion into the machine and drops into one of an endless chain of boxes. When the transport box containing this letter is at the proper destination case, the code causes the box to open and the letter is dropped into the case.

2. Operating Positions

There are four operating positions associated with the machine, and all are similar to the one shown in Figure 2. As has been said previously, the operator sits comfortably in front of the desk with the main frame of the machine on his left and the loading ramp, on which the incoming mail is placed, on his right.

A close-up view given in Figure 3 discloses the mechanism of the desk. The letters are at the extreme right of the photograph on an inclined ramp. Underneath the stack of letters is a series of chain drives that, by an intermittent motion, advance the stack toward an arm on which a suction device is mounted. This suction device is brought against the topmost letter in the stack, which it grasps. The arm is then withdrawn through the hole in the perforated plate and the

single letter thus removed from the stack is released and allowed to fall a short distance into a groove running the length of the desk in front of the operator.

In Figure 3, a small hook is visible against the lower right corner of the letter that has been pushed out into the reading position. A series of these hooks run in a slot along the front of the desk directly above the groove. They are spaced along their driving chain at a distance that will accommodate the longest piece of mail that is regularly processed on the machine, and they advance the letters along the groove, stopping each letter in front of the operator just long enough to allow him to read the address and depress the keys on his keyset in accordance with an established destination number or letter code.

The electric impulses obtained from the keyset shown in Figure 4 are recorded by memory devices similar to those used in automatic telephone exchanges. From the moment that the code is recorded, although the letter still has a long way to travel, its path is fixed and it will end its journey in the indicated destination case at the back of the machine.

After pausing in front of the operator, the hook pushes the letter to the left and into the body of the machine. Here the letter passes through a marking device that will print the operator's number on the envelope, or make

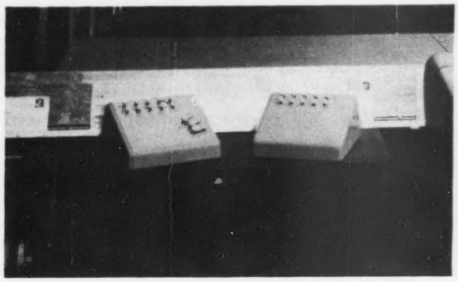

Figure 4—Operator's coding keyset.

Figure 3—The mechanism at an operating position. A pneumatic suction arm places each letter on a moving chain that brings them one-by-one in front of the operator.

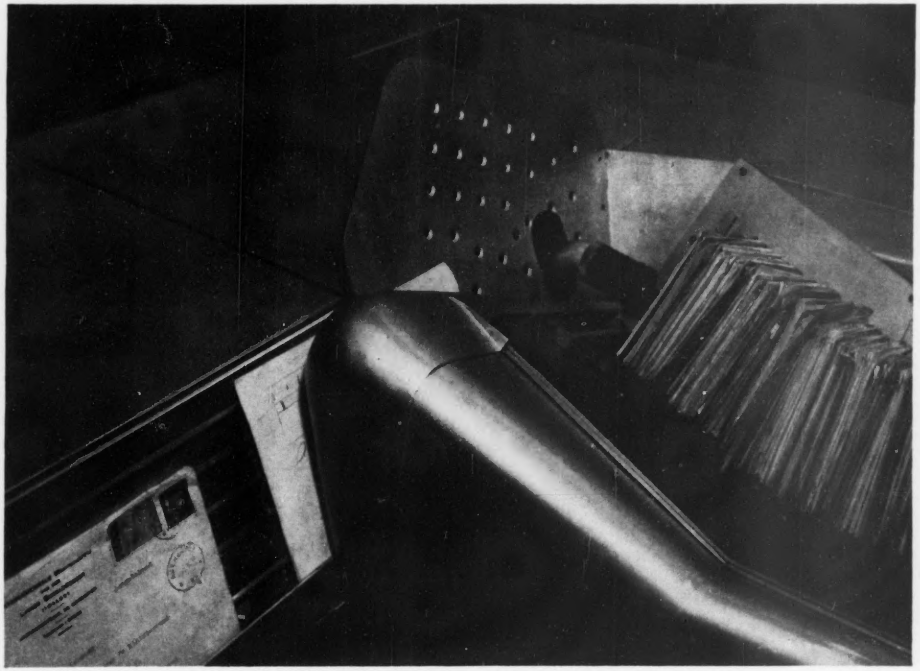

any other desired marking. A transfer device is next used to remove the letter from the groove on the desk and place it in one of the transport boxes that will carry the letter to the appropriate destination case.

3. Transfer Device

The mechanism of the transfer device is shown in Figure 5. The letter from the groove on the desk is pushed onto one of the blades of a horizontal turnstile. With the arrival of one of the troughs of the transport device under the turnstile, it revolves and the letter falls into the trough. There are several of these troughs on a short endless belt that moves at the same lineal rate as the long endless belt carrying the transport boxes. Each trough has a movable side that falls out to the same angle as the sloped reading panel. After the turnstile lets the letter fall into the trough, this movable side takes an upright position to enclose the letter within the trough.

Figure 5—The troughs on the transfer device and some other parts of the machine are shown below.

The gearing of the chain drives in the machine is such that the loaded trough, beginning its right-to-left journey on the underside of the endless chain, will be exactly over one of the transport boxes and will follow it along for a distance of several feet before raising and going back to the turnstile for another letter. A shutter on the bottom of the transfer trough is opened when the trough comes in contact with the top of one of the transport boxes and the letter falls into the lower box. This shutter is reclosed and the movable side drops into its sloped position again before the troughs return to the turnstile.

One of these transfer devices is used at each of the four operating positions, and the endless chain of transport boxes pass successively under each of the several transfer devices. The transport boxes are all empty as they approach the first operating position, where the transfer troughs load each fourth box. The rest of the transfer devices are successively shifted by one transport box so that there is always an empty box for each transfer trough at all four positions. Thus, the first position will have available to it transport boxes 1, 5, 9, 13 . . . while the second

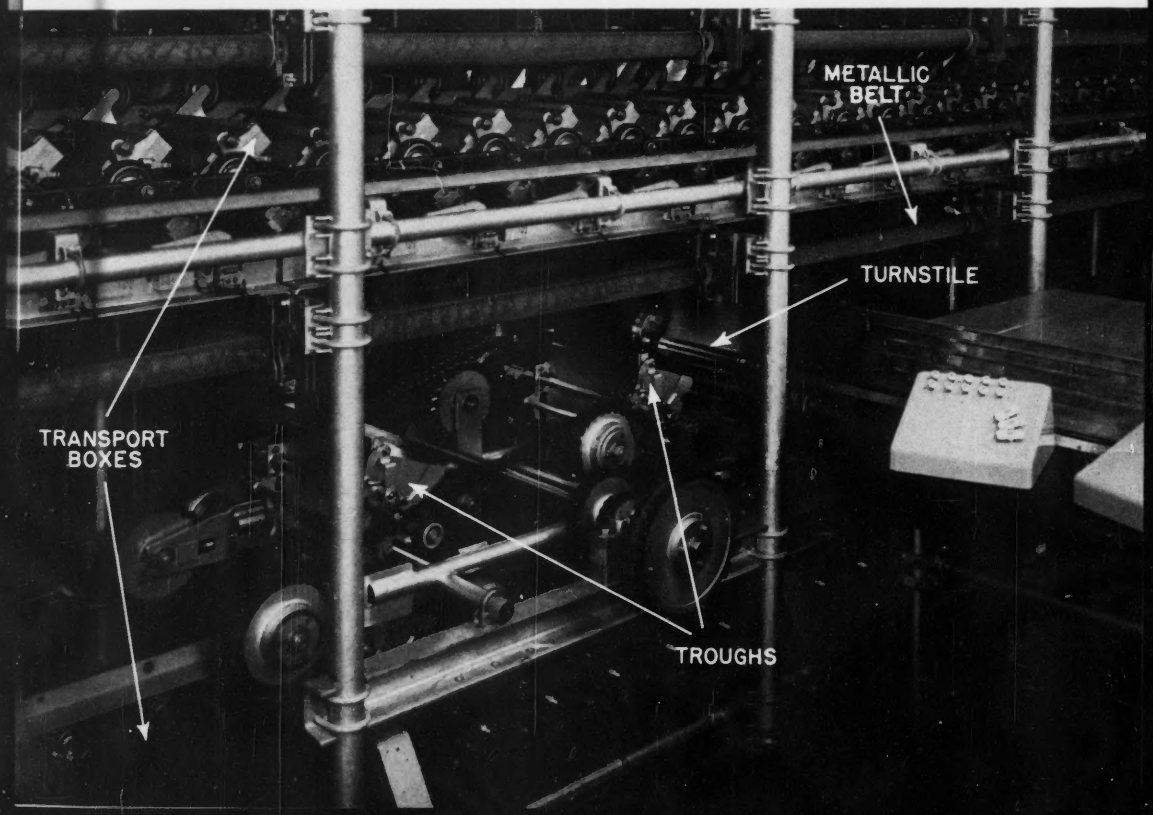

position will use boxes 2, 6, 10, 14 . . .; the third, 3, 7, 11, 15 . . .; and the fourth, 4, 8, 12, 16. . . .

4. Transport Chain

The 626 boxes of the transport chain are closed at top and bottom by movable shutters. The top shutters of the boxes are opened just before they come under the transfer devices and are closed after they pass the last one. The top shutters are necessary since the boxes are turned upside down several times in the course of their journey past the 300 destination cases. This

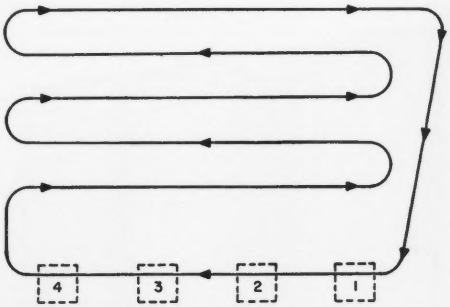

Figure 6—Direction of travel of the chain. The four operating positions are shown as broken squares.

transport chain consists of an endless series of boxes spaced 6 inches apart on a link-type cable that draws them along; the boxes themselves roll along metal bars on rubber rollers for silent operation.

The serpentine journey of the chain is illustrated in Figure 6; the 300 destination cases are disposed on 5 tiers of 60 cases each. The transport boxes successively pass in front of each destination case and then return to the starting point at the first operating position.

At the moment that a transport box containing a letter directed to a certain destination case passes in front of that case, the code that the operator punched on his keyset causes a small tripping device associated with the desired case to open the bottom shutter of the box and the letter falls onto a metallic mesh belt. For convenience, one of these belts serves for four cases (Figure 5) being sectioned by metallic panels to assure that the letter reaches the proper case as the belt carries it toward the rear of the machine.

An end view of the machine in Figure 7 shows the chutes used to direct the letter from the partitioned belts to the destination cases. The cases, shown in Figure 8, are designed so that when one is full an alarm sounds to summon an attendant. They are at a convenient height from the floor so that the attendant will not have to use a ladder or stoop over to remove the mail.

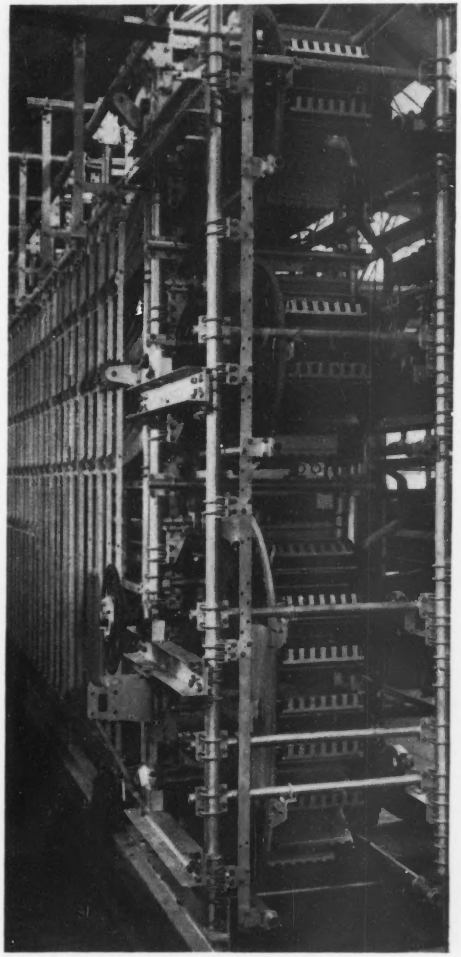

Figure 7—End view showing the rear of the machine.

5. Switching Devices

The electromechanical brain of the machine determines when the tripper associated with a particular destination case is to be operated to

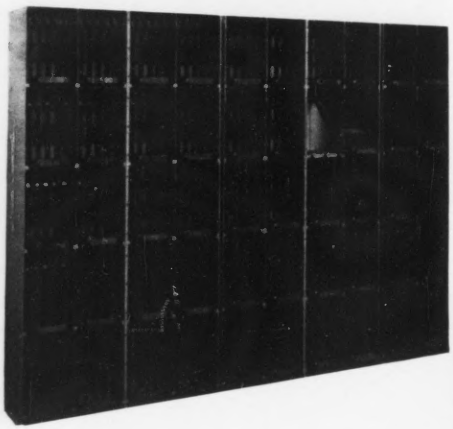

Figure 8—Destination cases to which the mail is distributed. They may be unloaded while sorting is in progress.

open the box then passing and drop the letter on the belt for delivery to the destination case. Rotary-type switches and relays perform this function. They are mounted on bays that need not be adjacent to the machine itself, but can be placed elsewhere and connected by cables. Racks of such equipment are shown in Figure 9.

As stated previously, each letter pauses in front of the operator, who reads the address and punches a 3-number code. The letter then continues its journey. The operator, of course, must know the proper code for each address by memory, but this presents no great difficulty for present-day postal operations commonly use such a system. Since the entire machine operates in a step-by-step synchronized method at a constant speed, the switching system need only compute how long it will take the letter in front of the operator to reach the proper destination case. Since the destination cases are placed 9 inches apart, a convenient method of computing time is to use 9-inch steps.

The block diagram of the switching system is given in Figure 10. Let us assume that the operator has just arrived at his seat and throws the switch that energizes the circuits associated with his desk. There are 6 registers (Figure 11) associated with each desk, and one of these will immediately be connected to the keyset. Suppose, then, that a letter stops in front of him and he punches the number of destination case 256 on the keyset. The register then computes that the letter is at this moment, say, Y, 9-inch steps away from case 256. But it also knows that it will take the letter Z steps to pass through the transfer device and be deposited in a transport box. These figures are then summed in the register and it is known that in exactly X 9-inch steps the tripper should be operated as the transport box containing our letter will be in front of destination case 256.

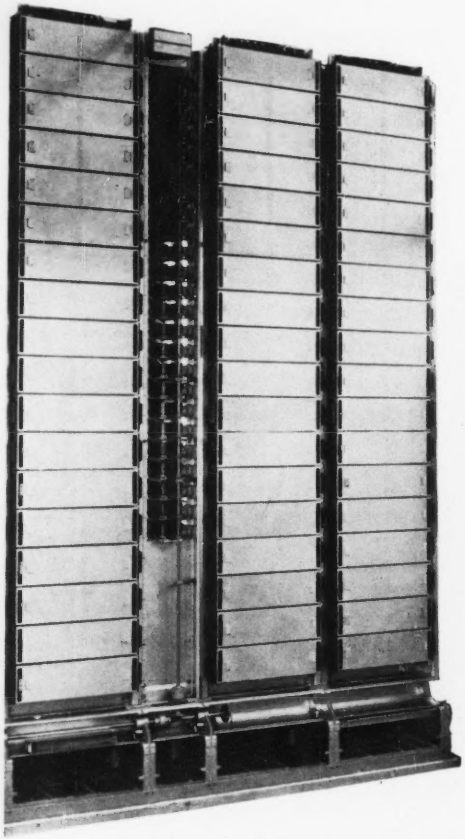

Figure 9—Some of the bays of control apparatus.

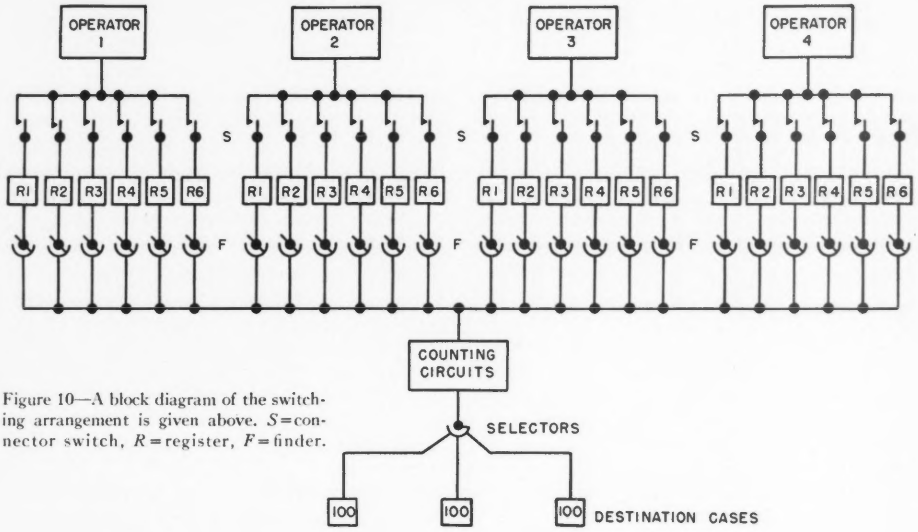

Figure 10—A block diagram of the switching arrangement is given above. S=connector switch, R=register, F=finder.

The register will then connect itself through a finder switch to one of the 200 counting circuits (Figure 12), and will give it the following instructions: "Connect yourself with destination case 256 and operate its tripper circuit when you have counted exactly X 9-inch steps from now." The register will then disconnect itself from the counting circuit and will be free to take another code from the operator's keyset. This entire operation takes but 5 seconds.

The letter enclosed in its box continues on its way and the counting circuit marks step-by-step the progress of the transport box toward the destination case. It should be noted that these two operations, the progress of the box and the marking of its position are performed independently of one another, and the only link is the synchronization between the mechanical motion of the chain and the counting of the 9-inch steps.

When the counting circuit has counted out the required X steps, the circuit finishes its task by sending an impulse to energize the tripper of destination case 256. At this precise moment, the transport box containing the letter will arrive in front of the case and the letter will be discharged through the shutter in the bottom of the box. Finally, the counting circuit disconnects itself from the tripper circuit and the tripper resumes its rest position before the arrival of the next transport box on the chain.

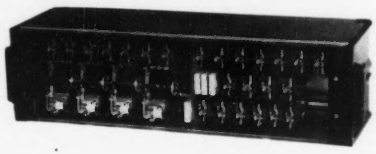

Figure 11—Calculating part of one of the 24 registers.

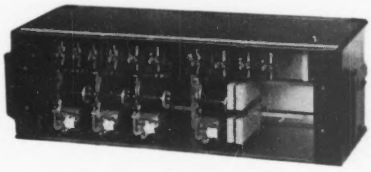

Figure 12—One of the 200 counting circuits.

6. *Conclusions*

The use of this distributing machine has increased the speed of sorting mail strikingly in

contrast with the time-worn methods that are prevalent throughout the world. With this machine, it is possible for an operator to classify 4200 letters per hour for 300 destinations. Manual methods permit the handling of only 1200 to 1600 letters for only 60 destinations in the same time, requiring several successive sortings before the mail is broken down into the required number of final destinations. It may be concluded that use of the machine increases the effectiveness of each operator by 4 or 5 times.

Another advantage of the machine is its great flexibility—machines can be assembled to suit local conditions and any number of operating positions can be incorporated. With the machine described here, it is obvious that in periods of light load, it can be manned with only one or two operators. The speed of the machine is adjustable and can be set to conform with the dexterity of the operators in reading the addresses and punching the keyset.

It may seem to the reader that the use of 626 transporting boxes in the chain is excessive; it would have been less expensive to use fewer boxes and run the chain at a faster speed. However, this would cause an increase in noise and wear on the moving parts. The machine has been constructed of the lightest possible materials to permit installation in a building without reinforcement of the floor, but great attention has been paid to making it as sturdy as possible. Some idea of the wear and tear that the machine undergoes may be gained from the fact that in the post office where it is installed 45 million letters are sorted on the machine in a year.

Instead of having to walk around to reach the various destination cases as is necessary in the manual method, the operators are seated comfortably in chairs. Their work consists only in reading the addresses of the envelopes passed in front of them and manipulating their keysets, which are comparable to an adding machine or typewriter. It should be noted that the letter is within the visual angle of the operator for about 2 seconds before the code number must be punched, an interval of time that is fully sufficient to allow for easy reading. Furthermore, if the operator makes an error in punching his code, or if he should find an illegible address on the letter in front of him, he has 3 seconds available in which to remove the letter from the reading desk and place it in a special pile or direct it to an "improper-address" destination case. This in no way disrupts the continuity of the sorting process.

One of the most important advantages of the machine is that the operator need not touch the letters with his hands, and thus has all 10 fingers available for use on the keyset. From a health standpoint, this means that he is not subjected to the danger of communicable diseases inherent in the handling of each letter. Similarly, he is relieved of the occupational hazards of poor blood circulation in one arm caused by carrying a load of mail in a fixed position while distributing it and of the foot troubles that result from constant standing and walking. Instead, he is seated comfortably at a desk and need only press a key to send each letter to its destination case. He has, in effect, been supplied with an exceedingly long arm to do his job with speed, accuracy, and comfort.

Manufacture of a High-Frequency Transmitting Tube

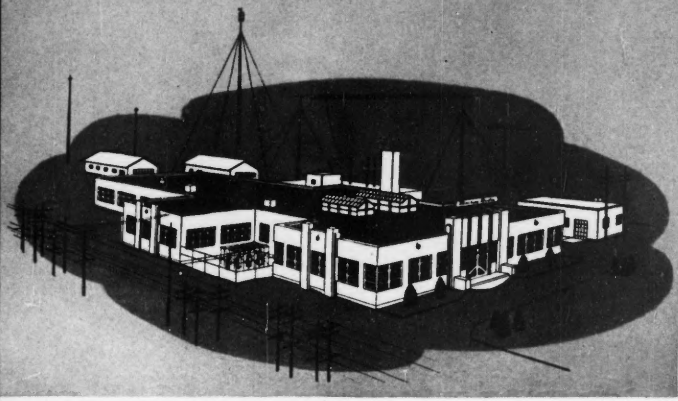

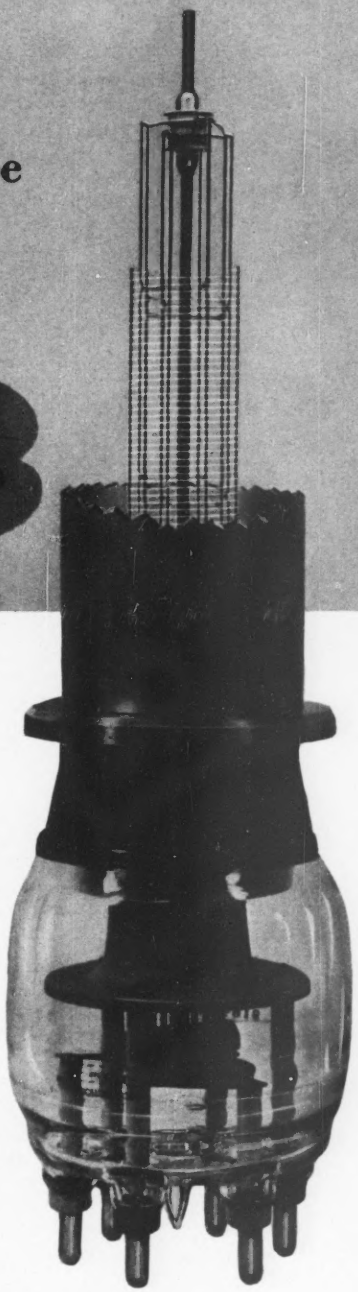

WHENEVER radio communication over very long distances must be established, as for point-to-point commercial telegraph service and for international high-frequency broadcasting, the generation of large amounts of radio-frequency power poses a major problem. A significant complication is that such services require the use of frequencies between approximately 3 and 30 megacycles per second. At the higher-frequency end of this band, transmitting tubes of the conventional types become so inefficient as to be unusable.

To meet the demand for high-power high-frequency transmitting tubes, Federal Telephone and Radio Corporation of Clifton, New Jersey, has developed and is now manufacturing the type *F-5918* triode. As may be seen in the accompanying cutaway view of this tube, simplicity of construction has been stressed along with sturdiness. A multistrand thoriated-tungsten filament is used, each of its 6 hairpin strands being mounted separately to prevent any stresses from warping the filament assembly when it heats up. The filament and grid connections are made to the pins on the glass base of the tube.

The *F-5918* triode is suitable for use as a radio-frequency amplifier, oscillator, and class-*B* modulator. Maximum ratings apply up to frequencies of 22 megacycles. The plate dissipation of this water-cooled tube is 70 kilowatts, and two tubes in push-pull class-*C* telegraph service will give an output of 400 kilowatts. As a class-*C* plate-modulated amplifier, two tubes will deliver in excess of 200 kilowatts. The manufacturing processes shown on the following pages characterize the production of most external-anode transmitting tubes.

1. In the illustration on the opposite page, the first operation in the fabrication of an anode is being performed. A thick disk of oxygen-free high-conductivity copper about a foot in diameter is centered over the die on a 250-ton drawing press. The ram of the press descends, forcing the copper through the die to produce a cupped shape. Successive drawings reduce the diameter of the cup and the thickness of the walls until the final form is obtained. Several stages of draw are shown at the right. Below, a lathe operator is machining the open end of the anode in preparation for the brazing operation shown next.

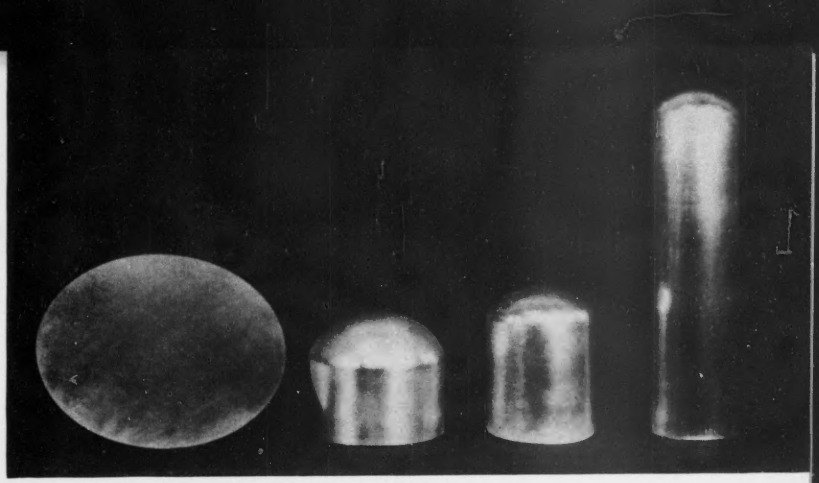

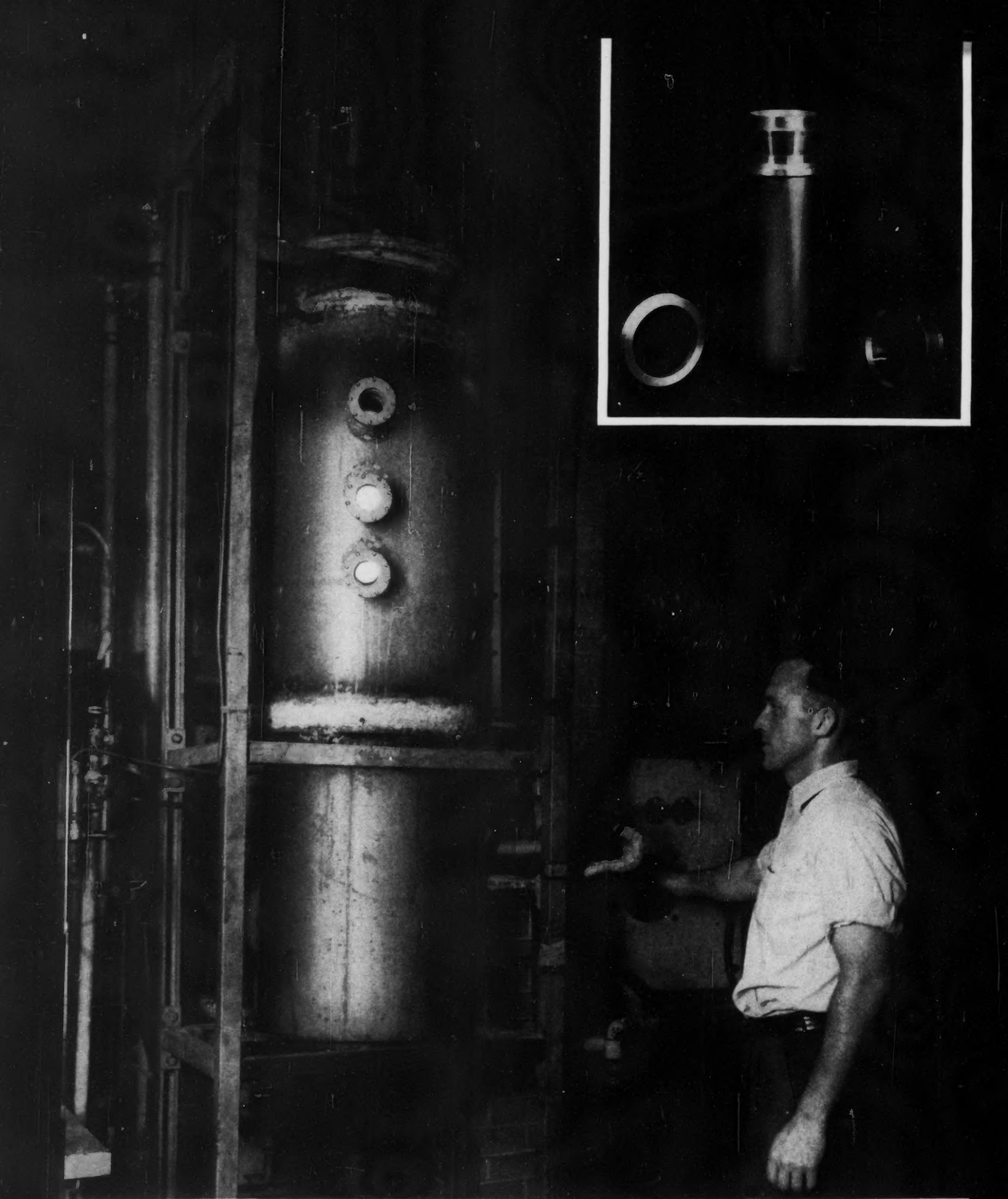

2. The copper mounting ring and a skirt are brazed to the machined end of the anode. A sturdy vacuum-tight seal must be obtained. The parts are assembled and placed in the furnace, where radiant heating raises the temperature until the brazing alloy melts. Inert gas prevents oxidation of the parts.

3. The next step is to fuse a glass blank to the end of the skirt. This blank will later be fused to the base assembly.

As the first step, flames are played on the metal skirt for a few seconds to form a layer of oxide to which the glass will adhere. Next, a large glass tube is brought over the skirt and heated until it fuses to the outside of the skirt. This tube is cut off leaving about a half-inch of free glass that is bent inside the skirt and fused there; this step is being performed at the right. To form a perfect seal, glass must be fused to both the inside and outside of the skirt.

The final step is illustrated below, where the end of the large glass tube has been squared off and high-temperature oxygen-hydrogen flames are used to fuse the glass tube to the glass-beaded skirt. When the final shape has been obtained, the anode will be placed in an annealing oven where it will be slowly brought down to room temperature.

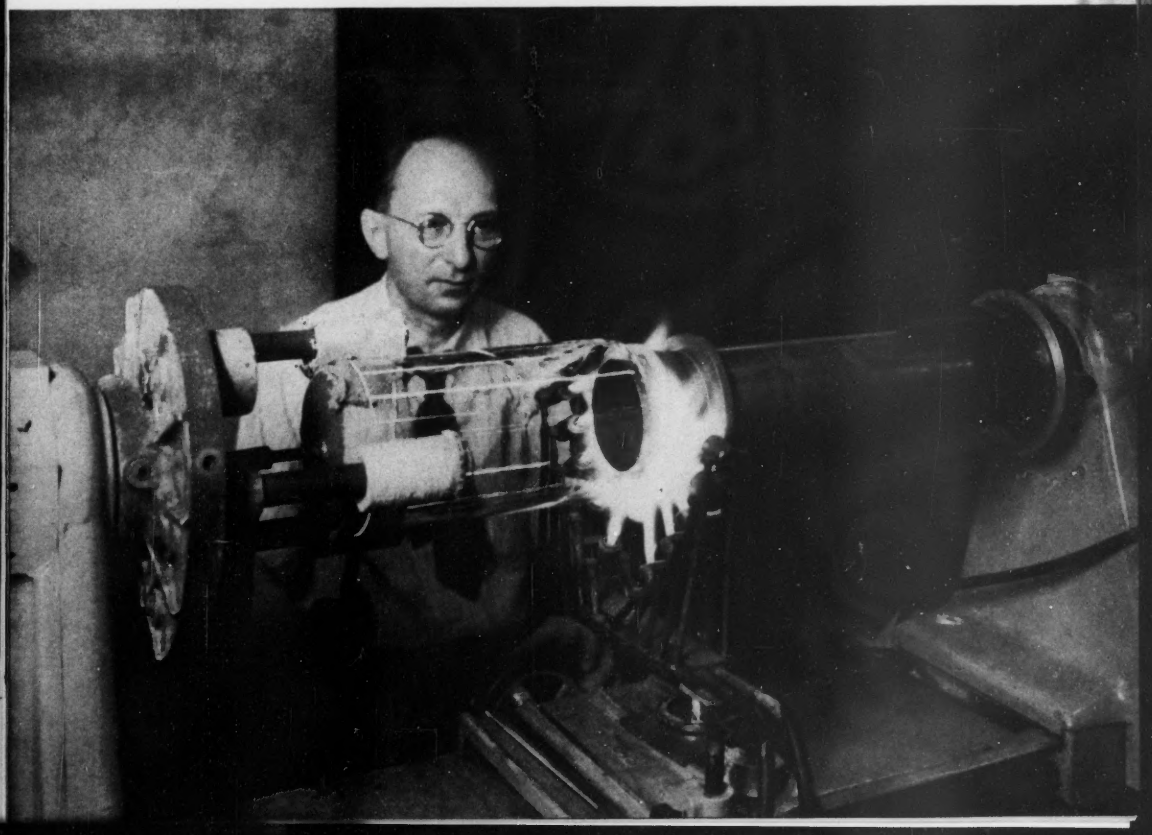

4. Extreme cleanliness is absolutely necessary throughout the manufacture of any transmitting tube that employs high operating voltages. If any dirt is left in the finished tube, even fingerprints, sparking is liable to occur or gas may be liberated and the tube is useless. In the illustration at the left, the finished anode, with the glass attached, is being washed with distilled water after being cleaned with hot acid. In addition to chemicals, sand-blasting is often used to remove scale and oxides from various parts. The anode will next be dried and the filament and grid assemblies sealed in it.

5. Below are illustrated the various parts that make up the base assembly of the tube. The large dish-shaped piece was pressed out of molten glass. The shorter terminal-pin assembly (bottom center) is one of three that will support the filament, and three of the longer ones will hold the grid. The parts that constitute one of these supports have been laid out to show the terminal cup (which will be glassed before fusing to the dish), and the various copper parts that are brazed to the terminal cup with the two brazing-alloy rings.

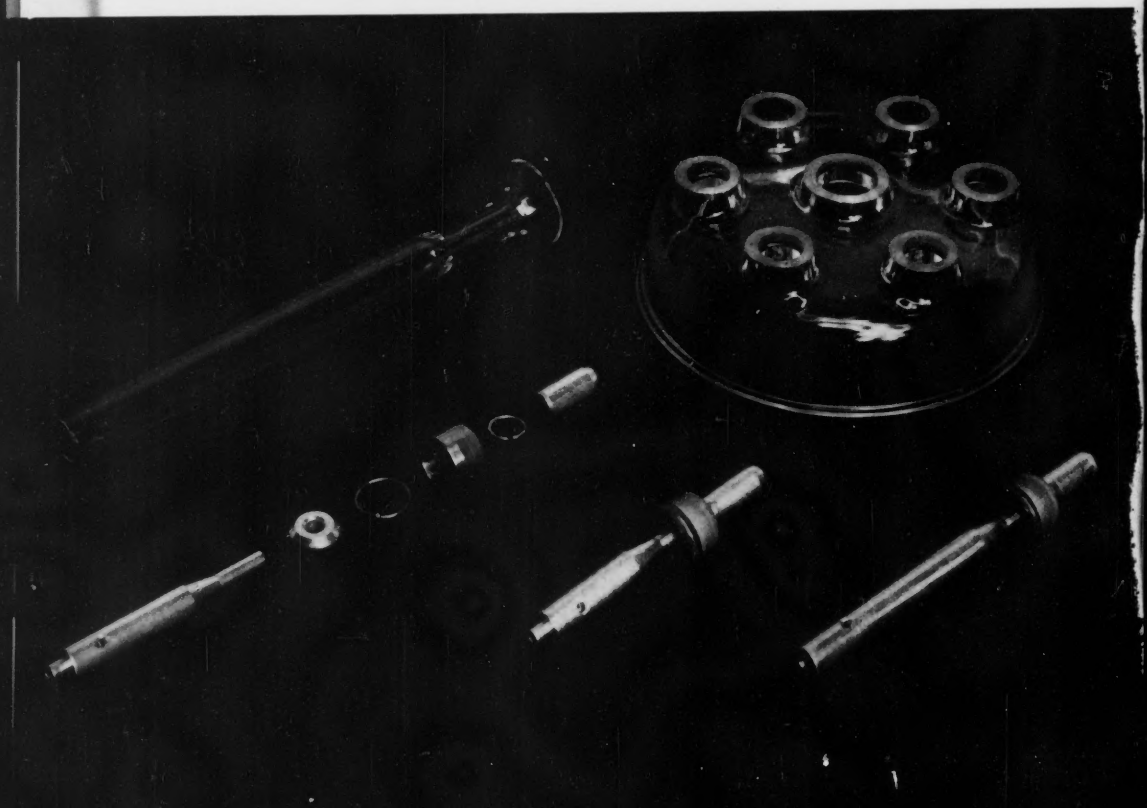

6. In the picture below, all the parts that are joined to the glass dish have been placed in their proper positions on a rotating jig. The jig holds the parts in exact alignment while the glass of the dish and that on the terminal cups are brought to a soft plastic state. The 6 small pipes on each side of the jig are oxygen–gas blowpipes; in addition, the operator is using a Mecker burner and a hand blowtorch to apply localized heat to various parts. Thick glass parts such as these must be heated and cooled very slowly or cracking is certain to occur.

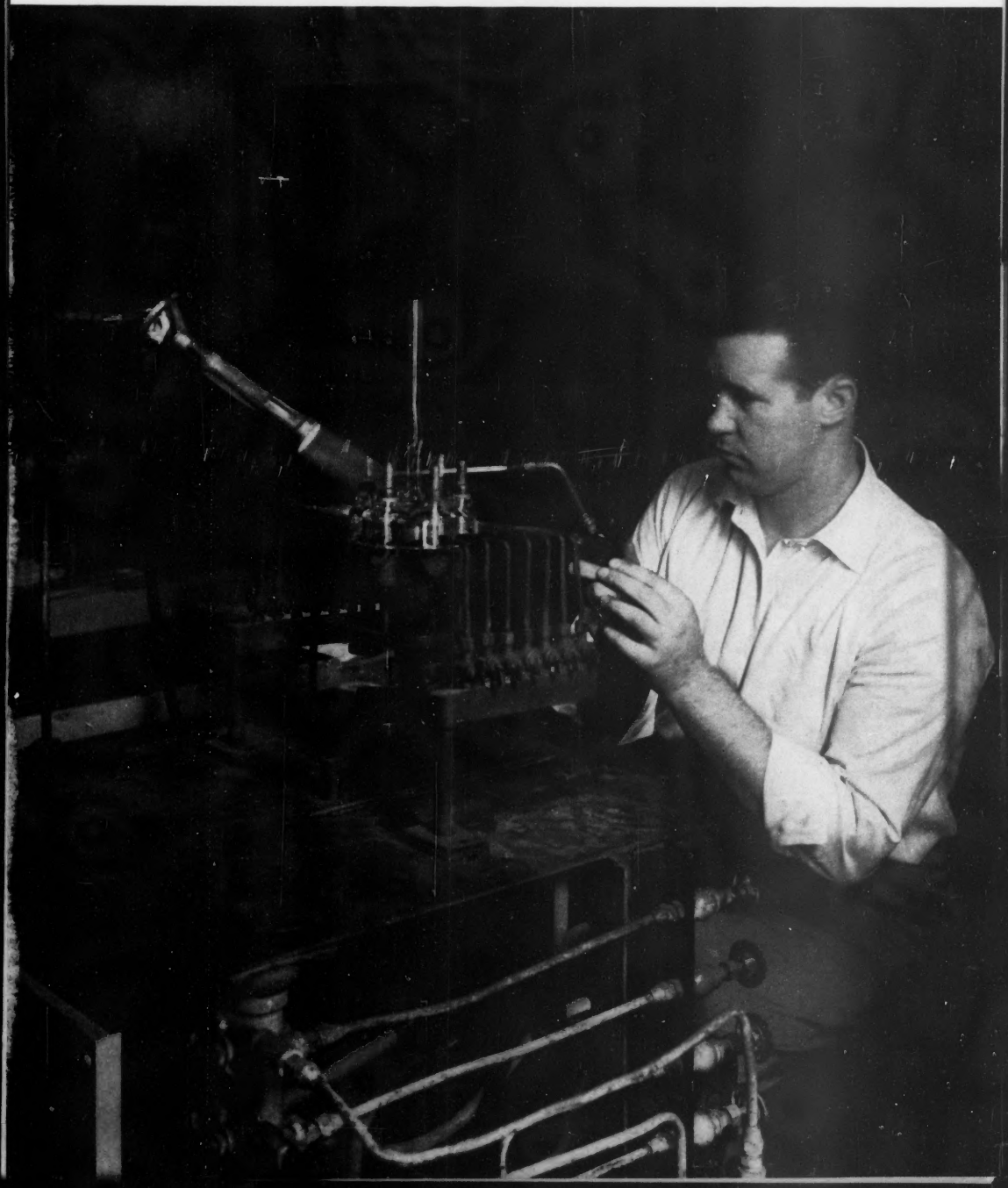

7. On the opposite page, an operator prepares to punch one of the supporting parts for the filament assembly from a smoking white-hot bar of molybdenum. This metal is extremely hard, having physical properties somewhat like tungsten, and can be punched only after being heated in a gas-fired furnace visable behind the woman's outstretched arm. Some of the finished pieces are on the table of the press.

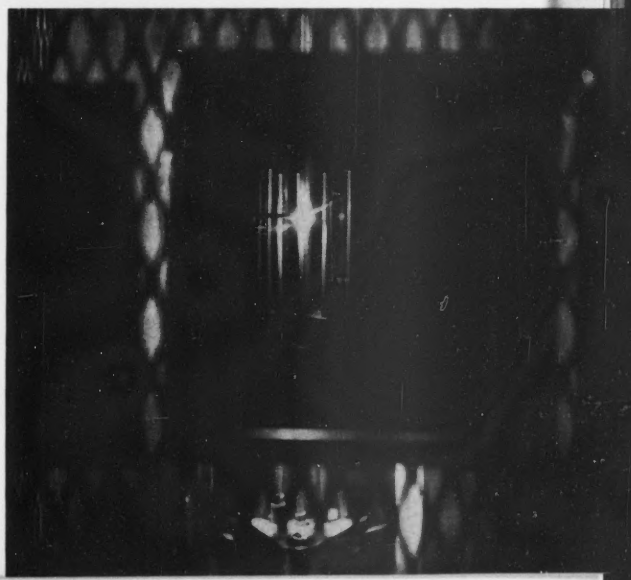

8. At the top of this page, an operator has completed assembly of the base and the supports for the filament and is installing the thoriated-tungsten hairpin filaments. He wears gloves to avoid contaminating the parts. Small clips of sheet molybdenum hold the tungsten against the heavier molybdenum support rods; when these clips are melted with an electric-arc torch (right), a firm bond is obtained. Inert gas is bled into the arc-welding chamber to prevent oxidation.

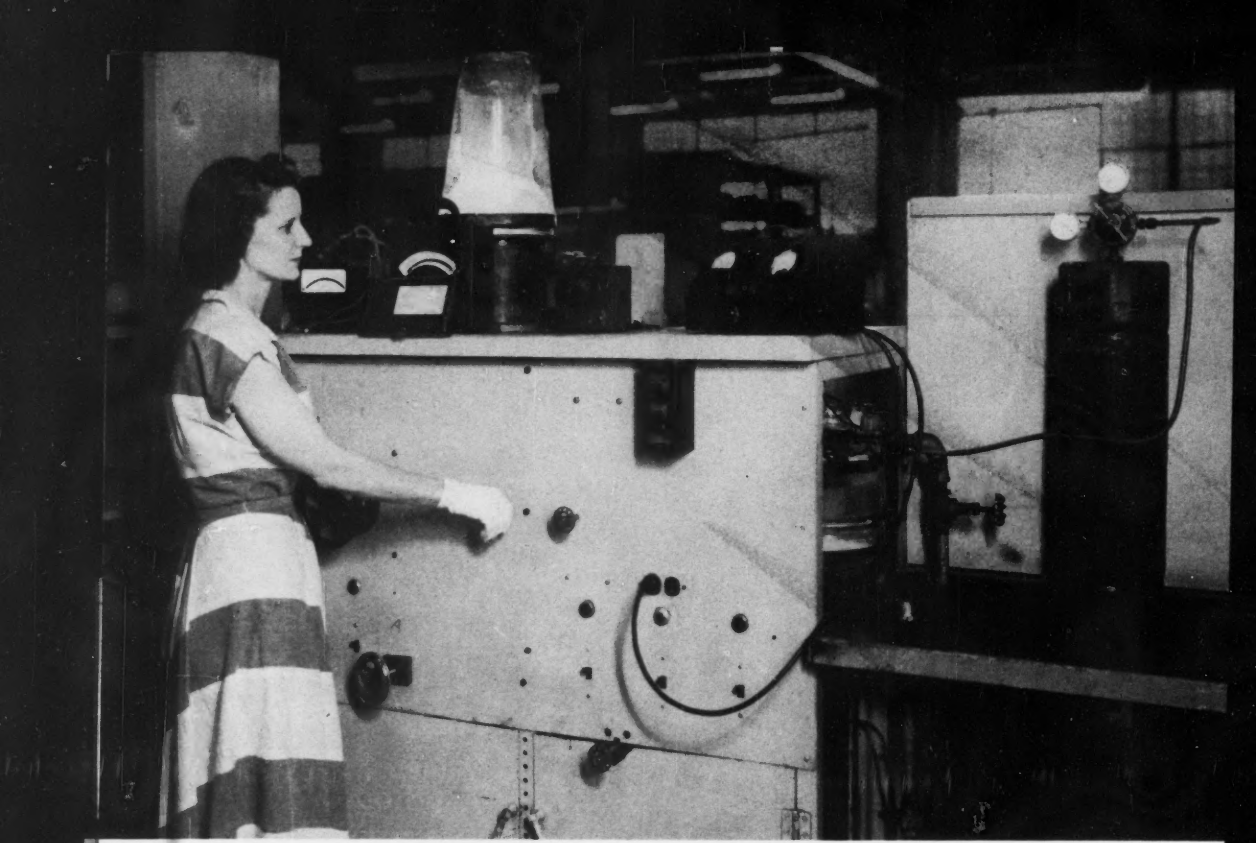

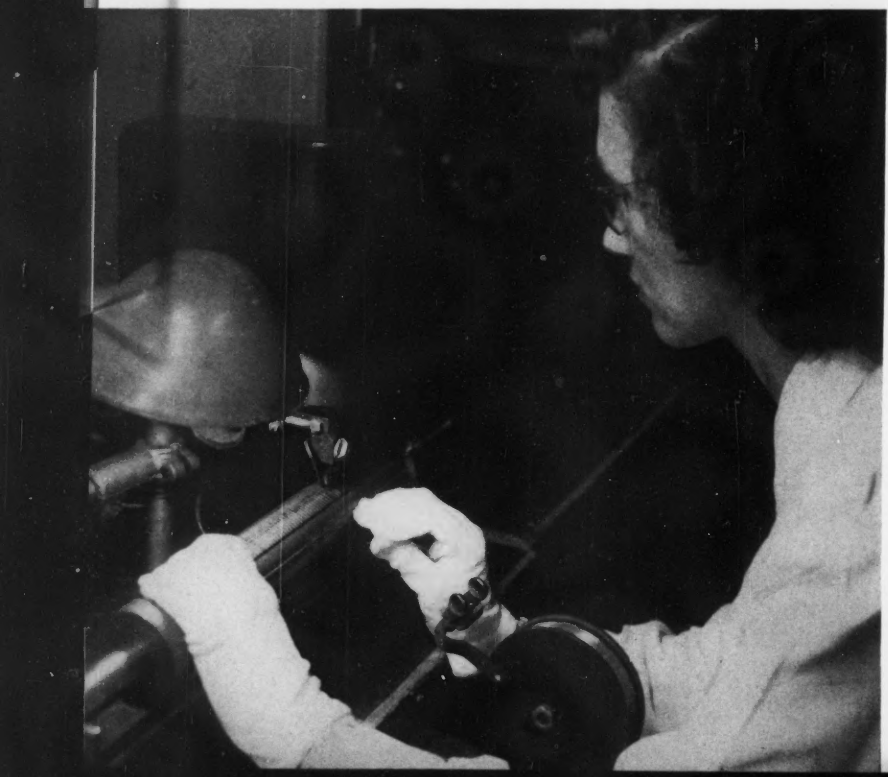

9. When the filament assembly is completed, it must be carburized. Thoriated tungsten requires this step to stabilize the rate at which the thorium contained in the tungsten is diffused toward the surface of the metal. Acetylene gas is bled into the glass vacuum chamber containing the filament, which is heated to a white heat by passing current through it. Changes in the electrical resistance of the filament indicate when the process is complete.

10. The grid is fabricated on the mandrel shown at the right. Molybdenum is used throughout the structure. Six relatively heavy supporting rods lie in slots along the mandrel, which is turned by hand. The thinner grid wires are fastened to each rod in turn by a spot-welding machine operated by a foot-pedal. Small spacers not visible here assure proper spacing of the turns of grid wire.

11. Before the grid may be mounted on the base assembly as at the left, it must be cleaned of all foreign matter. The operation is shown below.

The grid has been placed in one of the 4 bell jars in the machine. This is evacuated of all air, and high-frequency current is then applied to a coil that fits around the bell jar. By induction this causes currents to flow in the grid, which rapidly becomes white hot. All dirt is literally burned off the grid, and at the same time, any gas trapped in the metal of the grid is driven out and carried off through the vacuum pump.

Briefly, the effect of any spots of dirt on the grid is that these spots tend to become much hotter than the rest of the grid, and may actually become hot enough to emit electrons. Naturally, this alters the electrical characteristics of the tube, lowers the efficiency, and may actually become serious enough to destroy the tube by melting the grid.

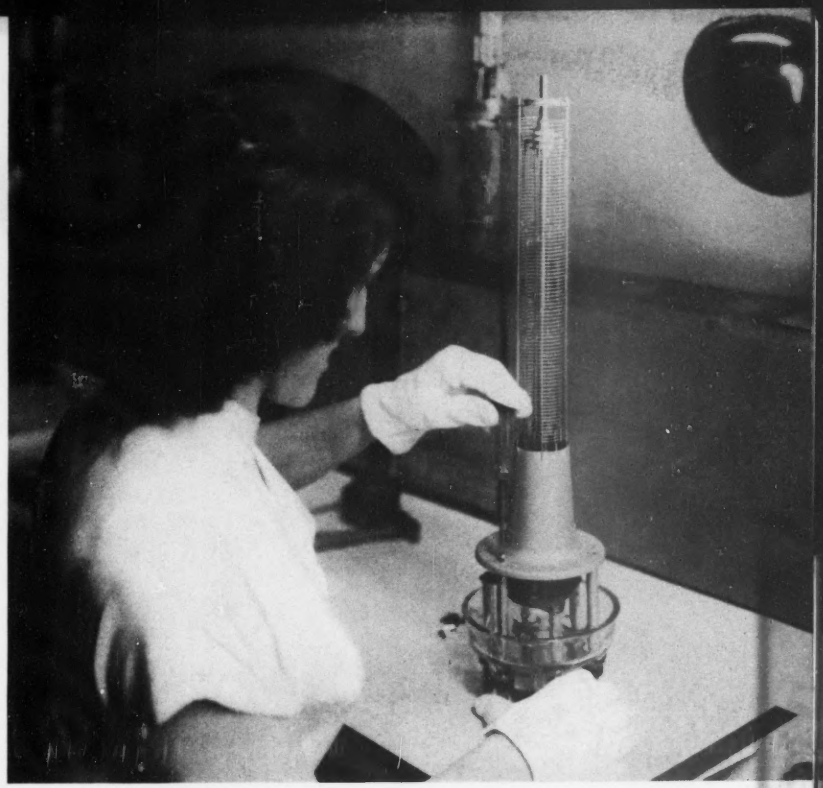

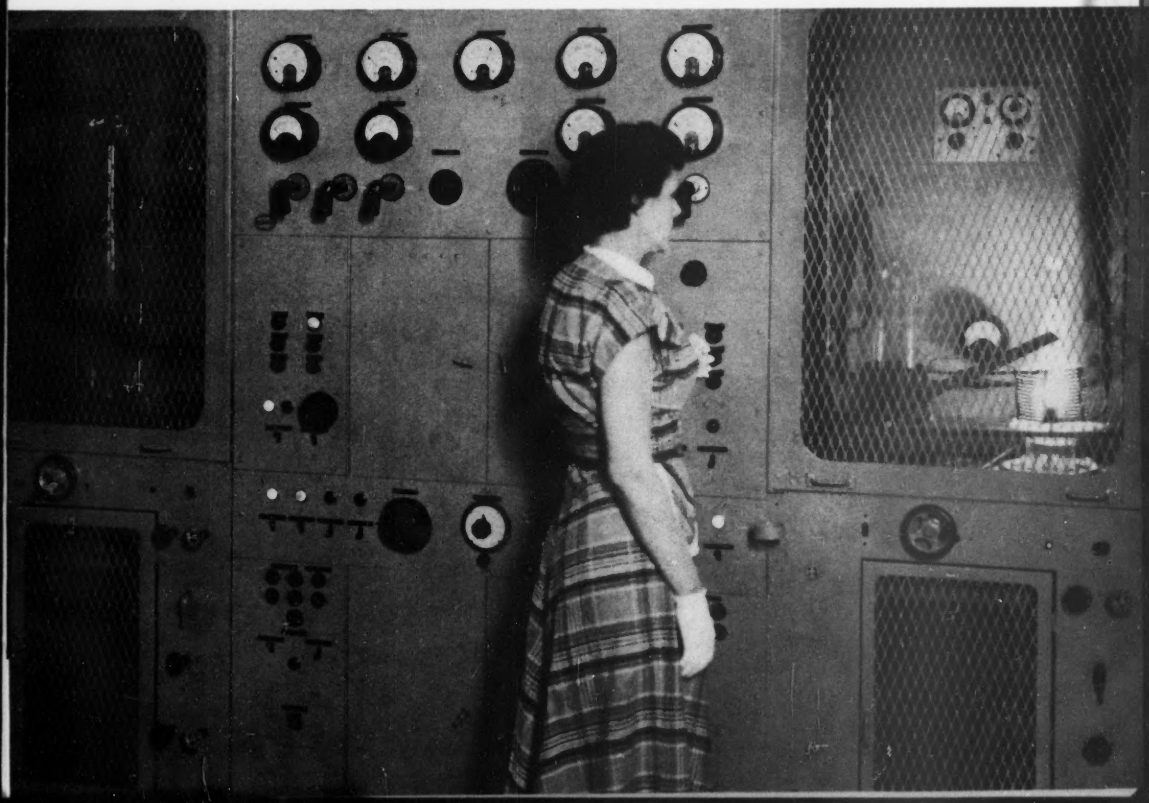

12. In the large glass lathe above, the headstock and tailstock rotate at exactly the same speeds. The tailstock holds the base assembly and this is carefully aligned with the anode in the headstock. When the preheating is finished, the operator will perform the final seal of the two parts by using greater heat.

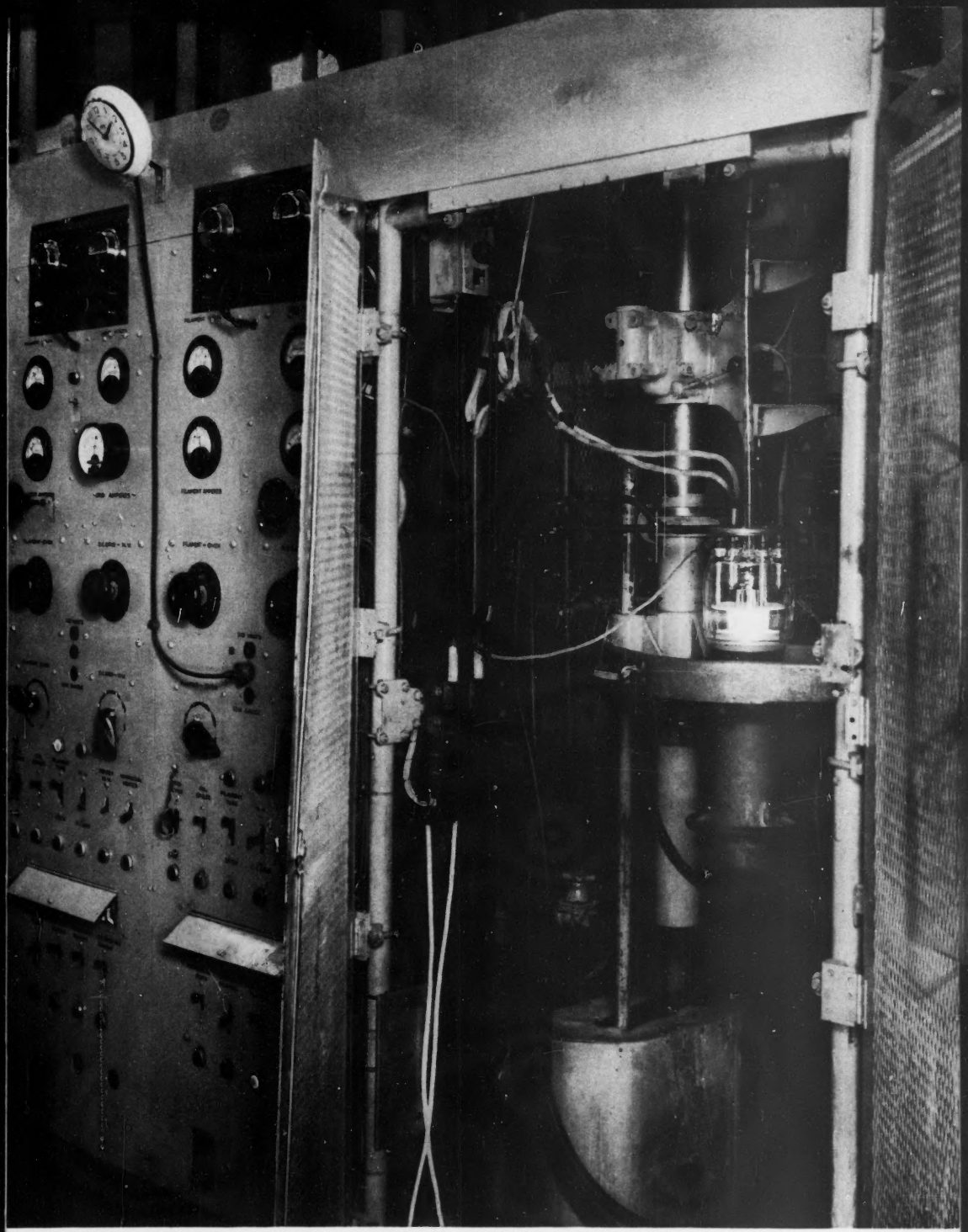

13. The safety doors of the exhaust station have been temporarily opened to show the tube in position. With a progressive series of steps, power dissipation in the elements of the tube is increased to drive all gases in the metals out before sealing off the exhaust tube. Gas flames on the anode assist the heating.

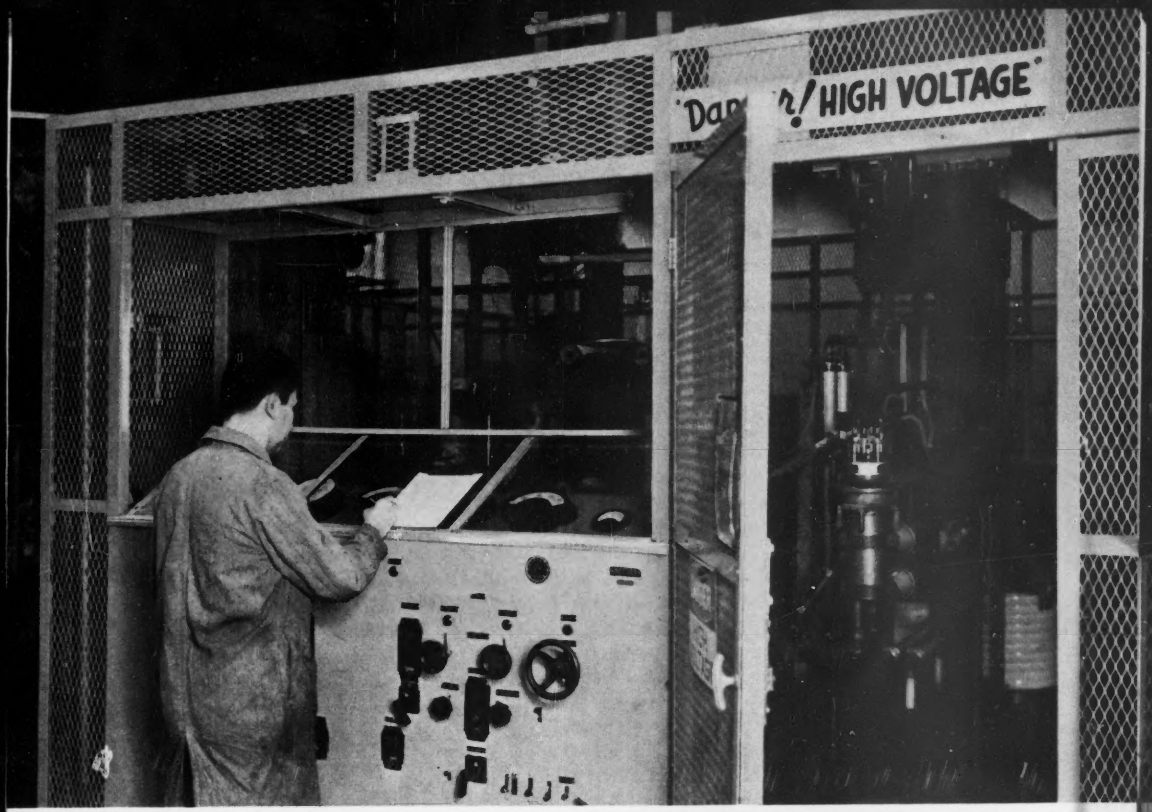

14. In the photograph above of a test set, the type *5918* tube has been placed in a water jacket, and a complete series of tests is being made of the various electrical characteristics of the tube. The tube is connected in a self-excited-oscillator circuit, the almost-200-kilowatt output being dissipated in a dummy water load.

15. On the opposite page is a view of a corner of the shipping department. The clerk is checking the tag that accompanies each tube through the testing department to be sure that all requirements have been met. After checking the packaging of the tube, it will be shipped to the customer. The tube is tied into the frame of the shipping container by a series of chains with springs at the ends. These insure that the tube will not strike the sides of the container if it should be dropped from any position. In shipping, a cardboard carton is slipped over the wooden framework shown in the picture.

16. At the right, Mr. Floyd Lantzer, chief transmitter engineer of station WLW, Cincinnati, Ohio, prepares to place a *F-5918* tube in one of the 200-kilowatt shortwave broadcasting transmitters at the station. Station WLW is an affiliate of the Crosley Broadcasting Corporation, and transmits some of the Department of State "Voice of America" programs to Europe.

Linear Electron Accelerator to One Million Volts

By A. T. STARR, G. KING, and L. LEWIN

Standard Telecommunication Laboratories, Limited; London, England

VARIOUS SYSTEMS of linear accelerators are discussed, and the problems of tolerance in dimensions and frequency investigated.

An accelerator employing an E_0 guide with irises has been constructed: the measured values of phase velocity agree with theory to within the observational error, which is about 1 per cent. With half a megawatt of power at 10 centimetres wavelength, a velocity corresponding to about 1·2 electron megavolts is achieved in a metre of guide: the injection velocity corresponds to 50 kilovolts. An X-ray output of $\frac{1}{2}$ roentgen per minute at 1 metre is obtained with a peak beam current of 60 milliamperes, but a 6-fold increase is available with the gun as constituted. The initial section is designed to collect only a small fraction of the beam in order to achieve a maximum acceleration in the length, and the order of collected current is 10 per cent.

A number of measuring instruments, for use with the accelerator, are described briefly.

The design of a 10-electron-megavolt accelerator to give 300 roentgens per minute is discussed. It is deduced that such an accelerator can be made on the basis of the present one, its length being about 3 metres and the input power 2 megawatts.

• • •

1. *Possible Types of Linear Accelerator*

It was felt in 1945 that the use of the high peak powers available with centimetre magnetrons could result in the design of a linear accelerator for electrons to produce a beam voltage of the order of several megavolts per metre of accelerator. Theoretical investigations have been carried out to ascertain the main properties of various accelerating systems.[1–10]

The following analysis was made to determine the most promising system. The possibilities considered are:—

A. E_0 guide with irises (corrugated waveguide).
B. E_0 guide with dielectric.
C. Zig-zag rectangular guide.
D. Coaxial line with resonant sleeves.
E. Resonators.

1.1 E_0 Guide with Irises

The simplest type is shown in Figure 1. A tube has at regular intervals circular plates with central holes. A wave travels through the central region with a phase velocity determined by the various dimensions and the free-space wavelength.

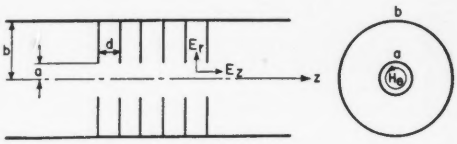

Figure 1—Simplest type of E_0 waveguide with irises.

The wave has a longitudinal component of electric force, a radial electric force, and an azimuthal magnetic force: when the electron and the phase of the wave have a velocity near that of light, the total radial force due to the electric and magnetic forces vanishes over the entire central region (not only at points on the axis). The longitudinal force does not vanish, but is constant over the central region.

For a given velocity of the electron and wave, the diameters of the iris holes and the guide can be varied, both increasing or decreasing together. The smaller the holes and guide, the greater is the acceleration for a given input power of wave, but the more critical are the dimensions for a given phase error per metre length of guide. Table 1 gives the tightest tolerance (which is for the guide diameter) for a variation of 1 per cent in the phase velocity. The free-space wavelength is 10 centimetres, the guide being designed for a phase velocity equal to that of light.

[1] Numbered references appear in Section 6 on page 194.

It is worth considering the choice of a lower frequency. If we were to assume that we need the same accuracy of phase velocity and that dimensional tolerances are to be proportional to the dimensions (i.e., fixed percentages), it can be shown that for a given acceleration per metre the power must be proportional to the square of the wavelength. But it is clear that if we still keep one adjustment per metre, the tolerance in the phase velocity is widened in proportion to the wavelength. Moreover, at 30 centimetres for example, it is easier to work to a tolerance of 0·015 inch in a 10-inch pipe than to 0·0044 inch in a 3-inch pipe. It would appear advantageous to use a longer wavelength.

1.2 E_0 Guide with Dielectric

This method suffers from two defects. It was felt that surface charges would upset the action, and the radio-frequency losses would be greater than in the guide with irises. Otherwise the action and tolerances are as for the E_0 guide. The recent proposal by Shersby-Harvie suggests that this type is worth reconsidering.

1.3 Zig-Zag Rectangular Waveguide

The magnetic force deflects the particles from a linear path, so that the path is more difficult to control. It is considered that this method is not worth pursuing.

TABLE 1

10 Centimetre E_0 Waveguide with Irises

Tube Diameter in Inches	3·37	3·22	3·14
Tolerance in Tube Diameter in Inches	±0·0044	±0·0024	±0·0014
Diameter of Iris in Inches	1·900	1·530	1·270
Frequency Tolerance in Megacycles per Second	±5·5	±2·6	±1·5
Attenuation per Metre in Decibels	0·2	0·45	0·82
Acceleration per Metre in Megavolts for 1 Megawatt Input	1·2	1·9	2·7
Acceleration per Metre in Megavolts for 2 Megawatts Input	1·7	2·7	3·8

1.4 Coaxial Line with Resonant Sleeves

Figure 2 shows one simple case; here the sleeves form a radial line between flat annular surfaces, and the dimensions are chosen so that the sleeves have zero impedance at the coaxial

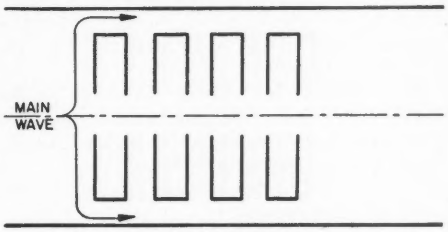

Figure 2—Coaxial waveguide with resonant sleeves.

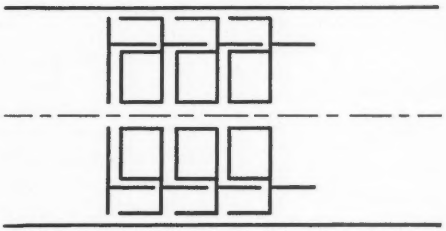

Figure 3—Coaxial line with sleeve labyrinth.

inner conductor. If this is done, the main wave travels with the velocity of light and high-voltage particles then travel continuously on a crest of voltage between the ends of the sleeves. It can be shown that such an arrangement will produce $\frac{1}{2}$ megavolt per metre with an input power of 1 megawatt.

Figure 3 shows a coaxial line with sleeve labyrinth; the latter steps up the voltage to give 2·2 megavolts per metre with an input power of 1 megawatt at 10 centimetres. The only tolerance of importance is that of the diameter of the holes forming the end of the high-voltage sleeve. It is found that a tolerance of ±0·0005 inch is needed if the parts are to be assembled without test, but it should be possible with this type of construction to adjust a few of the sleeves for the correct overall velocity after test. The loss is of the order of 1·0 decibel per metre.

The frequency tolerance is however very

stringent, being 1·0 megacycle at 3000 megacycles. The construction is somewhat complicated.

1.5 Resonators

1.5.1 Single Resonator

The simple type of resonator shown in Figure 4 will give 0·86 megavolt at 10 centimetres with an input power of 1 megawatt. The unloaded Q is 6000.

It is possible by altering the shape of the resonator (making the gap smaller and the resonator wider) to obtain a higher voltage, possibly by a factor of 2.

1.5.2 Cascade Resonators

For a given total power in the resonators, the total voltage is multiplied by the square root of the number of resonators.

Using 600 resonators in a 6-metre length, with 1 megawatt input power (0·2 megawatt being dissipated in a load), the output voltage is about 20 megavolts, and the frequency must stay within $\frac{1}{2}$ megacycle in 3000 megacycles.

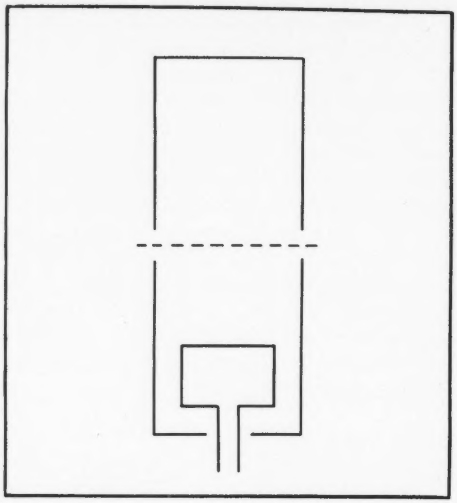

Figure 4—Single resonator.

2. Design of a Linear Accelerator

After careful consideration, it was considered that the E_0 guide with irises formed the most suitable type for initial experiments. A wavelength of 10 centimetres was chosen because of the availability of the Naval Type *277* modulator and transmitter, which produces about 0·5 megawatt peak power at that wavelength. Also, it was known that magnetrons giving 2 mega-

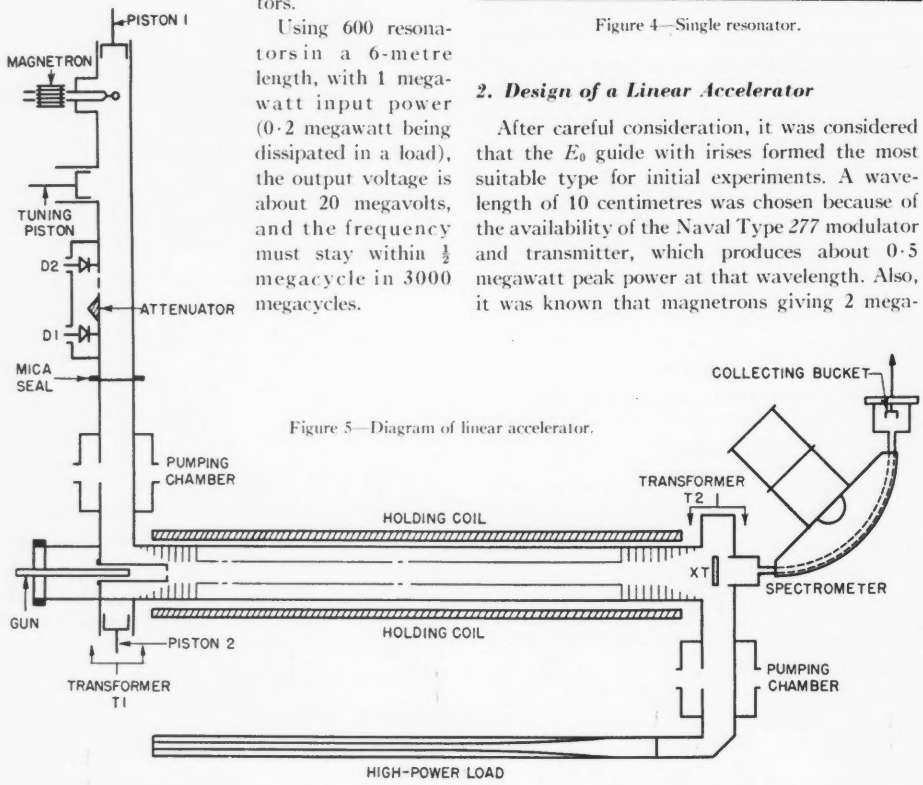

Figure 5—Diagram of linear accelerator.

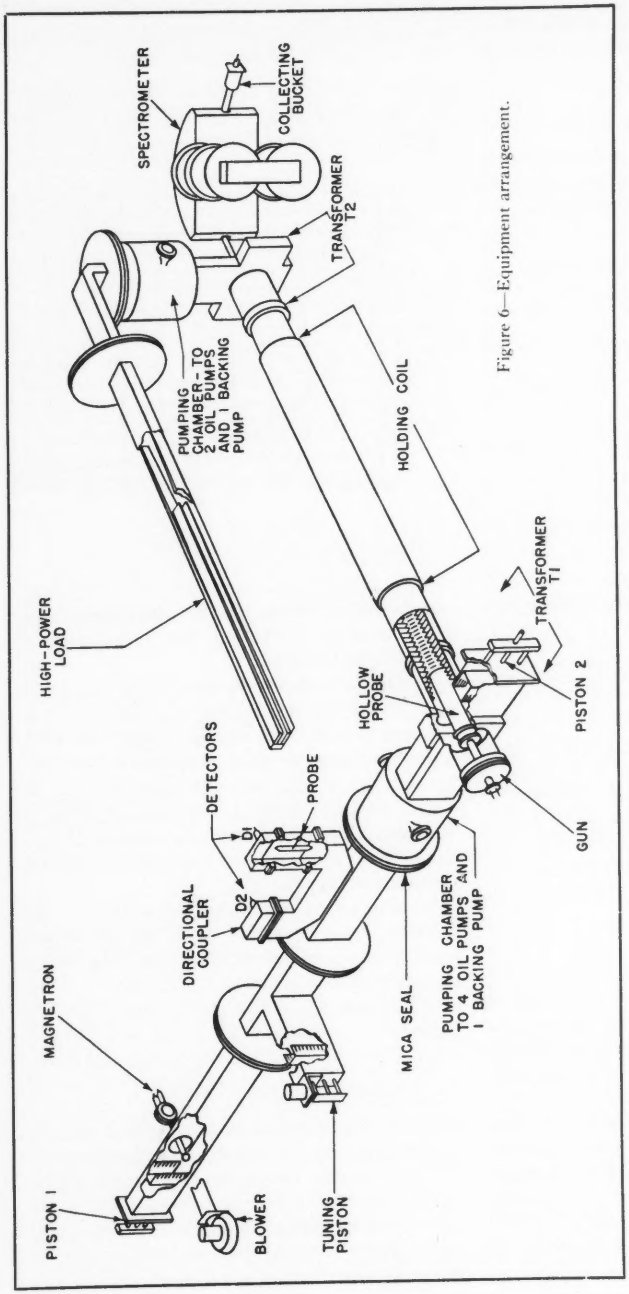

Figure 6—Equipment arrangement.

watts at this wavelength were being developed in Great Britain.

Figures 5 and 6 show the arrangement used. The magnetron *CV76* feeds a waveguide having internal dimensions of $3\frac{1}{2}$ by $1\frac{1}{2}$ inches via a probe. Piston 1 and the tuning piston together allow a reasonable range of frequency pulling of the magnetron with stable action and full output power. The microwave power, which is variable up to a maximum peak of 650 kilowatts, occurs in 2-microsecond pulses at a repetition rate of 500 cycles per second. This power is fed into the iris-loaded E_0 waveguide via a special transformer *T1*, in which there is a hollow earthed probe. The microwave power passes along the E_0 waveguide, and finally via a transformer *T2* into a high-power load.

An electron gun is situated inside the hollow probe and produces a beam of electrons at a voltage between 45 and 55 kilovolts: the driving voltage for the gun is bled from the modulator supplying the magnetron pulse.

The accelerated electrons strike a target *XT*, which is insulated from earth for measurement, or they pass into the spectrometer tube and, after deflection, are collected and measured in the collecting bucket *B*.

There are pumping chambers at the input and output of the E_0 guide: the first has four Metrovac *03* oil pumps and a backing pump, and the latter near the load has two oil pumps and a backing pump.

There is a holding coil over the waveguide to reduce dispersion of the electron beam as much as possible.

2.1 Design and Construction of the Guide

If we consider an electron velocity nearly equal to that of light, the relevant equations connecting the dimensions, wavelength, and phase velocity are

$$b \doteqdot \frac{\lambda}{2\pi}\left[2{\cdot}405 - 0{\cdot}982\,\frac{2J_1(ka) - kaJ_0(ka)}{2Y_1(ka) - kaY_0(ka)}\right], \quad (1)$$

$$\delta b \doteqdot \frac{1{\cdot}964a^2}{\lambda}\,\frac{\delta\alpha}{[2Y_1(ka) - kaY_0(ka)]^2}, \quad (2)$$

$$E_z = \frac{7\lambda}{a^2}P^{\frac{1}{2}}, \quad (3)$$

where

λ = free-space wavelength
$k = 2\pi/\lambda$
α = light velocity/phase velocity
a = iris radius
b = tube radius
E_z = axial field strength in volts per centimetre
P = input power in watts.

If we choose a stress of 1 megavolt per metre for a power of 0·5 megawatt and a wavelength of 10 centimetres, we find that $a = 2{\cdot}23$ centimetres: then the first equation gives $b = 4{\cdot}14$ centimetres, i.e., a diameter of 3·26 inches and $\delta b = 0{\cdot}0028$ inch for $\delta\alpha = 0{\cdot}01$. In practice, a slightly larger diameter of $3{\cdot}32 \pm 0{\cdot}0005$ inches was chosen: the much tighter tolerance was adopted for use in the initial accelerating section where the iris diameters are much smaller.

2.2 Accelerating Section

It is convenient to inject the electrons into the guide at 50 kilovolts: it is then necessary to design a guide in which the velocity varies along the axis in a way suitable to accelerate electrons starting with a velocity of 0·415 times that of light.

The inner diameter of the guide was kept fixed at 3·32 inches and the iris diameters were varied from 1·170 to 1·614 inches over a distance of 97·5 centimetres: at the end of this distance the velocity of the electron should be 0·953 times the velocity of light, corresponding to 1·17 electron megavolts. The tolerance is

$$\delta b = \frac{1{\cdot}96\lambda}{4\pi^2}\,\frac{\alpha\delta\alpha}{[Y_0(ka) - 2Y_1(ka)/ka]^2}. \quad (4)$$

For $a = 1{\cdot}17$ inches, $ka = 0{\cdot}93$, the denominator is found from Figure 7 as 3·4; to keep the phase error per metre constant, we take $\alpha\delta\alpha = 0{\cdot}01$,

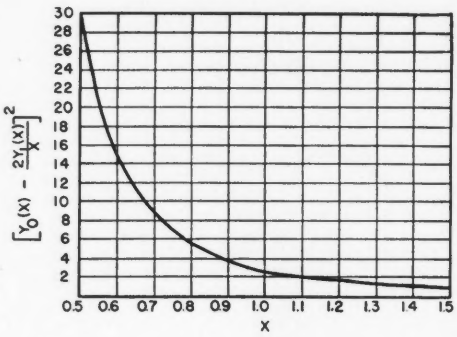

Figure 7—Plot of $\left[Y_0(X) - \frac{2Y_1(X)}{X}\right]^2$ against X.

and then $\delta b = 0{\cdot}0006$ inch and thus the tolerance in the diameter is 0·0012 inch. A tolerance of $\pm 0{\cdot}0005$ inch was taken.

In practice, the irises are 0·344 inch apart, with 0·002-inch tolerances. The guide is constructed of rings and annular plates, the whole assembly being soldered together: it has been found that a vacuum-tight assembly can be made, and no special vacuum envelope is necessary. This arrangement is convenient as it has a small diameter and the holding coils are therefore not bulky.

Measurements were made on a section with velocity equal to that of light, and the experimental results agreed with the theory to within the experimental errors of 1 per cent.

Measurements of attenuation have not been made.

2.2 Microwave Input Circuits

The directional coupler in Figure 6 and the crystal detectors *D1* and *D2* measure the power incident to the input transformer of the E_0 guide and the reflected power, respectively; they therefore give simultaneous readings of the peak power entering the accelerator and the standing-wave ratio of the system.

A probe in the transmitter box picks up a small radio-frequency power, which is supplied to a spectrum analyser that indicates the precise frequency relative to that of a continuous-wave oscillator. This arrangement serves to monitor the spectrum of the output of the magnetron. The magnetron output probe is in air, and the vacuum seal is a mica plate placed after the directional coupler. The rest of the system, up to and including the load, is vacuum tight.

The E_0–H_1 transformer is a modification of normal practice: the irises are tapered over a length of 3 inches, and the cylindrical probe of the gun (which is at earth potential) protrudes into the tapered irises. By suitable adjustment, a voltage standing-wave ratio of 0·8 can be achieved over a 6-megacycle band: at a spot frequency, a value greater than 0·95 can be achieved.

2.3 Output Circuit and Load

The output transformer *T2* is like the input transformer *T1*: the only difference is that the probe insertion is very small.

The load is an American design made to drawings kindly supplied by Telecommunication Research Establishment.

A later development[12] is a method due to Shersby-Harvie and Mullet in which the radio-frequency power at the output of the accelerator guide is fed back to the input.

2.4 Modulator and Transmitter

The modulator and transmitter is the Naval Type *277* slightly modified: the output was increased, by adjustment of the input variac, to give 50 kilovolts to the magnetron, which then gave an output up to 650 kilowatts peak power.

2.5 Gun

Figure 8 shows the gun and the trifilar winding used as a choke feed for the heater current and the control electrode. In early experiments, the cathode was oxide coated and had a moderate life. It was capable of sending a beam of 400 milliamperes peak through the guide in the absence of a radio-frequency field.

2.6 Pumping

The guide was exhausted via non-radiating slots by six Metrovac diffusion pumps, type *03*.

The pumps each remove 20 litres per second at a pressure of 10^{-4} to 10^{-5} millimetre. When the radio-frequency power is first switched on, gas is produced and acceleration stops for 30 seconds or more depending on whether or not the system has been let down to air recently: acceleration restarts when the pressure drops to 1 to 3×10^{-4} millimetre.

Starting from atmospheric pressure, the backing pumps alone reduce the pressure to that for the oil diffusion pumps to operate in 10 minutes: the pressure drops to 10^{-5} millimetre in one hour, and to 10^{-6} in several hours.

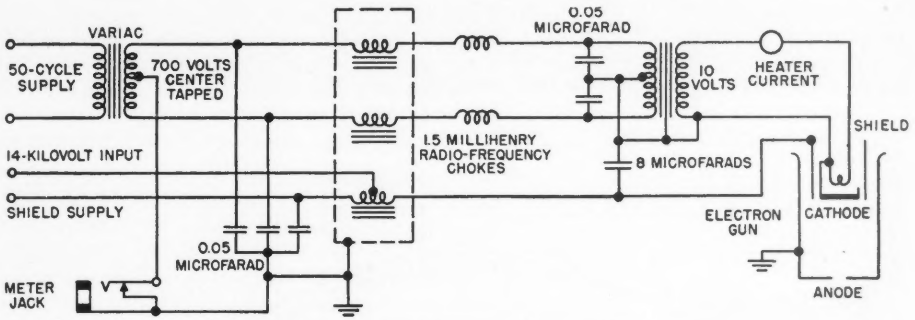

Figure 8—Electron gun and power supply circuit.

2.7 Holding Coils

Provision is made for a holding field of 120 gauss.

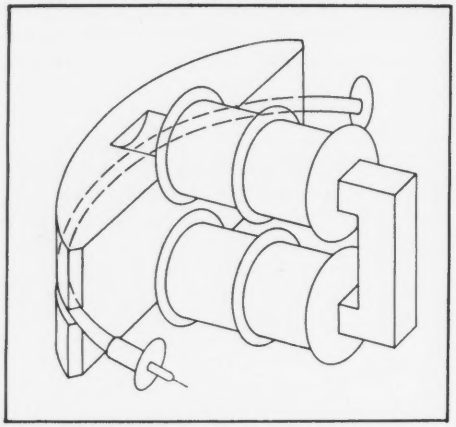

Figure 9—Magnetic spectrometer. The electron path is subjected to the magnetic field over a 90-degree arc.

2.8 Measuring Apparatus

A General Electric Company geiger counter type *GM2*, mounted in a lead housing about $1\frac{1}{2}$ inches thick, was used to measure the X-ray intensity: rough estimates of voltage were obtained by lead plates 0·5, 1, and 1·5 centimetres thick over the aperture. The output was fed to a 4-decade counter and, under the conditions of use, 1 microroentgen per second gives 280 counts per minute.

For the purposes of preliminary tuning, a 5-litre aluminium cylinder was used as an ionisation chamber, and the voltage was measured by a triode electrometer.

Figure 9 shows a magnetic spectrometer for measuring the velocity of the electrons: it is capable of measuring velocities up to that corresponding to 20 electron megavolts.

Figure 10 shows the spectrometer tube and electron gun. The main layout is shown in Figure 11.

3. Experimental Results

Figure 12 shows the output (peak) current in the spectrometer as a function of electron voltage for a radio-frequency input of 0·6 megawatt; the electron voltage is not certain to within 20 per cent as the magnetic spectrometer was not designed for this low range. It was estimated that the output is effectively 1·2 electron megavolts based on the methods of measuring the hardness of normal X-ray tubes.

The output current at the end of the spectrometer tube was 0·25 microampere mean (i.e., 250-microamperes peak), and it is not known precisely what current this corresponds to at the end of the accelerator tube: it is estimated that the mean current is 6 microamperes on the basis of the X-ray output, which was 0·5 roentgen

Figure 10—Spectrometer tube and electron gun.

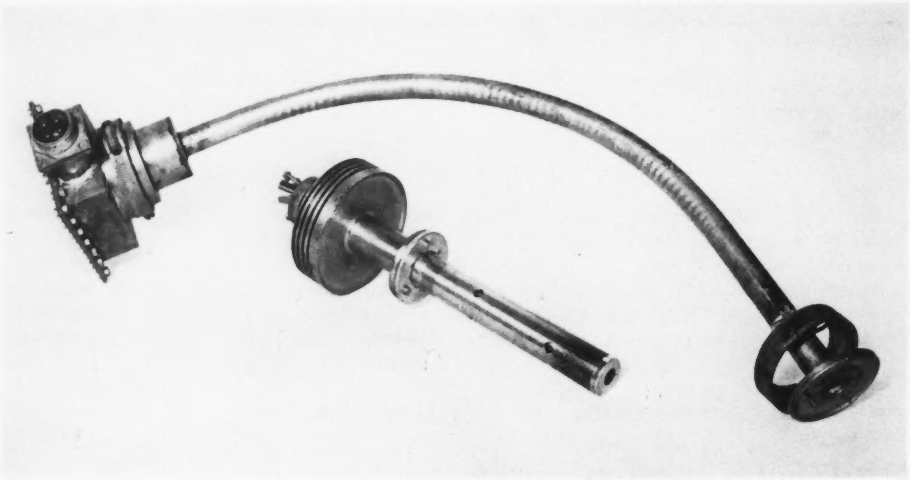

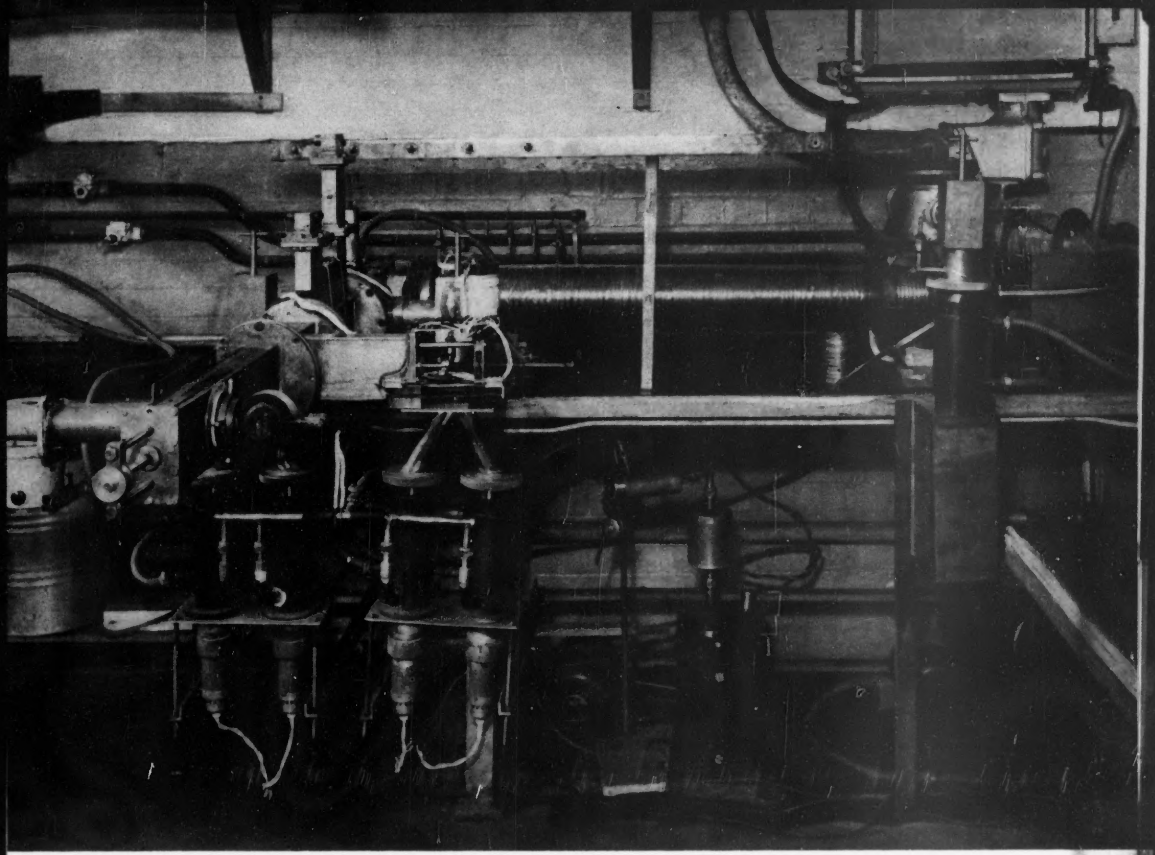

Figure 11—The main layout of the accelerator.

per minute at 1 metre. In this experiment, a beam current of 60 milliamperes was used, whereas a maximum of 400 milliamperes was available.

With this output of 0·5 roentgen per minute at 1 metre, i.e., 3 roentgens per minute at 40 centimetres, a 10-millimetre copper filter reduced the output to 1·8 roentgens per minute and the half-value thickness of copper was 12 millimetres. We are informed that the million-volt tube at St. Bartholomew's Hospital, having a permanent filter of 4·2 millimetres of steel and 2 millimetres of lead, has a half-value copper thickness of 9·3 millimetres. Part or all of this difference is due to the fact that the hospital target is a reflection target, and the present is a transmission type.

It is interesting to compare the results of the accelerator with that described briefly in reference 3 of the bibliography. The Telecommunication Research Establishment early accelerator used 1 megawatt and 0·5 metre of waveguide, and gave a peak of 0·54 electron megavolt, and more than 70 per cent of the gun current (emerging into the guide) is accelerated.

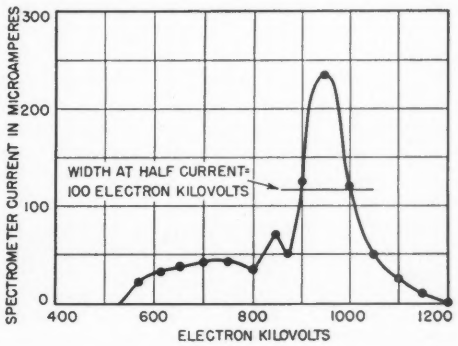

Figure 12—In the graph above, peak output current in the spectrometer is plotted against electron voltage for a radio-frequency input of 0·6 megawatt.

The present accelerator using 0·6 megawatt, 1 metre of guide, gives a peak voltage of about 1·0 electron megavolt with a collection efficiency of about 10 per cent. This difference in collection efficiency is due to the fact that the present design was for collection over a small phase angle near the peak, at 0·5-megawatt input, so as to produce a maximum acceleration in the length. It is felt that adequate current at high voltages is obtainable with the lower collection efficiency, but it may be worth while to increase the figure from 10 to 30 per cent by redesign.

4. Possible Future Developments

With the use of a 2-megawatt magnetron, it appears from Table 1 that an acceleration of about 3 megavolts per metre is attainable with the mechanical standards already achieved.

To produce an accelerator of 10 electron megavolts and 300 roentgens per minute at 1 metre (unfiltered), it is possible to design for a guide length of 3 metres or so. If we assume an attenuation twice the theoretical value, viz., 1 decibel per metre, and an accelerator 3 metres long, the decrease in output voltage due to the loss is 15 per cent. This diminution can be allowed for in the design by choosing slightly smaller iris diameters.

The beam current required is given roughly by

$$\text{roentgens per minute at 1 metre} = 2 \cdot 1 \cdot 10^{-6}\ (\text{kilovolts})^{2 \cdot 6}$$

by Kaye and Binks in the *British Journal of Radiology* for 1940. It is valid between 0·5 and 2 electron megavolts. There appears to be some evidence that the exponent 2·6 is somewhat high for voltages above 5 electron megavolts, but pending accurate information no great error is anticipated by using this value. Taking values of 300 roentgens per minute at 1 metre and 10^4 kilovolts, we find that a beam current of 5·6 microamperes is needed. It appears that the current obtained in the present model need not be increased much, if at all, for the desired output.

5. Acknowledgments

The authors express their deepest gratitude to Mr. Innes of St. Bartholomew's Hospital for his co-operation and encouragement, and for X-ray measurements; and to Mr. D. W. Fry of Telecommunication Research Establishment, Great Malvern, for kindly giving them drawings of the high-power load.

They acknowledge the great help given by their colleagues Mr. E. Pethick, in the monitoring and measuring circuits, and Mr. P. A. Shatford in the vacuum work.

6. Bibliography

1. W. D. Allen and J. L. Symonds, "Experiments in Multiple-Gap Linear Acceleration of Electrons," *Proceedings of the Physical Society*, v. 59, pp. 622–629; July, 1947.
2. L. J. Chu and W. W. Hansen, "Theory of Disc-Loaded Waveguides," *Journal of Applied Physics*, v. 18, pp. 996–1008; November, 1947.
3. D. W. Fry, R. B. R. Shersby-Harvie, L. B. Mullett, and W. Walkinshaw, "Travelling-Wave Linear Accelerator for Electrons," *Nature*, v. 160, pp. 351–353; September 13, 1947.
4. E. L. Ginzton, W. W. Hansen, and W. R. Kennedy, "Linear Electron Accelerators," *Review of Scientific Instruments*, v. 19, pp. 89–108; February, 1948.
5. J. Halpern, E. Everhart, R. A. Rapuano, and J. C. Slater, "Preliminary Studies on the Design of a Microwave Linear Accelerator," *Physical Review*, v. 69, p. 688; June, 1946.
6. J. C. Slater, "Design of Linear Accelerators," *Reviews of Modern Physics*, v. 20, pp. 473–518; July, 1948.
7. W. Walkinshaw, "Theoretical Design of Linear Accelerator for Electrons," *Proceedings of the Physical Society*, v. 61, pp. 246-254; September, 1948.
8. R. B. R. Shersby-Harvie, "A Proposed New Form of Dielectric-Loaded Wave-Guide for Linear Electron Accelerators," *Nature*, v. 162, p. 890; December 4, 1948.
9. J. D. Cockcroft, "The Development of Linear Accelerators and Synchrotrons for Radiotherapy and for Research in Physics," *Proceedings of the Institution of Electrical Engineers*, Part I, v. 96, pp. 296–303; November, 1949.
10. G. R. Newbery, "The Microwave Linear Electron Accelerator," *British Journal of Radiology*, v. 22, pp. 473–486; August, 1949.
11. D. W. Fry, R. B. R. Shersby-Harvie, L. B. Mullett, and W. Walkinshaw, "Travelling-Wave Linear Accelerator for 4-MeV Electrons," *Nature*, v. 162, pp. 859–861; November 27, 1948.
12. R. B. R. Shersby-Harvie and L. B. Mullett, "A Travelling Wave Linear Accelerator with R.F. Power Feedback, and an Observation of R.F. Absorption by Gas in Presence of a Magnetic Field," *Proceedings of the Physical Society, B*, v. 62, pp. 270–271; April, 1949.

Crystal Triodes*

By T. R. SCOTT

Standard Telecommunication Laboratories, Limited; London, England

THE PAPER reviews first the various forms of crystal triode so far developed and comments on their characteristics. A brief résumé is then given of the various materials proposed and of the types of control that have been applied to modify the characteristics of triodes made therefrom. A discussion of testing procedure follows.

In view of the scarcity of information to date on applications and circuit design a section on this aspect is included.

• • •

List of Principal Symbols

I_c = collector bias current in milliamperes
I_e = emitter bias current in milliamperes
i_c = instantaneous collector current in milliamperes
i_e = instantaneous emitter current in milliamperes
V_c = collector bias voltage in volts
V_e = emitter bias voltage in volts
v_c = instantaneous collector voltage in volts
v_e = instantaneous emitter voltage in volts
R_L = collector load resistance in ohms
α = current gain.

1. Introduction

The crystal triode or transistor was formally introduced to the technical public by the Bell Telephone Laboratories on 30th June, 1948. Private demonstrations were made in this country from July, 1948, onwards, and at the 33rd Physical Society Exhibition in April, 1949, two exhibitors displayed the device. Since June, 1948, much has been written about this component, and there have been many discussions in many places. So far, however, no formal technical paper has appeared in this country on the subject. Even at this date it is perhaps too early to present a reasoned appreciation of the place of this component in the electrical field. In the few months of its public life, opinion has swayed to and fro on the controversial subject of its relationship to the thermionic valve. Will the valve become obsolete in face of this strong competition? Or will the crystal triode remain a scientific curiosity while the valve continues to perform as an industrial component?

A somewhat lengthy commercial appreciation of the component has recently appeared in the United States.[1] In the author's opinion, however, it is now clear that the crystal triode and its derivatives will have definite applications and that probably the correct view in the controversy mentioned above is that the crystal triode is an excellent auxiliary to the thermionic valve, performing functions that the valve might achieve with difficulty, or uneconomically, but not competing with the valve in applications that the valve fulfils easily and economically. Further, there are distinct signs that combinations of valve and crystal triode will appear, so that it will in some cases be difficult to make distinctions. The object of the paper is to expose sufficient evidence regarding the performance of components of this type to justify the above view.

One remark must be made here regarding nomenclature. In deference to British practice the component is herein called the crystal triode in preference to the American name transistor. It is already obvious that "triode" will not meet the situation. In this paper electrode arrangements will be described that are not triodes. Other multi-electrode types are known to be under development. It is too early to say whether the name "transistor" is sufficiently broad in meaning to meet the eventual scope of this class of components. Arguments on nomenclature are not included in the paper.

* Reprinted from *Proceedings of the Institution of Electrical Engineers*, Part III, v. 98, pp. 169–177; May, 1951. Presented before the Radio Section of the Institution of Electrical Engineers in London on 6 December, 1950.

This is an "integrating" paper. Members are invited to submit papers in this category, giving the full perspective of the developments leading to the present practice in a particular part of one of the branches of electrical science.

[1] Numbered references appear in Section 7 on p. 208.

Further, no attempt is made in the paper to deal with the underlying physical theory, although much of the technical literature issued to date has done so. A complete treatise on the physics of the component is known to be in

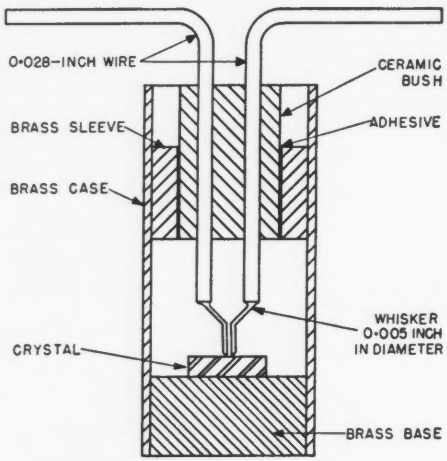

Figure 1—Cross-section of type-*A* crystal triode.

preparation.[2] In the author's opinion the immediate development programme in this field should be devoted to chemical and engineering investigations into the phenomena exposed by direct experimental work. Thereafter, when sufficient experimental data are amassed, the physicist may be able to offer a complete theoretical explanation of the phenomena.

Since some of the physical concepts involved may be novel to engineers, attention is drawn to the excellent editorial note[2] in the *Bell System Technical Journal* for July, 1949, which deals simply but adequately with these concepts. It, perhaps for obvious reasons, deals insufficiently with the all-important *p-n* junction which is covered by Shockley[3] in one of the five papers introduced by the above editorial note.

Intensive work during the war on diodes, i.e. point-contact rectifiers (see, for example, Torrey and Whitmer[4]), utilizing silicon or germanium, undoubtedly stimulated post-war interest in these semi-conducting metals and led to work that finally brought about the development of the crystal triode. There are, however, quite marked distinctions between the present form of triode and the diode and the former is not readily derived from the latter. The more the crystal triode is developed into a useful component, the greater appears to be the difference in form and in processing.

In a brief review such as is given in the paper it is also impossible to deal adequately with the metallurgy and physics relating to germanium. Much has been published elsewhere on this subject. Reference might be made to a descriptive paper by Dunlap.[5]

While, as has been mentioned above, there has been a very large number of papers and lectures devoted to this component in the course of its short life, not all of them have been published in full. The references in the bibliography have been made as wide as possible but are obviously not comprehensive.

2. *Electrode Arrangements and Characteristics*

2.1 Original Form

The crystal triode as first demonstrated to the public on 30th June, 1948, and as first formally described by Bardeen and Brattain[6] in the July of that year is illustrated in Figures 1 and 2. It comprised in effect a high back-voltage rectifier (diode) utilizing *n*-type (or excess semi-conductor) germanium as the crystal but having an additional point-contact electrode (cat's whisker) inserted in the assembly very close to the normal point electrode. The circuit was as shown in Figure 2, the two point-contacts being called the emitter and the collector respectively and being biased in the original models with direct-current potentials of + 0·5 to 1·0 volt and −70 volts respectively.

The emitter impedance is comparatively low, of the order of 300 ohms while the collector impedance is high, of the order of 10 000 and 50 000 ohms. If the emitter current is varied by a signal voltage, there will be a corresponding variation in collector current.

In the 1949 Kelvin Lecture, Professor Mott[7] has explained the physical concept of "positive holes" in the theory of conduction in a non-metal. References[2, 3] have been given above to other technical articles on this subject. Bardeen and Brattain[8] have also given their theory in considerable detail. It is, therefore, only necessary

here to state that Bardeen and Brattain claimed that the flow of holes from the emitter into the collector altered the normal current flow from the base to the collector in such a way that the change in collector current may be larger than the change in emitter current. The collector while operated in the reverse direction, being a rectifier, has a high impedance and may be matched to a high-impedance load.

A large ratio of output to input voltage of the same order as the ratio of the reverse to the forward impedance of the point is obtained. There is a corresponding power amplification of the input signal.

This type of crystal triode was comparatively easy to assemble in the laboratory. Practically any germanium crystal suitable for a high-back-voltage diode could be used, and with some care and ingenuity the application of the two point-contact electrodes close together (Bardeen and Brattain specified 0·005 to 0·025-centimetre spacing) could be achieved.

Using a 20-kilohm load at 5 kilocycles per second, insertion gains of the order of 25 to 35 decibels could be obtained. Since there is normally about 10-decibel mismatch in the circuit, the actual power gains were of the order of 15 to 25.

Bardeen and Brattain claimed that crystal triodes could be operated as amplifiers up to 10 megacycles per second. Very few crystals, however, gave such performance. Figure 3 illustrates a typical frequency characteristic.

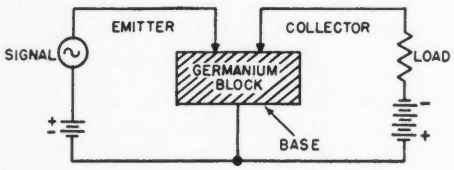

Figure 2—Schematic of type-*A* crystal-triode circuit.

More recently the Bell Telephone Laboratories have modified their claims and quoted 4 megacycles per second as the effective top value of *n*-type germanium. This is, however, not the effective top value of all germanium crystals under all conditions and this point will be discussed in greater detail below.

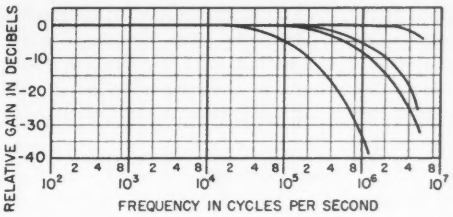

Figure 3*—Frequency characteristics of a group of type-*A* crystal triodes.

Typical characteristics of six *n*-type germanium crystal triodes of this original type are given in Table 1.

TABLE 1

Emitter Current I_e in Milliamperes	Collector Current I_c in Milliamperes	Collector Load Resistance R_L in Ohms	Collector Voltage v_c in Volts	Insertion Gain in Decibels
1·07	3·0	20 000	8·3	29·1
1·38	2·5	20 000	7·6	28·3
0·58	2·5	20 000	8·2	29·0
0·37	1·5	20 000	4·8	24·4
0·80	0·40	20 000	3·5	21·4
0·85	2·3	20 000	3·2	20·6

Tests were taken at 5 kilocycles per second; owing to impedance mismatch in operating the triode between a 520-ohm generator and a 20 000-ohm load, the gain includes about 10 decibels from this cause.

While this original crystal triode was of profound interest it had many obvious defects. It did not provide, at least regularly and uniformly, any appreciable current amplification; it was noisy; its frequency range was restricted; its power output (of the order of 25 milliwatts) was small. Work, therefore, was put in hand in many laboratories in order to overcome these defects.

2.2 Double-Surface Crystals

One defect not mentioned above is that of applying two point-contact electrodes close together as a commercial manufacturing process. Some ingenuity has been displayed in overcoming this manufacturing difficulty and one solution has already been announced by Little[9] of the Bell Telephone Laboratories. As will be

* This graph is substituted for the original Figure 3, which was erroneously retained in the original publication although the text concerning it had been deleted from the paper.

seen later, there is some hope that eventually point-contact electrodes will be unnecessary. However, it was natural that development would trend right away to the simplification of this problem. One such development has been that of

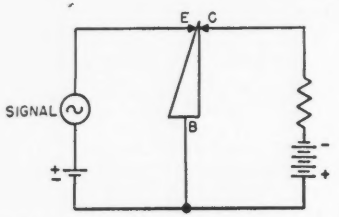

Figure 4—Diagrammatic representation of wedge-type crystal-triode.

the double-surface crystal. In October, 1948, Mr. Kinman demonstrated in this country a type shown diagrammatically in Figure 4 in which the emitter and collector face each other at the apex of a ground wedge. Bell Telephone Laboratories refer to a corresponding development by Shive.[10] He utilized *n*-type germanium, specified a maximum thickness of germanium between emitter and collector of 0·01 centimetre employing a collector bias of −50 to −100 volts and quoted *inter alia* a current amplification of 1·5. However, their main effort has obviously been concentrated on the so-called coaxial type described by Kock and Wallace[11] and illustrated in Figure 5.

The laboratories with which the author is associated have, in view of developments mentioned in Section 2.3 below, produced a similar type with spacing (crystal thickness) up to 0·075 centimetre, collector bias of under 30 volts and current amplification in excess of 2. The increased spacing obviously simplifies manufacture.

2.3 Other Electrode (Point-Contact) Arrangements

Another natural line of research was the effect of using more than two point-contact electrodes. However, little has been published on this subject. At an Institute of Radio Engineers symposium held at Princeton, New Jersey, on 21st June, 1949, Haegele[12] read a paper on crystal triodes. This dealt with a multi-electrode crystal used as a mixer at frequencies of the order of 100–150 megacycles per second. The electrode arrangement comprised point contacts in a triangle spaced about 0·002 inch. In the laboratories with which the author is associated, considerable work has been carried out by White and others on the effect of additional electrodes. Some of this work can be mentioned here.

White[13] and his colleagues have tried out a variety of arrangements of electrodes with some interesting results. It is quite clear, however, that all these results are profoundly affected by

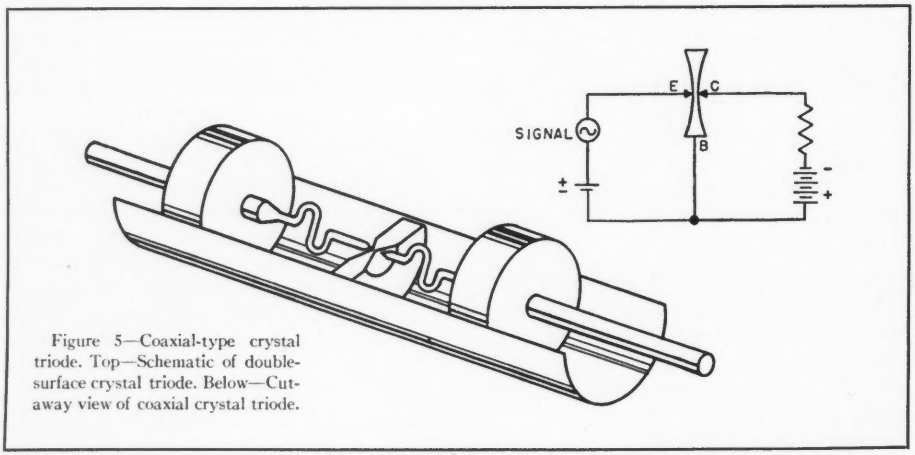

Figure 5—Coaxial-type crystal triode. Top—Schematic of double-surface crystal triode. Below—Cut-away view of coaxial crystal triode.

the materials employed, both of the electrodes and the semi-conductor. A great number of experiments providing statistical data is, therefore, necessary to establish the merits or demerits before any of these unusual electrode systems can be fully evaluated. It is, however, worth while to record some of the interesting phenomena recorded so far, namely:

A. Good characteristics can be obtained by using three point-contact electrodes, two close-spaced and the third spaced at least 0·025 centimetre away. Of the two close-spaced electrodes, one is invariably the collector, the other in certain cases can be utilized as the base, leaving the emitter comparatively widely spaced. Although the area contact normally used as the base is not included in the circuit, it is apparently necessary to have it in physical existence if the electrodes are to be formed.

B. Duplication of emitters *per se* appears to have little effect, but if one of the emitters is worked normally and the other is made still more positive in bias the current gain obtained is increased by a factor of 2 or 3.

C. Duplication of collectors gives some increased gain, e.g., two collectors may give $\sqrt{2}$ times the gain from one.

D. If a gold wire is used as the emitter and an electro-forming process is employed, the optimum spacing from the collector appears to be of the order of 0·07 centimetre. (This is the basis of one of the double-surface types referred to in Section 2.2 above.)

In general, neglecting possible manufacturing difficulties, there seems to be a case for increasing the number of point-contact electrodes in order to increase gain. It must again be stressed, however, that all these results are greatly dependent upon the materials employed and the electro-forming process applied. Reference is made below (Section 3.2) to the electro-forming process and its effect on the characteristics of the crystal triode. It may be noted that in the laboratories in question the best results obtained from silicon so far have been by using the electrode arrangement mentioned in *A* above. Statistical work on electrode arrangements may in the end prove to be a powerful weapon in elucidating the theory of crystal triodes and in assessing the suitability of various materials. As stated earlier, some of these arrangements raise the question of the suitability of the term "triode."

2.4 Crystal Triodes without Point Contacts

At the Princeton symposium of the Institute at Radio Engineers referred to in Section 2.3, Pearson[14] in the course of describing work on single-crystal filament-type triodes mentioned one type in which the emitter was an *n-p* junction rather than a point contact (Figure 6). The collector and base are metal sprayed. While such types may at present be purely experimental,

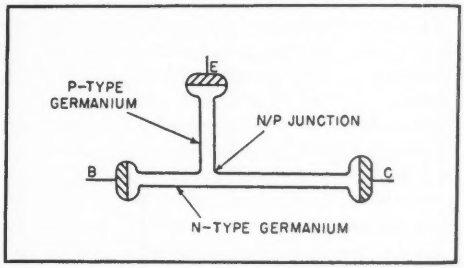

Figure 6—Filamentary transistor (Pearson) with *n-p* barrier.

they at least reveal possibilities of considerable changes in design and structure in the future. They are, of course, of fundamental interest in experiments tending to reveal the semi-conductor mechanism involved in triode action.

2.5 Photo-Transistor

It would be wrong to close this section of the paper without reference to the Bell Telephone Laboratories' development of a new photo-conductivity cell which was disclosed by Shive.[15] Its importance lies in the fact that it introduces possibilities of additional controls and effects by means of photo-electric effects.

3. Materials and Control

3.1 Different Types of Semi-Conductor

At the time of the first announcement of the discovery of the crystal-triode action, it was stated that feeble effects were obtainable from silicon. In Section 2.3 it was pointed out that stronger effects can be obtained from silicon by the three-point-contact electrode arrangement. Silicon is also referred to by Bardeen, Brattain, and Gibney.[16] No other direct mention of materials other than germanium has been published. It is believed, however, that slight amplification

has been observed from some of the oxides, e.g., cuprous oxide. There are, however, two significant facts that suggest that other semi-conductors will be found to produce analogous characteristics.

In 1925 Lilienfeld[17] patented a series of semiconductor devices for controlling the flow of an electric current between two terminals of an electrically conducting solid system by establishing a difference of potential between certain elements of the system. He claimed it was particularly adaptable to the amplification of oscillating currents. The arrangements proposed are somewhat difficult to construct with the accuracy necessary to produce reasonable amplification, although it is understood that laboratory models have manifested some degree of amplification. It would appear, however, that given the right electrode conditions some sulphides and oxides could be employed as semi-conductor material for crystal amplifiers. It is noteworthy, also, that about this time Ohl[18] took out a patent on multi-electrode (point-contact) devices for amplification and the like by crystals, the currents being magnetically controlled. Obviously over 20 years ago engineers were groping for the clues necessary to originate crystal-triode development.

In 1949 in the laboratories with which the author is associated Beck[19] *et al.* observed phenomena in connection with oxide-coated cathodes that led them to investigate crystal-triode action in oxides at high temperature. In the arrangement originally set up the cathode (indirectly heated) formed the base, an emitter point-contact was provided and for a collector a wire loop was used. With the oxide and collector at 1000 degrees Kelvin results similar to those obtained at ordinary temperatures from germanium crystal triodes in respect of amplification and oscillation were obtained. Work on this interesting phenomenon continues.

We, therefore, see that apart from germanium there are possibilities that silicon, some sulphides and some oxides may be employed. In the author's opinion the field is likely to become much broader even than this as development and research proceed.

For the present, however, interest centres round germanium and there is no doubt but that a great variety of interesting devices can be built up from this material.

At first it was thought that only *n*-type germanium could produce such effects. Later it was shown that *p*-type material could also be used. In point of fact *n*-type and *p*-type material are intermixed in both cases and the only real criterion is the polarity of the biasing potential applied to the collector; for *n*-type germanium it is negative, for *p*-type it is positive.

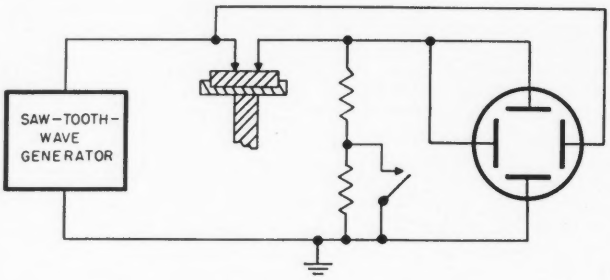

Figure 7—Electro-forming circuit.

However, there are apparently somewhat different characteristics from the two types. In the author's experience it is possible from *p*-type material to obtain an appreciable reduction in noise. According to Pfann,[20] the *p*-type gives an increased frequency range up to 15 megacycles per second. According to Ryder,[21] the *p*-type effective limit is 11 megacycles per second, as distinct from a probable top limit of 4 megacycles per second for *n*-type. There are, of course, other factors that affect both the noise and the frequency range. Brown[22] has shown that he could extend the frequency range to 30 megacycles per second by applying a magnetic field.

In the laboratories with which the author is associated, frequencies between 30 and 40 megacycles per second have been achieved, both with and without the use of magnetic fields. It is reported elsewhere that proposals have also been made for control of the characteristics by electrostatic fields. Incidentally, it is apparent that the top limit of frequency for crystal-triode

action has moved up from 10 megacycles per second originally quoted to something of the order of 50 megacycles per second.

3.2 Electro-forming

Reference has been made in the literature quoted and also in the present paper to electro-forming. It is not clear that in all cases the same thing is meant by this term. It may, therefore, be useful to describe one particular form of electro-forming developed by Matthews and White.[23] The triode to be treated is included in a circuit of the type illustrated in Figure 7. A generator of saw-tooth waves having a low-impedance output circuit capable of supplying currents up to 100 milliamperes has one terminal connected to ground and the other connected to the emitter. The circuit is completed by two resistors connecting the collector electrode to ground and a switch is provided by means of which one of the resistors can be short circuited. The testing device comprises a cathode-ray tube of conventional type, only the deflecting plates of which are shown. The horizontal deflection of the cathode ray is proportional to the voltage applied between the emitter and collector, and the vertical deflection is proportional to the current that passes between the two electrodes. Keeping the emitter positive with

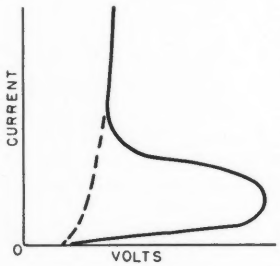

Figure 8—Electro-forming characteristics.

respect to the collector and having selected the resistances so that normally a small current flows in the forming circuit, it is found that in general the curve traced on the oscillograph screen is the full-line curve shown in Figure 8. This curve shows the current in the circuit as ordinates plotted against the voltage of the generator as abscissae for the forward or scanning strokes of the saw-tooth waves. A different return curve is traced during the flyback strokes but this is of no interest and is barely visible owing to the rapidity of return of the spot to zero. It will be seen that the full curve has a loop with a portion having a negative slope, indicating a negative resistance condition between the electrodes.

In order to form the crystal triode, the switch is momentarily closed, thus short-circuiting the resistor and greatly increasing the current in the circuit. When the switch is re-opened, it is usually found that the loop of the curve will have become reduced and in some cases will have completely disappeared. The curve on the screen is then as shown by the dotted line completed by the straight part of the initial curve. If the loop does not disappear completely the first time, by repeating the process two or three times the loop can be entirely removed. When the loop has been removed from the voltage/current characteristic, the crystal triode is in the condition in which it produces its maximum current gain.

Interesting results can be obtained by using different samples of germanium, different surface treatments, different metals for electrodes (emitter and collector), and different degrees of purity in the metals.

If the process of electro-forming is overdone, the loop with the negative slope may reappear in the voltage/current curve. By repeating the process the loop can be made to disappear again. We thus get the idea of various "electronic" states in the triode, the progress from state to state being produced by the forming current. In due course, when the full story of interrelation between materials and electro-forming is completed, there should be a better basis for the development of a physical theory of triode action.

3.3 Control Electric Fields

Bardeen, Brattain, and Gibney[16] have described arrangements in which control electrodes of metal or electrolyte are added to the normal array of electrodes (emitter, collector, base). These control electrodes are used to produce strong electric fields in the semi-conductor to modify the conductivity of the semi-conductor. It has unfortunately been impossible to study

this disclosure in sufficient detail to render it possible to include a full discussion thereof in the paper. There is little doubt, however, that devices of this nature may open up new possibilities in respect of materials employed.

3.4 Interim Conclusions

It is quite clear that at this stage with two varieties of germanium, with the possibilities from other semi-conductors, and with important work proceeding on the effect due to the nature of the electrodes and on the effect of electro-forming—without taking into account the possibilities of magnetic and electrostatic control—it is much too early to attempt to define the limitations of the crystal triode. Two at least of the initial alleged disabilities, namely noise and restricted frequency range, appear to be slowly but surely disappearing.

4. Testing

4.1 General

As mentioned in Section 2.1 above, the original testing of crystal triodes was on an insertion-gain basis. However, this soon proved to be inadequate. Lehovec[24] has proposed a simple test circuit using two pentodes (see Figure 9), that gives direct currents and voltages at any operating point, corresponding alternating-current values for zero and infinite collector load resistance, and current and voltage amplification values.

$$\left.\begin{aligned} v_e &= R_{11}i_e + R_{12}i_c \\ v_c &= R_{21}i_e + R_{22}i_c. \end{aligned}\right\} \quad (1)$$

For the calculation of the coefficients it is sufficient to measure v_e and i_e at zero collector load resistance and v_e and v_c at infinite collector load resistance. The important circuit qualities of crystal triodes can then be expressed, according to Lehovec, in terms of R_{11}, R_{12}, R_{21}, and R_{22} as shown in Table 2.

Lehovec also gives a convenient way to arrange the results of this type of test (see Table 3A). The first or left-hand group contains the direct currents and voltages that describe the operating point. The second group contains in the upper line the alternating currents and voltages at zero collector load resistance and in the lower line the

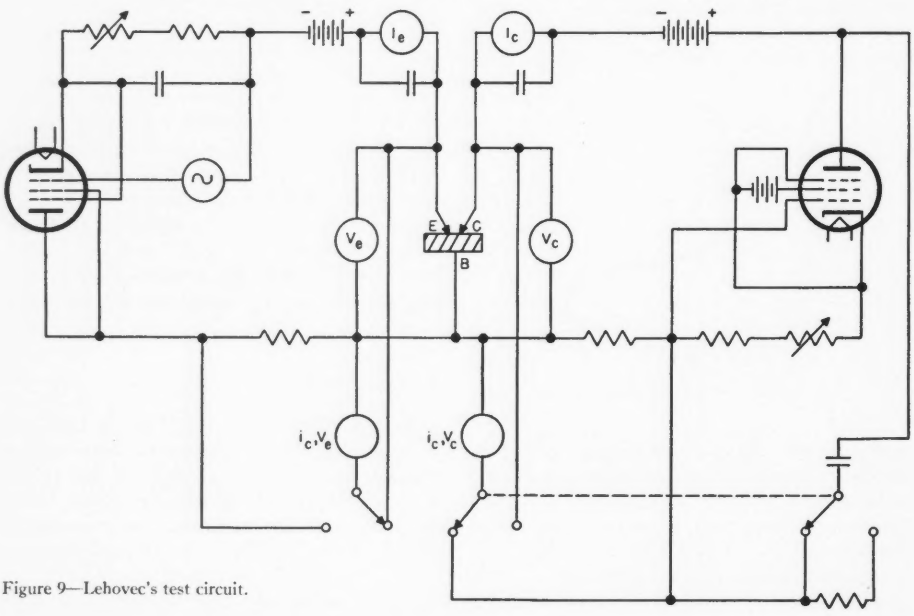

Figure 9—Lehovec's test circuit.

TABLE 2

IMPORTANT CIRCUIT QUALITIES OF CRYSTAL TRIODES

(1) Short-circuit stability	$\delta = \frac{R_{12}R_{21}}{R_{11}R_{22}} < 1$
(2) Input impedance (collector load resistance is R_L)	$R_{11} - \frac{R_{12}R_{21}}{R_{22}+R_L}$
(3) Output impedance (external resistance in emitter circuit is R_e)	$R_{22} - \frac{R_{12}R_{21}}{R_{11}+R_e}$
(4) Power amplification (output power/input power)	$\frac{R^2_{21}}{R_{11}R_{22}} \frac{R_L}{(R_L+R_{22})} \frac{1}{(1-\delta+R_L/R_{22})}$
(5) Maximum current amplification (zero load)	R_{21}/R_{22}
(6) Maximum voltage amplification (infinite load)	R_{21}/R_{11}
The following values refer specifically to $\delta<1$ and a load resistance matched for maximum available power amplification:	
(7) Load resistance matched for maximum power amplification	$R_{22}(1-\delta)^{\frac{1}{2}}$
(8) Input impedance at maximum power amplification	$R_{11}(1-\delta)^{\frac{1}{2}}$
(9) Maximum power amplification	$\frac{R^2_{21}}{R_{11}R_{22}} \frac{1}{\{1+(1-\delta)^{\frac{1}{2}}\}^2}$
(10) Insertion gain at maximum power amplification	$\frac{R^2_{21}}{4R^2_{11}} \frac{1}{\{1+(1-\delta)^{\frac{1}{2}}\}^2}$
(11) Insertion gain (at maximum power amplification)/maximum power amplification	$R_{22}/4R_{11}$
(12) Current amplification at maximum power gain	$\frac{R_{21}}{R_{22}} \frac{1}{1+(1-\delta)^{\frac{1}{2}}}$
(13) Voltage amplification at maximum power gain	$\frac{R_{21}}{R_{11}} \frac{1}{1+(1-\delta)^{\frac{1}{2}}}$

corresponding values for infinite collector load resistance. The third group gives the current amplification at zero collector load resistance and the voltage amplification at infinite collector load resistance. The fourth group contains the four coefficients, which are calculated from the direct-current components in the second group according to

$$\left.\begin{aligned} |R_{11}| &= (v_e/i_e)_\infty \\ |R_{12}| &= [(v_e)_\infty - (v_e)_0]/(i_c)_0 \\ |R_{21}| &= (v_c/i_c)_\infty \\ |R_{22}| &= (v_c)_\infty/(i_c)_0. \end{aligned}\right\} \quad (2)$$

The above equations follow immediately from (1) if first $(i_e)_\infty$ and then $(v_c)_0$ are set equal to zero. In Table 3B values for some crystal triodes are given.

For a quick test, one is often more interested in the maximum current amplification, and the maximum voltage amplification is obtained without further calculation from the alternating

TABLE 3A

ARRANGEMENT OF MEASURED VALUES

I_e I_c	i_e	$(v_e)_0$	$(i_c)_0$	0	$(i_c/i_e)_0$	$\lvert R_{11}\rvert$	$\lvert R_{12}\rvert$
V_e V_c	i_e	$(v_c)_\infty$	0	$(v_c)_\infty$	$(v_c/v_e)_\infty$	$\lvert R_{21}\rvert$	$\lvert R_{22}\rvert$

TABLE 3B

TEST VALUES FOR COMMERCIAL GERMANIUM CRYSTAL TRIODE

0·5 milliamperes	2·0 milliamperes	100 microamperes	18 millivolts	132 milliamperes	0	1·32	240 ohms	182 ohms
0·13 volts	22·5 volts	100 microamperes	42 millivolts	0	3·1 volts	74	31 000 ohms	23 500 ohms

collector current at zero collector load resistance.*

While a considerable amount of work is going on in connection with the development of more refined methods of testing, e.g., by bridge methods, there is no doubt that Lehovec's proposals

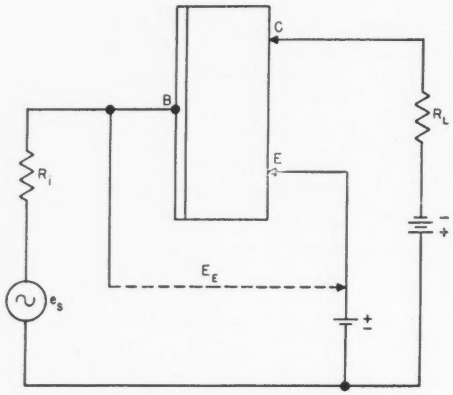

Figure 10—Base-input connection.

are sound for normal usage in the present state of the art. There are, however, two additional measurements that should be taken to make the tests realistic. First, it is necessary to be very sure that the alternating currents and voltages are not distorted but are pure sine waves if the intrinsic values of R are desired. For this purpose it is advisable to put an oscilloscope across the valve voltmeter in Figure 9 to ensure that overloading, etc., is not present. Secondly, it is convenient before applying the Lehovec tests to determine the V_c, V_e conditions at which maximum insertion gain is obtained. Tests on the Lehovec basis can then be confined to the values adjacent to the optimum V_c and V_e and need not be unnecessarily extensive.

4.2 Special Tests

Frequency runs, noise measurements, stability, and life testing all require standardization of methods and, in due course, of tolerances. For the moment it would be undesirable to be too expansive about such tests. Life tests seem to indicate longevity and a fair measure of stability at least after an initial settling-down period. Some crystal triodes are extremely stable, and doubtless as manufacturing techniques improve the percentage of these will increase. Temperature over the range -80 to $+70$ degrees centigrade appears to have little or no effect provided the triode is well made mechanically.

Since the noise voltages depend (cf. Montgomery[25]) on direct-current bias and possibly more particularly on the direct-current collector voltage in some cases it may be desirable to aim at low direct-current biases (there are other reasons for this—see Section 5) and to determine the characteristics at such voltages rather than to obtain maximum gain and use this as the criterion.

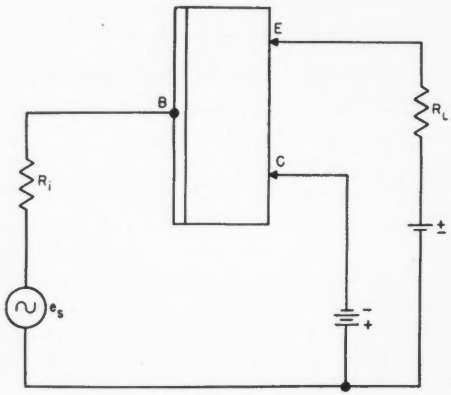

Figure 11—Emitter-output connection.

5. *Applications and Circuit Design*

5.1 Amplification

With the art changing so rapidly, it is difficult to foretell the range of applications in the future. The frequency range has already been increased. Maximum output is now officially stated at 600 milliwatts[28] in place of 25 milliwatts as originally quoted. It is believed that this value has been exceeded and a 1-watt output attained. It remains to be seen whether or not noise can be controlled when output and working frequency

* Bardeen and Brattain used this representation of transistors in a lecture given in October, 1948, in Princeton, New Jersey, for the local section of the American Institute of Electrical Engineers.

are raised towards the maximum. Nevertheless, it is already quite clear that audio-frequency and carrier-frequency amplifiers can be built to give 15 to 20 decibels gain and 25 milliwatts output. Such amplifiers compare in performance with those containing valves and have the advantage that they can, if properly made, be worked off 2 to 3 volts direct-current supply. There are many applications where this simplification of power supplies is of great interest, e.g., the telephone subscriber's set.

There is a difficulty in that the input impedance is so low and the output impedance is comparatively high in the conventional grounded-base circuit. This is opposite in sense to valve amplifiers and causes a revision of circuit details and components. For example, in an audio receiver in a hearing aid or a telephone subscriber's set a crystal receiver with high impedance fits in better to the triode circuit than a magnetic (low-impedance) receiver.

There appears to be some evidence, not clearly designated in publications, that the intrinsic input and output impedances of a triode can be varied somewhat; if so, this difficulty may be at least partially removed.

In a paper on the circuit design of triodes Webster, Eberhard, and Barton[26] have described some amplifier arrangements that differ from the initially described type, which they call the "emitter-input" arrangement. They describe and analyse the circuit design of the "base-input" and "emitter-output" types which are illustrated in Figures 10 and 11 respectively. Comparative experimental results of the three types given by these authors are quoted in Table 4. It would appear, however, that crystal triodes with specially selected characteristics are required to produce some of the results quoted. Some of the characteristics may be only interesting as examples of the versatility of the triode. For example the number of practical applications for the unique characteristics of the base-input connection is very small indeed.

It now appears that Bardeen and Brattain had foreseen a variety of circuit devices as the following extract from one of their patent applications[27] shows:

> From the standpoint of its external behaviour and uses, the device resembles a vacuum tube triode; and while the electrodes are designated emitter, collector and base electrode, respectively, they may be externally interconnected in the various ways which have become recognized as appropriate for triodes, such as the conventional, the "grounded grid," the "grounded plate" or cathode follower, and the like. However, the analogies among the circuits is, of course, no better than the analogy between emitter and cathode, base electrode and grid, collector and anode. By feeding back a portion of the output voltage in proper phase to the input terminals, the device may be caused to oscillate at a frequency determined by its external circuit elements, and among other tests, power amplification was confirmed by a feedback connection which caused it to oscillate. It has been found that the performance of the device is expressed, to a good approximation, by the following functional relations:
>
> $$I_e = f(V_e + R_F I_c) \qquad (I)$$
> $$I_c = I_c^0(V_c) + aI_e \qquad (IA)$$
>
> where
>
> I_e = emitter current.
> I_c = collector current.
> $I_c^0\ (V_c)$ = collector current with emitter disconnected.
> V_e = voltage of emitter electrode measured with respect to base electrode.
> V_c = voltage of collector electrode measured with respect to the base electrode.
> R_F = an equivalent resistance independent of bias.
> a = a numerical factor which depends on the bias voltages.
> $f(V_e)$ gives the relation between emitter current and emitter voltage with the collector circuit open.
>
> The interpretation of the foregoing equation (I) is that the collector current lowers the potential of the surface of the block in the vicinity of the emitter relative to the base

TABLE 4

CHARACTERISTICS OF AMPLIFIER CONNECTIONS

	Emitter Input	Base Input	Emitter Output
Input impedance	700 ohms	5 000 ohms	20 000 ohms
Output impedance	30 000 ohms	10 000 ohms	500 ohms
Power gain	16 decibels	23 decibels	16 decibels
Voltage gain	40:1	20:1	less than 1:1
Current gain	about 1:1	10:1	40:1
Maximum power output with tolerable distortion	2×10^{-2} watt	2×10^{-2} watt	10^{-4} watt

electrode by an amount $R_F I_e$ and thus increases the effective bias voltage on the emitter by the same amount. The term $R_F I_e$ thus represents positive feedback.

It is quite obvious that some interesting amplifier circuits can be designed round crystal triodes, but unless power supply introduces special requirements and difficulties there does not appear to be any marked superiority of crystal triodes over vacuum tubes in respect of type of application.

For radio-frequency amplifiers, since the noise apparently follows an inverse square-law with frequency, e.g. doubling the frequency reduces the noise to a quarter of its value, the position is simpler. Using two stages of intermediate-frequency amplification, we can produce 30- to 35-decibels gain. It is thus possible to design and produce a radio set of 60-decibels gain with a tolerable noise level using crystal triodes instead of valves. Such a set built round three crystal triodes can be constructed to consume less than 500 milliwatts and yet produce sufficient volume for normal purposes.

Since this paper was originally drafted an interesting article on the circuit design of the crystal triode by Ryder and Kircher[28] has been published. It should, however, be emphasized that numerical data in such articles are very much dependent on the triode characteristics selected and that it is too early yet to be specific about the component's characteristics.

5.2 Pulse Circuits

The greatest field of application for crystal triodes, however, appears at present to be in connection with circuits associated with pulse technique. Here the disabilities of high noise and low output are not important. Triodes with appreciable current gain ($\alpha > 2$) can work in two stable conditions (Eccles-Jordan) or in one stable and one unstable condition (flip-flop). From such circuits counting, dividing, pulse generating, and regenerating devices can be obtained. Many such circuits and devices have been worked out, constructed, and tested. The circuits are in general much simpler than those employing hard valves, and they are more sensitive. They are even preferable to circuits employing modern gas tubes and are more versatile.

An example of trigger-circuit simplicity is shown in Figures 12A and 12B. The former is the normal double-triode Eccles-Jordan circuit employing valves which is used so widely for binary counting, as, for example, in conjunction with Geiger-Müller counters. The circuit in Figure 12B is the crystal-triode equivalent which provides the double stability action with much greater simplicity in circuit and supplies together with increased sensitivity and speed of operation. The action is dependent on positive feedback introduced by the base resistance when triodes are employed with $\alpha > 1$.

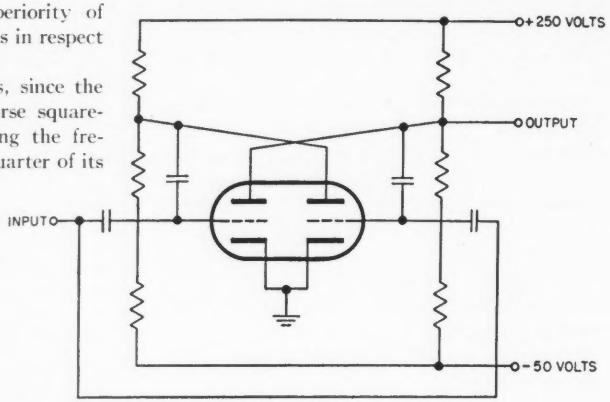

Figure 12A—Eccles-Jordan circuit employing thermionic valves.

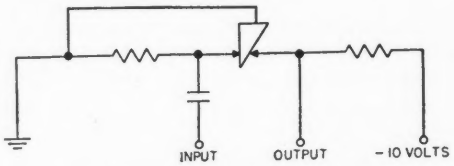

Figure 12B—Eccles-Jordan circuit employing crystal triodes.

It is quite clear that the development of pulse systems on cables can be materially assisted by employing crystal triodes as the basis of repeaters; the power consumption will be small, at low volt-

age, and will easily be supplied by the cable itself. It should be noted that triodes are capable of producing high peak output; e.g. it is possible to produce peaks of the order of $1\frac{1}{2}$ watts although the mean output is only a few milliwatts.

In Figure 13 a pulse repeater is shown that can be inserted in a line and be fed with power down the line. Such a circuit will give power gains of about 35 decibels, a peak pulse-power output of one to two watts, and is operated satisfactorily using $\frac{1}{2}$-micro-second pulses. It could be manufactured so small that it could fit inside a normal line-terminating insulator. The circuit is of the blocking-oscillator type and provides pulse-shaped regeneration.

Practical commercial applications in respect of computers, counters, pulse-code modulation, electronic switching, etc., should become common just as soon as triodes are commercially available in sufficient quantity to satisfy demands. Life and stability appear to be satisfactory, making due allowance for a certain percentage of defective triodes in current prototype manufacture. A counting circuit containing nine triodes has been working consistently for four or five months to date.

5.3 Oscillators

In this field the frequency restrictions appear to be somewhat less and development is still bringing in higher frequencies. Up to about 45 megacycles per second, it is at present possible to produce experimental transmitters, of very limited output but of interesting characteristics for special applications in the radio field. It is rumoured that higher frequencies have been attained and that push-pull arrangements with suitable cooling devices have given more than 250-milliwatts output.

Here again the circuits are simplified as compared with those associated with hard valves. A sine-wave oscillator has been constructed which appears to be much more stable than its thermionic valve counterpart.

Apparently the Jet Propulsion Laboratory[29] of the California Institute of Technology has built up a very small radio transmitter round the triode for uses in rockets for the transmission of data during flight.

Webster, Eberhard, and Barton[26] in the paper referred to above have described two oscillator circuits both making use of negative resistance effects in the base lead. One is a two-terminal sine-wave generator, the other a simple relaxation oscillator which will furnish either pulse or saw-tooth waveform.

Reeves[30] has also dealt in some detail with triode circuits particularly those utilizing positive feedback. As illustrations of this technique, he developed pulse repeater circuits and binary pulse counting circuits of the type illustrated in Figures 12 and 13.

In the field of small-output oscillators the crystal triode has undoubtedly a place in the future.

6. *Conclusions and Acknowledgments*

In view of the remarkable progress in the development of the crystal triode during the very short period of time in which such development has been in play, it is quite clear that an interesting and useful electronic component has arrived. Perhaps it is premature to talk of arrival since considerable metallurgical and manufacturing development may still be required before this component is commercially available at a reasonable and competitive price. The performance of laboratory and prototype models described herein begets confidence in the future of the

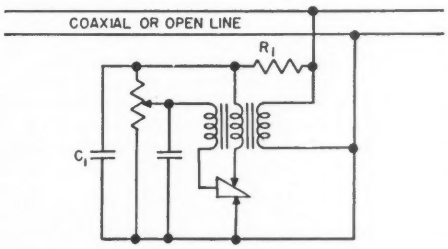

Figure 13—Two-terminal pulse repeater employing a crystal triode. R_1 and C_1 provide decoupling.

triode once some of the less desirable apparent characteristics (noise, low output, restricted frequency range, etc.) are brought strictly under control. It is reasonably clear that this will happen.

As envisaged in the introduction, the crystal triode is not really a straight competitor to the

thermionic valve but rather a complement to it in that it, in certain cases, simplifies circuit design and power supply. This would appear to be particularly the case in connection with pulse technique. Perhaps at a later date the same may be true in connection with lower-power transmission at medium wavelengths. The position at ultra-high frequency is quite obscure at present.

There appear to be good grounds for believing that we are at the threshold of a new stage in electronics in which the well-known devices, such as valves, rectifiers, etc., are supplemented by a range of semi-conductor devices that oscillate, modulate, amplify, etc., and that give the electronic engineer an opportunity of producing simple and fool-proof circuits for many applications which at present are with difficulty met by complex circuits and temperamental components.

The author has to acknowledge considerable assistance from his colleagues in the laboratories, in particular Mr. C. de B. White. He has also to thank Standard Telecommunication Laboratories, Limited, for permission to present the paper and to include therein unpublished work carried out in their laboratories.

7. *Bibliography*

1. Editorial, *Consumer Reports*; September, 1949.
2. Editorial, *Bell System Technical Journal*, v. 28, p. 335; 1949.
3. W. Shockley, "Theory of *p-n* Junctions in Semiconductors and *p-n* Junction Transistors," *Bell System Technical Journal*, v. 28, p. 435; 1949.
4. H. C. Torrey and C. A. Whitmer, "Crystal Rectifiers," McGraw-Hill Book Company, New York, New York; 1948.
5. W. C. Dunlap, "Germanium, Important New Semiconductor," *General Electric Review*, v. 52, p. 9; February, 1949.
6. J. Bardeen and W. H. Brattain, "The Transistor, A Semi-Conductor Triode," *Physical Review*, v. 74, p. 230; 1948.
7. N. F. Mott, "Semi-Conductors and Rectifiers," The Fortieth Kelvin Lecture, *Proceedings of the Institution of Electrical Engineers*, v. 96, Part 1, p. 253; 1949.
8. J. Bardeen and W. H. Brattain, "Physical Principles Involved in Transistor Action," *Physical Review*, v. 75, p. 1208; 1949.
9. J. B. Little, "New Structure for Transistors," Institute of Radio Engineers, Princeton Symposium on Semiconductor Devices, June 21, 1949.
10. J. N. Shive, "The Double Surface Transistor," *Physical Review*, v. 75, p. 689; 1949.
11. W. E. Kock and R. L. Wallace, "The Coaxial Transistor," *Electrical Engineering*, v. 68, p. 222; 1949.
12. R. W. Haegele, Institute of Radio Engineers, Princeton Symposium on Semiconductor Devices, June 21, 1949. Later published as "Crystal-Tetrode Mixer," *Electronics*, v. 22, p. 80; October, 1949.
13. C. de B. White and K. A. Matthews, British Patent Application 8906/49.
14. G. L. Pearson, Institute of Radio Engineers, Princeton Symposium on Semiconductor Devices, June 21, 1949. See also W. Shockley, G. L. Pearson, M Sparks, and W. H. Brattain, "Modulation of the Resistance of a Germanium Filament by Hole Injection," *Physical Review*, v. 76, p. 459; 1949.
15. J. N. Shive, "Germanium Photoconductivity Cell," Institute of Radio Engineers, Princeton Symposium on Semiconductor Devices, June 21, 1949. (See also J. N. Shive, "A New Germanium Photo-Resistance Cell," *Physical Review*, v. 76, p. 574; 1949.)
16. J. Bardeen, W. H. Brattain, and R. B. Gibney, British Patent Application 5203/49.
17. J. E. Lilienfeld, United States Patents 1,745,175, 1,877,140, and 1,900,018.
18. R. S. Ohl, United States Patent 1,765,607. French Patent 677,049.
19. A. H. W. Beck, A. B. Cutting, and A. D. Brisbane, British Patent Application 30706/48.
20. W. G. Pfann, Institute of Radio Engineers, Princeton Symposium on Semiconductor Devices, June 21, 1949. See also item 28 below. See also W. G. Pfann and J. H. Scaff, "The P-Type Germanium Transistor," *Physical Review*, v. 76, p. 459; 1949.
21. R. M. Ryder, Institute of Radio Engineers, Princeton Symposium on Semiconductor Devices, June 21, 1949. See also item 28 below.
22. C. B. Brown, Institute of Radio Engineers, Princeton Symposium on Semiconductor Devices, June 21, 1949. Later published as "Magnetically Biased Transistors," *Physical Review*, v. 76, p. 1736; 1949.
23. K. A. Matthews and C. de B. White, British Patent Application 8902/49.
24. K. Lehovec, "Testing Transistors," *Electronics*, p. 88; June, 1949.
25. H. C. Montgomery, Institute of Radio Engineers, Princeton Symposium on Semiconductor Devices, June 21, 1949. See also item 28 below.
26. W. M. Webster, E. Eberhard, and L. E. Barton, "Some Novel Circuits for the Three-Terminal Semiconductor Amplifier," *R.C.A. Review*, v. 10, p. 5; 1949.
27. J. Bardeen and W. H. Brattain, British Patent Application 23808/48.
28. R. M. Ryder and R. J. Kircher, "Some Circuit Aspects of the Transistor," *Bell System Technical Journal*, v. 28, p. 367; 1949.
29. F. W. Lehan, "Transistor Oscillator for Telemetering," *Electronics*, p. 90; August, 1949.
30. A. H. Reeves, British Patent Application 27894/48.

Cross-Talk Considerations in Time-Division Multiplex Systems*

By SIDNEY MOSKOWITZ, LISCUM DIVEN,† and LOUIS FEIT

Federal Telecommunication Laboratories, Incorporated; Nutley, New Jersey

AN EXPERIMENTAL study was made of the effects on interchannel cross talk of the bandwidth characteristics of the transmission medium in pulse-time multiplex systems. Pulse-amplitude modulation and pulse-position modulation systems are considered. The effects of various types of high- and low-frequency response are discussed from both experimental and theoretical points of view.

• • •

1. Introduction

One of the significant problems present in the development of pulse-multiplex communication systems is interchannel cross talk. An investigation was conducted to determine the factors that would permit the design of a system combining high interchannel cross-talk ratios with maximum economy of bandwidth. Pulse-position and pulse-amplitude modulation[1,2] were investigated.

Pulse-amplitude modulation is of considerable importance, inasmuch as some form of it is used in many pulse-multiplex systems. In its simplest form, it is derived by sampling a signal at fixed time intervals. These pulse samples comprise the pulse-amplitude-modulated signal. If these modulation samples are transformed to time displacement of the pulses with respect to a fixed time reference (such as a marker pulse), pulse-position modulation results.

One common form of cross talk is caused by carryover of energy from one pulse to the following pulse. Thus, cross talk may occur from one channel to the following channel, decreasing rapidly as the pulses are further separated in time. This cross talk may be expressed as the ratio of the signal output of a given channel under normal modulation to the signal output of

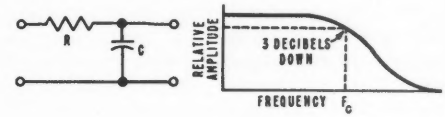

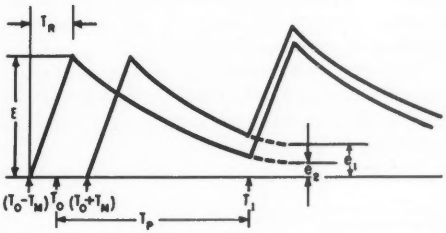

Figure 1—Effect of high-frequency response on cross talk in pulse-position modulation using a resistance–capacitance filter.

$$\text{Cross-talk ratio} = \frac{\exp\,(T_P/RC)}{\sinh\,(T_M/RC)}\left(\frac{T_M}{T_R}\right).$$

the same channel resulting from the modulation of some other channel. This ratio is customarily expressed in decibels.

2. Pulse-Position Modulation

In analyzing the effect of bandwidth on pulse carryover, it is necessary to investigate the effect of the response–frequency characteristic of the transmission system on the shape of the pulses. Two types of high-frequency response will be considered, a slow and an extremely rapid rate of high-frequency cutoff.

2.1 Slow Rate of High-Frequency Cutoff

A slow rate of cutoff may be obtained by a resistance–capacitance circuit of the type shown in Figure 1. Such a circuit represents either the

* Reprinted from *Proceedings of the I.R.E.*, v. 38, pp. 1330–1336; November, 1950. Presented at the National Convention of the Institute of Radio Engineers on March 7, 1949, in New York, New York.

† Now with Motorola, Incorporated, Pheonix, Arizona.

[1] F. F. Roberts and J. C. Simmonds, "Multichannel Communication Systems," *Wireless Engineer*, v. 22, pp. 538–549; November, 1945: and pp. 576–580; December, 1945.

[2] V. D. Landon, "Theoretical Analysis of Various Systems of Multiplex Transmission," *RCA Review*, v. 9, pp. 287–351; June, 1948: and pp. 438–482; September, 1948.

standard resistance-coupled amplifier without peaking circuits or its band-pass analogue, the single-tuned circuit.

The relative amplitude–frequency response of such a circuit may be expressed as

$$E_0 = E_I \cos [\tan^{-1} (F/F_c)], \qquad (1)$$

where F is the frequency considered and F_c is the cutoff frequency, which is equal to $1/(2\pi RC)$, at which point the relative amplitude drops 3 decibels. Figure 1 shows the type of response given by this circuit. The rate of cutoff approaches 6 decibels per octave.

The effect of such a response on a pulse of voltage may be calculated by simple transient analysis. With a rectangular input pulse, the rise time T_R of the received pulse increases with increasing transmission-circuit time constant RC until a value of T_R equal to the width of the original pulse is obtained. If RC is increased further, T_R remains constant.

The cross talk introduced by transmission of time-modulated pulses through a medium having the type of frequency characteristic described can be calculated as follows.

Referring to Figure 1, two adjacent pulses of period T_P and rise time T_R are shown. The first pulse is time modulated by a displacement T_M from its resting position T_O and therefore moves between T_O+T_M and T_O-T_M, producing carryover e_1 and e_2.

At one extreme, the carryover is

$$e_1 = E \exp -[(T_P - T_M)/RC].$$

At the other extreme, the carryover is

$$e_2 = E \exp -[(T_P + T_M)/RC].$$

The peak-to-peak variation in amplitude of the pulse, because of carryover, is then

$$e_1 - e_2 = E\left\{\exp\left[-\left(\frac{T_P - T_M}{RC}\right)\right] - \exp\left[-\left(\frac{T_P + T_M}{RC}\right)\right]\right\}.$$

This may be rewritten as

$$\begin{aligned} e_1 - e_2 &= E[\exp -(T_P/RC) \exp (T_M/RC) \\ &\quad - \exp -(T_P/RC) \exp -(T_M/RC)] \\ &= E \exp -(T_P/RC)[\exp (T_M/RC) \\ &\quad - \exp -(T_M/RC)]. \end{aligned}$$

The ratio of pulse amplitude to carryover is then

$$\begin{aligned} &\frac{E}{e_1 - e_2} \\ &= \frac{1}{\exp -(T_P/RC)[\exp (T_M/RC) - \exp -(T_M/RC)]} \\ &= \frac{\exp (T_P/RC)}{\exp (T_M/RC) - \exp -(T_M/RC)} \\ &= \frac{\exp (T_P/RC)}{2 \sinh (T_M/RC)}. \end{aligned}$$

Since $F_c = 1/(2\pi\ RC)$,

$$\frac{E}{e_1 - e_2} = \frac{\exp (2\pi F_c T_P)}{2 \sinh (2\pi F_c T_M)}.$$

This cross talk is expressed in terms of amplitude variation. It can be shown[3,4] that in pulse-position modulation there is an improvement factor of $2(T_M/T_R)$, which may be applied to signal-to-noise ratio or to cross talk.

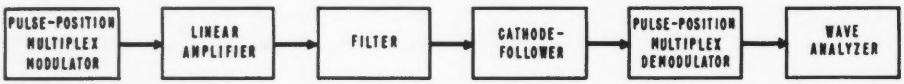

Figure 2—Equipment used for cross-talk measurements on pulse-position modulation.

The output cross-talk ratio then becomes

$$\text{cross-talk ratio} = \frac{\exp (2\pi F_c T_P)}{\sinh (2\pi F_c T_M)} \left(\frac{T_M}{T_R}\right). \qquad (2)$$

This formula may also be expressed in terms of the time constant RC.

$$\text{Cross-talk ratio} = \frac{\exp (T_P/RC)}{\sinh (T_M/RC)} \left(\frac{T_M}{T_R}\right). \qquad (2A)$$

To check the results that might be expected from the use of (2), a series of experiments were

[3] E. M. Deloraine and E. Labin, "Pulse-Time Modulation," *Electrical Communication*, v. 22, pp. 91–98; 1944.

[4] S. Moskowitz and D. D. Grieg, "Noise-Suppression Characteristics of Pulse-Time Modulation," *Proceedings of the I.R.E.*, v. 36, pp. 446–450; April, 1948.

run using a commercial pulse-position-modulation multiplex system in which

$T_M = 1$ microsecond
$T_R = 0.3$ microsecond (for low values of F_c)
$T_P = 5$ microseconds.

The inherent cross talk in the terminals was 66 decibels, and this was therefore the highest cross-talk ratio that could be measured. A block diagram of the setup used is shown in Figure 2. Resistance–capacitance filters of various cutoff frequencies were inserted at the point indicated, and cross talk at a modulating frequency of 1000 cycles was measured with a General Radio *736A* wave analyzer. Only adjacent-channel cross talk was considered.

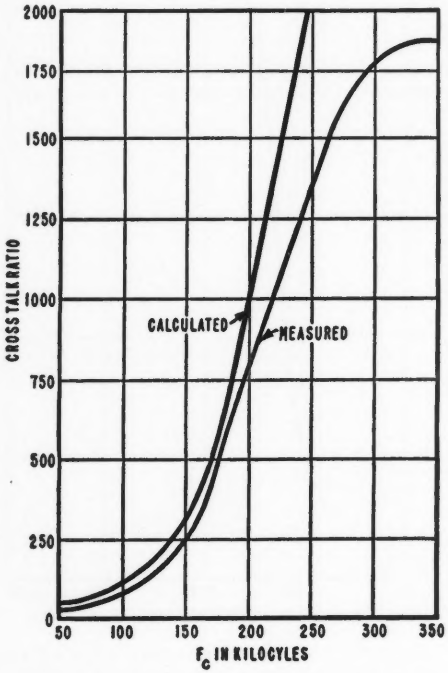

Figure 3—Cross-talk ratio versus bandwidth for pulse-position modulation. High frequencies have been attenuated by a filter as shown in Figure 2, where $F_C = 1/(2\pi RC)$.

The results of these tests, together with the values derived from (2), are plotted in Figure 3. It will be noted that the experimental results agree closely with theory, except at high cutoff frequencies, where the inherent cross talk in the equipment used becomes the limiting factor.

2.2 Rapid Rate of High-Frequency Cutoff

The cross talk arising from sharp cutoff of the transmission response was also studied. Such a response is approached in intermediate-frequency amplifiers. If a rectangular pulse is passed through a low-pass system having uniform frequency and linear phase characteristics up to a certain frequency, and zero response above this frequency, the equation of the resulting pulse can be shown to be[5]

$$e = E\{\mathrm{Si}\,[n\pi(t'+\tfrac{1}{2})] - \mathrm{Si}\,[n\pi(t'-\tfrac{1}{2})]\},$$

where

$$\mathrm{Si}(X) = \int_0^x [(\sin u)/u]\,du$$

e = output voltage at any instant
E = input pulse amplitude
$n = 2F_cW$
F_c = cutoff frequency
W = width of input pulse
$t' = T_P/W$
T_P = pulse period.

For such a theoretical transmission system, the cross talk may be derived as follows.

The carryover at one extreme of modulation is

$$e_1 = E\left\{\mathrm{Si}\left[n\pi\left(\frac{T_P - T_M}{W} + \frac{1}{2}\right)\right] - \mathrm{Si}\left[n\pi\left(\frac{T_P - T_M}{W} - \frac{1}{2}\right)\right]\right\}$$

and at the other extreme it is

$$e_2 = E\left\{\mathrm{Si}\left[n\pi\left(\frac{T_P + T_M}{W} + \frac{1}{2}\right)\right] - \mathrm{Si}\left[n\pi\left(\frac{T_P + T_M}{W} - \frac{1}{2}\right)\right]\right\}.$$

[5] E. A. Guillemin, "Communication Networks," v. 2, John Wiley and Sons, Inc., New York, New York; 1935: p. 485.

The peak-to-peak carryover ratio is then

$$\frac{E}{e_1-e_2}=\left\{\mathrm{Si}\left[n\pi\left(\frac{T_P-T_M}{W}+\frac{1}{2}\right)\right]-\mathrm{Si}\left[n\pi\left(\frac{T_P+T_M}{W}+\frac{1}{2}\right)\right]+\mathrm{Si}\left[n\pi\left(\frac{T_P+T_M}{W}-\frac{1}{2}\right)\right]-\mathrm{Si}\left[n\pi\left(\frac{T_P-T_M}{W}-\frac{1}{2}\right)\right]\right\}^{-1}. \quad (3)$$

The build-up time of the pulse, after transmission through this system, is $1/(2F_c)$ so that, if $E/(e_1-e_2)$ is denoted by ψ, the net cross-talk ratio will be

$$\text{cross-talk ratio}=4\psi T_M F_c. \quad (4)$$

The characteristics of a filter or transmission medium as given in the above analysis cannot be met in practice. A fair approximation can be made, however, by means of a low-pass π-section filter having a general characteristic as shown in Figure 4. This filter had a rate of cutoff of approximately 20 decibels per octave. Tests on the same terminal equipment were made using such filters between modulator and demodulator. The results of these tests are shown in Figure 5. From these data, substantiated by theory, a high-frequency cutoff of about 500 kilocycles is sufficient to obtain a cross-talk ratio of about 70 decibels. If a slow rate of cutoff is maintained such as that given by low-Q transmission circuits, transmission lines, or resistance–capacitance video-frequency circuits, a half-power point at about 350 kilocycles would give an equally satisfactory cross-talk ratio.

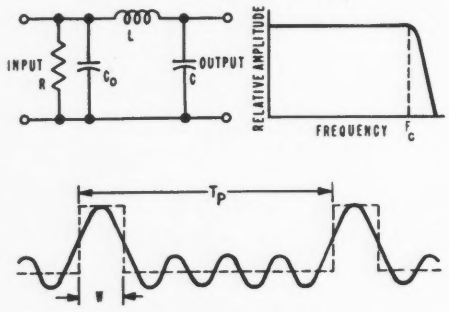

Figure 4—Effect of high-frequency response on cross talk in pulse-position modulation using a low-pass filter. For the π network $C_0RC_c=78{,}900$, $C=2C_0$, $C_0LF_c^2=12{,}670$, in micromicrofarads, microhenries, ohms, and megacycles.

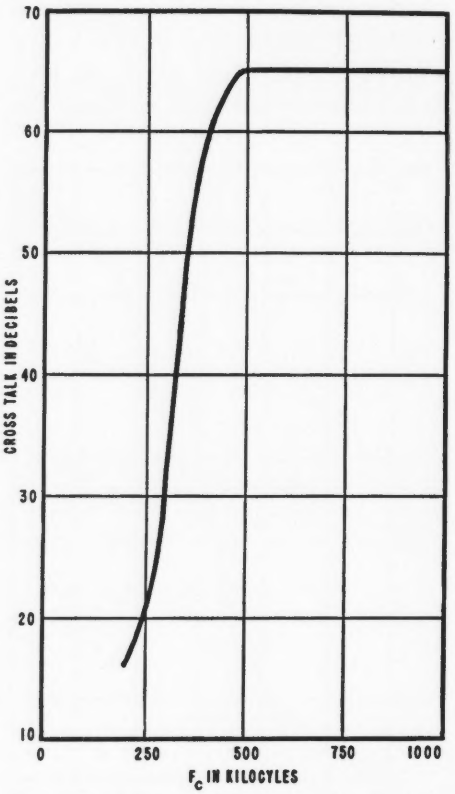

Figure 5—Cross talk plotted against bandwidth for pulse-position modulation. High frequencies have been attenuated by the π filter shown in Figure 4.

2.3 Low-Frequency Cutoff

The effect of low-frequency cutoff has also been considered. If a slow rate of cutoff such as that given by the resistance–capacitance circuit of Figure 6 characterizes the transmitting medium, the pulse will be distorted as shown. The response–frequency plot of such a circuit is also shown in this figure and is given by

$$\text{relative amplitude}=\cos\tan^{-1}F_c/F, \quad (5)$$

where $F_c=1/(2\pi RC)$.

The voltage e at any time $(T-W)$, where W is the width of the pulse, is

$$e=-E[1-\exp-(W/RC)]\exp-[(T-W)/RC].$$

At one extreme of modulation, the carryover to the next pulse is

$$e_1=-E[1-\exp-(W/RC)]\exp-[(T_P-W+T_M)/RC].$$

At the other extreme, the carryover is

$$e_2=-E[1-\exp-(W/RC)]\exp-[(T_P-W-T_M)/RC].$$

The peak-to-peak carryover is then

$$\begin{aligned}e_2-e_1&=-E[1-\exp-(W/RC)]\{\exp-[(T_P-W)/RC]\}[\exp(T_M/RC)-\exp-(T_M/RC)]\\&=-E[1-\exp-(W/RC)]\{\exp-[(T_P-W)/RC]\}[2\sinh(T_M/RC)].\end{aligned}$$

The ratio of pulse amplitude to carryover is

$$\frac{E}{e_2-e_1}=\frac{-\exp[(T_P-W)/RC]}{2[1-\exp-(W/RC)]\sinh(T_M/RC)}.$$

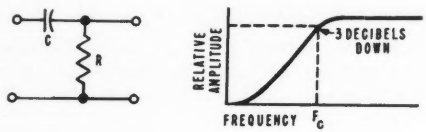

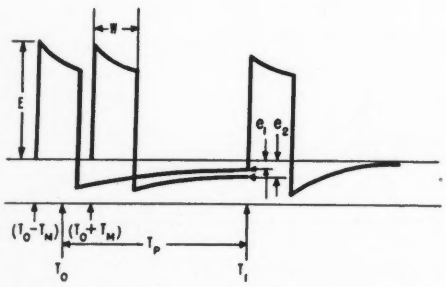

Figure 6—Effect of low-frequency response on cross talk in pulse-position modulation using a resistance–capacitance filter.

$$\text{Cross-talk ratio}=\frac{-T_M\exp[(T_P-W)/RC]}{T_R[1-\exp-(W/RC)][\sinh(T_M/RC)]}.$$

Applying the pulse-position-modulation improvement factor $2T_M/T_R$, the following equation is obtained.

Output cross-talk ratio

$$=\frac{-T_M\exp[(T_P-W)/RC]}{T_R[1-\exp-(W/RC)][\sinh(T_M/RC)]}. \quad (6)$$

Substituting $F_c=1/(2\pi RC)$,

output cross-talk ratio

$$=-\frac{T_M\exp[2\pi F_c(T_P-W)]}{T_R[1-\exp(-2\pi F_cW)](\sinh 2\pi F_cT_M)}. \quad (6A)$$

Note that the cross talk introduced by poor low-frequency response is opposite in polarity to

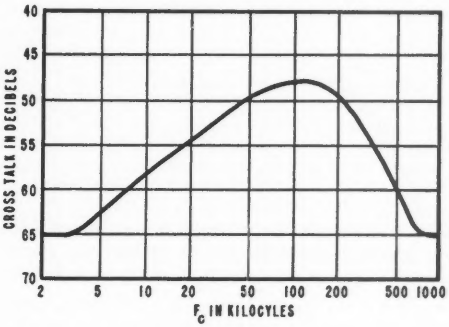

Figure 7—Cross talk plotted against bandwidth for pulse-position modulation. Low frequencies have been attenuated by a resistance–capacitance filter having a cutoff frequency of $F_c=1/(2\pi RC)$. The high-frequency cutoff is at 3 megacycles.

that caused by poor high-frequency response. Further inspection of (6A) shows that the cross-talk ratio may be high at two values of F_c. The latter fact is borne out by the experimental results plotted in Figure 7.

The physical explanation of this curve is simply that, at very low values of cutoff frequency, the pulse is passed by the coupling network without distortion, so that no appreciable carryover occurs. At higher values of cutoff frequency, cross talk is present because of the carryover from channel to channel as shown in Figure 6. As the cutoff frequency is raised still further, the pulse becomes differentiated and returns to the base line some time before the next channel occurs, again resulting in negligible carryover.

2.4 Combined High- and Low-Frequency Cutoff

The fact that cross talk due to high-frequency attenuation is of opposite phase from cross talk due to low-frequency attenuation indicates that by suitably choosing the high and low cutoff frequencies some form of cancellation might produce a system featuring high cross-talk ratios with very narrow bandwidth. Results of experiments along this line are plotted in Figure 8. In each case, the high-frequency response was kept to a value that would not greatly affect cross talk, and the low-frequency cutoff was varied. Notice that in curve 3, where the over-all bandwidth between the 3-decibel points was considerably less than 1 megacycle, a cross-talk ratio of 73 decibels was obtained, whereas the inherent cross talk in the system was only 66 decibels. Thus, some of this inherent cross talk was actually cancelled out. In investigating causes of cross talk in a given system, it is important to remember that a good cross-talk figure may be the result of some form of accidental cancellation of two forms of cross talk arising from different sources.

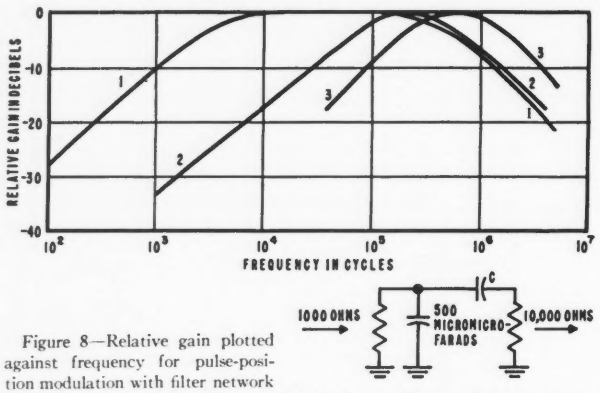

Figure 8—Relative gain plotted against frequency for pulse-position modulation with filter network shown. Values of C in micromicrofarads and of cross talk in decibels are, respectively, for curve 1, 4500 and 62; curve 2, 132 and 38; and curve 3, 4.8 and 73.

2.5 Miscellaneous Considerations

The formula given in Figure 1 is also useful in determining the spacing between adjacent pulses, and thus the number of channels that may be employed in a given bandwidth. The smaller the pulse spacing, the larger is the required bandwidth for a given deviation and cross-talk figure. In the case of the sharp-cutoff filter, however, this is not necessarily true. Because of the oscillations on the base line resulting from the distortion of the pulse, the pulses may be positioned such that the peaks and troughs of the overshoot can cause cross-talk cancellation. Thus, a position may be found where cross-talk ratio is a maximum, whereas moving the pulse in either direction will cause the cross-talk ratio to decrease. With pulse-position modulation, it will be found that this type of cross talk varies considerably with percentage modulation, depending on the peak deviation used. Such cross talk also may occur accidentally, due to ringing resulting from long inductive leads, insufficient decoupling of circuits containing inductances, and other causes.

3. Pulse-Amplitude Modulation

3.1 High-Frequency Cutoff

The interchannel cross talk caused by poor high-frequency response may be studied in a manner similar to that used in the above dis-

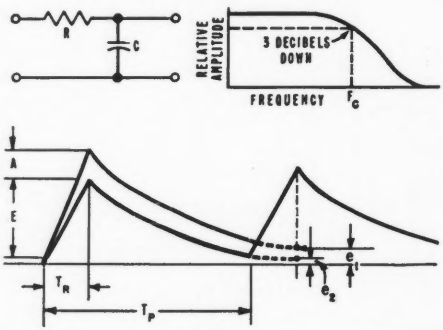

Figure 9—Effect of high-frequency response on cross talk in pulse-amplitude modulation using a resistance–capacitance filter. $M = A/E$ = modulation factor. Cross-talk ratio = exp (T_P/RC). Cross talk in decibels for 100-percent modulation = 8.68 T_P/RC.

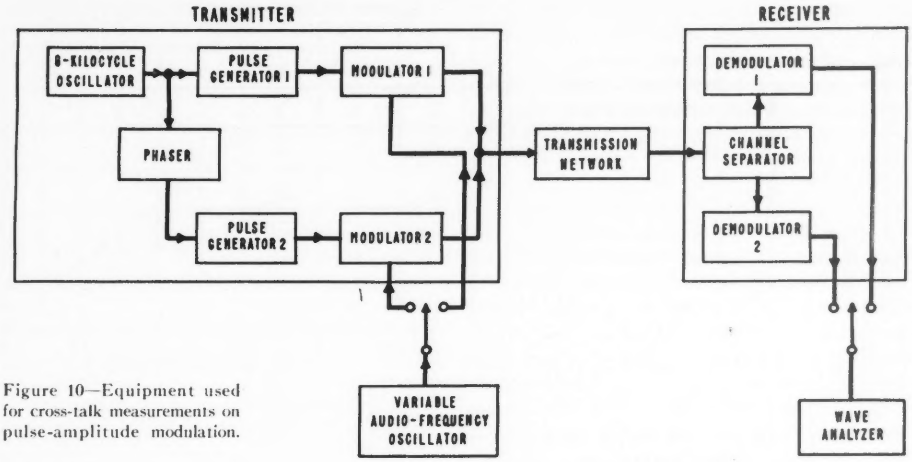

Figure 10—Equipment used for cross-talk measurements on pulse-amplitude modulation.

cussion. The expression is derived by the same procedure, with the exception that the displacement of the pulse under modulation is one of amplitude and not a time deviation, and that there is no pulse-position-modulation improvement factor in this case. Referring to Figure 9, at one extreme of modulation, the carryover is

$$e_1 = E \exp [-(T_P/RC)](1+M).$$

At the other extreme of modulation, the carryover is

$$e_2 = E \exp [-(T_P/RC)](1-M).$$

The peak-to-peak amplitude variation of the pulse due to carryover is then

$$e_1 - e_2 = 2ME \exp -(T_P/RC).$$

Since the peak-to-peak output of the channel when modulated in the normal fashion is $2ME$, the cross-talk ratio becomes

$$\frac{2ME}{e_1 - e_2} = \frac{2ME}{2ME \exp -(T_P/RC)}.$$

$$\text{Cross-talk ratio} = \exp (T_P/RC). \qquad (7)$$

Taking the logarithm to the base 10 of both sides and multiplying by 20, gives

$$\text{cross-talk ratio in decibels} = \frac{8.68T_P}{RC}. \qquad (8)$$

3.2 Low-Frequency Cutoff

Because of the presence of an audio-frequency component in pulse-amplitude modulation, the effect of low-frequency attenuation must be considered from a different standpoint. This audio-frequency component represents a change in the average value of the signal with modulation. When a pulse-amplitude-modulated signal is passed through a coupling network that does not transmit the direct-current component, displacement of the base line occurs. This displacement will vary in accordance with the modulation. The result is that when one channel is modulated, *all other channels* are affected.

Since an exact mathematical analysis is rather involved, an experimental procedure was followed similar to that used in the experiments with pulse-position modulation. A block diagram of the equipment is shown in Figure 10.

The transmitter consisted of a two-channel pulse-amplitude modulator with a pulse-repetition rate of 8 kilocycles and a pulse width of approximately 3 microseconds. A phasing network was incorporated so that the relative position in time of the two channels could be adjusted at will. Standard resistance–capacitance coupling networks of the type shown in Figure 6 and having various time constants were inserted at the point marked "transmission network." The desired channel was demodulated and cross talk measured by means of a wave analyzer as previously described.

The results are shown in Figure 11. The inherent cross talk in the system due to high-

frequency carryover was 70 decibels. It is interesting to note the dependence on modulating frequency, and the extremely large time constants that are required if high cross-talk ratios are to be obtained at low modulating frequencies. For example, to obtain a figure of 56 decibels with a modulating frequency of 200 cycles, a 0.25-microfarad coupling capacitor and a 1-megohm grid resistor would be required. The cutoff frequency of this network is only 0.6 cycle! This, of course, represents only one coupling network. The requirements become far more severe in a multistage amplifier having several such networks in cascade. The use of such large coupling capacitors introduces new problems, such as the effect on the high-frequency response of capacitance to ground, and changes in the direct-current grid bias of the following tube resulting from leakage currents.

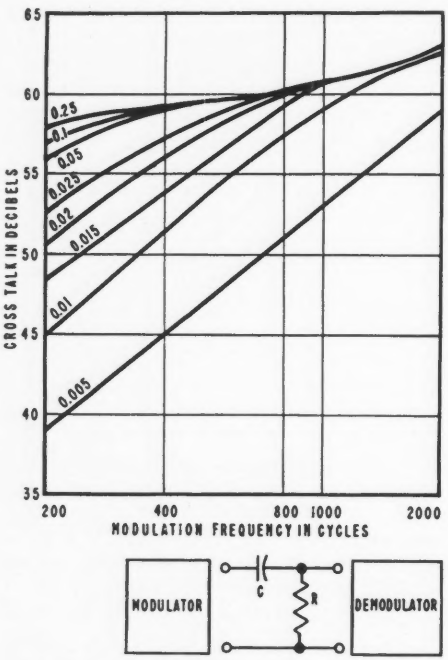

Figure 11—Cross talk plotted against modulation frequency for 2 pulse-amplitude-modulated channels. The pulse-repetition rate is 8000 cycles. The designations on the curves correspond to the product of C and R (microfarads×megohms) in the coupling circuit shown.

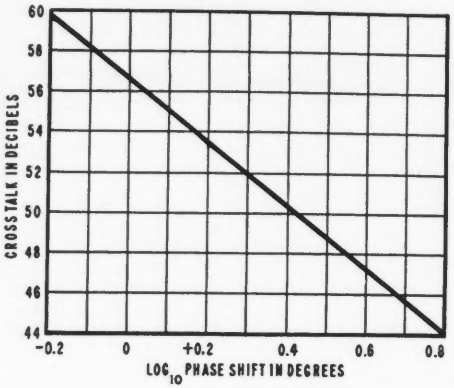

Figure 12—Cross talk as a function of the logarithm of the phase shift of the coupling network for pulse-amplitude modulation.

The separation between the two channels was varied and the cross talk at 1000 cycles measured for two values of transmission time constant. Cross-talk ratio was found to be independent of channel spacing.

The effect of the coupling network may be expressed in several ways: in terms of time constant, cutoff frequency, or in phase shift at a certain frequency. A convenient empirical relation may be derived by taking the data of Figure 11 and plotting cross talk in decibels against $\log_{10}$ phase shift in degrees, where $\tan \theta = F_c/F$. This is shown in Figure 12. Since the result is a straight line, the equation of the curve is

$$\text{cross talk in decibels} = 56.7 - 15.8 \log_{10} \theta. \quad (9)$$

To obtain a cross-talk figure of better than 56.7 decibels, a phase shift of less than one degree is required. In applications where it may be found impractical to obtain the required low-frequency response by using large coupling capacitors, the usual methods of correcting the low-frequency response may be applied, providing all the stages involved are linear. However, it is advisable to determine the effect on the phase response of slight variations in component tolerances. Adjustment of such compensating networks may be found to be extremely critical. Any other networks that may affect low-frequency response must also be controlled, such as screen-grid and cathode by-pass networks.

Theory of Space-Charge Waves in Cylindrical Waveguides with Many Beams*

By PHILIP PARZEN

Federal Telecommunication Laboratories, Incorporated; Nutley, New Jersey

IN A REPORT [1] by Haeff, the theory of the propagation of space-charge waves in unbounded coincident electron beams is discussed. Haeff's theory, however, does not account for the effect of the surrounding waveguide and the separation of the electron beams on gain and bandwidth.

This effect has been calculated approximately by an integral-equation method; and it has been found that in general the maximum gain and bandwidth both decrease. Furthermore, the energy transported is mostly in the form of alternating-current kinetic energy in the electron beam; and very little of it is in the form of electromagnetic-field energy in the waveguide. Hence, the input and output circuits for such a device would be similar to those of a klystron rather than those of a traveling-wave tube.

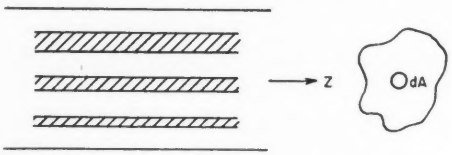

Figure 1.

1. General Considerations of Electron-Beam-Wave Interaction

Consider the case of a cylindrical waveguide, as shown in Figure 1, filled by many electron beams with varying initial longitudinal velocities.

We shall make the usual assumptions that only the longitudinal electric field $\bar{E}_z$ acts on the beam (the other components being neutralized by the infinite longitudinal magnetic focusing field), and the small-signal approximations[2] are in meter-kilogram-second units

$$\left.\begin{aligned} v_{it} &= v_i + \tilde{v}_i \exp[j(\omega t - hz)] \\ \rho_{it} &= \rho_i + \tilde{\rho}_i \exp[j(\omega t - hz)]; \; \tilde{v}_i \ll v_i, \; \tilde{\rho}_i \ll \rho_i, \end{aligned}\right\} \quad (1)$$

where ρ_i is the initial direct-current density of the electrons whose direct-current velocity is v_i. The subscript t denotes the total quantity and the tilde the alternating-current part. The longitudinal current density

$$\left.\begin{aligned} J_t &= J + \tilde{J} \exp[j(\omega t - hz)] \\ \tilde{J} &= \textstyle\sum_i (\rho_i \tilde{v}_i + \tilde{\rho}_i v_i). \end{aligned}\right\} \quad (2)$$

By deriving the wave equation including the space charge and using (1), (2), and the continuity equation, the variation of E_z is given by

$$\left.\begin{aligned} \nabla_t^2 \bar{E}_z + (k^2 - h^2)\bar{E}_z &= \frac{j\zeta}{k}(k^2 - h^2)\tilde{J} \\ \nabla_t^2 &= \frac{\partial^2}{\partial x^2} + \frac{\partial^2}{\partial y^2} \\ k &= \frac{\omega}{c} = \frac{2\pi}{\lambda}, \end{aligned}\right\} \quad (3)$$

where ζ = impedance of free space.

Equation (3) may be considered to represent the forced spatial vibrations of the waveguide caused by the beams; and $\bar{E}_z$ and $\tilde{J}$ may accordingly be expanded in the orthogonal modes of the free vibrations (waveguide without beams).

In the case of $\tilde{J} = 0$, there exist orthogonal modes given by

$$\left.\begin{aligned} \bar{E}_z &= \bar{E}_{zn} \exp[-jh_n z] \\ \nabla_t^2 \bar{E}_{zn} &+ (k^2 - h_n^2)\bar{E}_{zn} = 0. \end{aligned}\right\} \quad (4)$$

$$\left.\begin{aligned} \int_G \bar{E}_{zn} E_{zm}^* \, dA &= 0, \quad \text{if } n \neq m \\ &= N_n, \text{ if } n = m, \end{aligned}\right\} \quad (5)$$

* This development was sponsored by the Signal Corps Engineering Laboratories of the United States Army. A paper on this subject was delivered at the joint meeting of the American Section of the International Scientific Radio Union and the Washington Section of the Institute of Radio Engineers in Washington, District of Columbia, on May 2, 1949.

[1] A. V. Haeff, "The Electron-Wave Tube—A Novel Method of Generation and Amplification of Microwave Energy," *Proceedings of the I.R.E.*, v. 37, pp. 4–10; January, 1949.

[2] J. R. Pierce, "Theory of the Beam-Type Traveling-Wave Tube," *Proceedings of the I.R.E.*, v. 35, pp. 111–123; February, 1947: see p. 114.

where E^* is the conjugate of E, and G is the cross-section of the waveguide. Thus, for the case of $\tilde{J} \neq 0$, let

$$\left.\begin{aligned} \tilde{E}_z &= \sum \alpha_n E_{zn} \exp[-jhz] \\ J &= \sum b_n E_{zn} \exp[-jhz]. \end{aligned}\right\} \tag{6}$$

Substituting these into the wave equation, and equating Fourier coefficients

$$\alpha_n = \frac{j\zeta(k^2-h^2)}{k} \frac{b_n}{h_n^2-h^2}, \tag{7}$$

$$\tilde{E}_z = \frac{j\zeta(k^2-h^2)}{k} \sum_k \frac{\tilde{E}_{zn}}{(h_n^2-h^2)N_n} \int_G \tilde{J}\tilde{E}^*_{zn}\, dA. \tag{8}$$

The relation between $\tilde{J}$ and $\tilde{E}_z$, which is obtained from the equations of motion, is

$$J = \frac{\omega\eta\tilde{E}_z}{j} \sum_i \frac{\rho_i}{(\omega - hv_i)^2}; \quad \eta = \frac{e}{m}. \tag{9}$$

Thus, the following integral equation is obtained for E_z.

$$\tilde{E}_z(s) = \int_G K(s,t)\, \tilde{E}_z(t)\, d\,A, \tag{10}$$

$$\left.\begin{aligned} K(s,t) &= \sum_n \frac{\tilde{E}_{zn}(s)\, \tilde{E}^*_{zn}(t)\, T(t)}{\{1+[\gamma_n^2/(h^2-k^2)]\}N_n} \\ \gamma_n^2 &= k^2 - h_n^2. \end{aligned}\right\} \tag{11}$$

$$\left.\begin{aligned} T(t) &= \sum_i \frac{\omega_i^2}{(\omega - hv_i)^2} \\ \omega_i^2 &= \frac{\eta\rho_i}{\epsilon_0} \end{aligned}\right\} \tag{12}$$

and (s) and (t) denote any two points in G.

$T(t)$ is a function of the direct-current velocities and densities of the various beams and its variation is a measure of the variation of the density and velocity across the waveguide.

2. *Special Cases, i = 2*

Consider two simple cases of (10) for two beams.

2.1 Case A. Two Thin Annular Beams with Symmetrical Properties in a Circular Waveguide.

For the case of two thin annular beams with symmetrical properties in a circular waveguide,[3] reference is made to Figure 2. Here $T(t) = 0$ except for small annular rings of cross-sectional areas S_1 and S_2, respectively, in which $T(r)$ is constant and independent of θ. It is necessary to

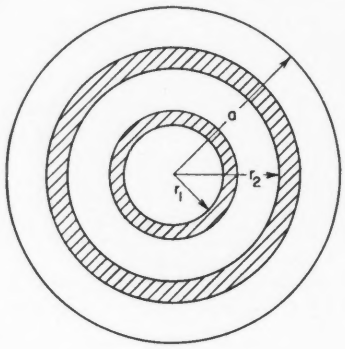

Figure 2.

sum over the symmetrical modes only, replacing the integrals in (10) by sums.

$$\left.\begin{aligned} E_z(r_1) &= E_z(r_1)\, S_1K(r_1,r_1) \\ &\quad + E_z(r_2)\, S_2K(r_1,r_2) \\ E_z(r_2) &= E_z(r_1)\, S_1K(r_2,r_1) \\ &\quad + E_z(r_2)\, S_2K(r_2,r_2). \end{aligned}\right\} \tag{13}$$

Looking for solutions of the form

$$h = \frac{\omega}{v} + u, \quad u \ll \frac{\omega}{v},$$

$$v = \frac{v_1+v_2}{2},$$

and letting

$$\left.\begin{aligned} x &= \frac{\alpha_{12}^2}{\alpha_{11}\alpha_{22}}, \quad 0 \leqslant x \leqslant 1 \\ Y &= \frac{\alpha_{22}}{\alpha_{11}} \\ \omega_1^2 &= Y\omega_2^2 \end{aligned}\right\} \tag{14}$$

the eliminant of (13) is

$$\frac{1}{\alpha_{11}} = \omega_1^2 \left[\frac{1}{(\omega - hv_1)^2} + \frac{1}{(\omega - hv_2)^2} + \frac{(x-1)\omega_1^4}{(\omega - hv_1)^2(\omega - hv_2)^2} \right], \tag{15}$$

$$\alpha_{ij} = (S_iS_j)^{\frac{1}{2}} \sum_n \frac{E_{zn}(r_i)\, E_{zn}(r_j)}{[1+(\gamma_n/\beta)^2]N_n}, \tag{16}$$

where $\beta = \omega/v$. It should be noted that α_{11} and α_{22} measure the effect of the individual beams, while

[3] This problem has also been treated by J. R. Pierce, "Double-Stream Amplifiers," *Proceedings of the I.R.E.*, v. 37, pp. 980–985; September, 1949: see page 983. However, the effect of geometry and beam separations are accounted for by electrostatic approximations. The method outlined here is more general.

α_{12} measures the effect of the separation of the beams.

Thus $x=1$ corresponds to coincident beams and $x=0$ to the case where the beams are far apart. Now let

$$\left.\begin{aligned}\delta&=\frac{v_1-v_2}{2}\\ \Delta&=\frac{\omega\delta}{v\omega_1\alpha_{11}^{1/2}}\\ H&=\frac{uv}{\omega_1\alpha_{11}^{1/2}},\end{aligned}\right\} \tag{17}$$

then (15) reduces to

$$1=\frac{1}{(\Delta-H)^2}+\frac{1}{(\Delta+H)^2}+\frac{x-1}{(\Delta-H)^2(\Delta+H)^2}, \tag{18}$$

if $\left|\frac{\omega\delta}{v}\pm uv\right|\gg\mu\delta$. Thus

$$H^2=\Delta^2+1\pm(4\Delta^2+x)^{1/2}. \tag{19}$$

Thus, maximum gain is given by $|H^2|_{\max}=x/4$ and maximum bandwidth is given by $\Delta^2\leqslant 1+x^{1/2}$.

Thus, both the maximum gain and bandwidth decrease as the beams are separated. When the beams are coincident, there is still a reduction in gain and bandwidth because of geometry. In this case, the maximum gain and bandwidth is proportional to $\alpha_{11}^{1/2}$ which can be maximized by making γ_i/β as small as possible or the mean electron velocity should be as small as possible.

2.2 Case B. Cylindrical Waveguide Entirely Filled with a Homogenous Mixture of Two Electron Beams

The case of a cylindrical waveguide entirely filled with a homogeneous mixture of two electron beams is considered to show how the space-charge waves differ from ordinary field waves in a waveguide. Let $\mu=P/T$, where P is the electromagnetic energy transported across the waveguide per unit of time, and T is the amount of excess alternating-current kinetic energy similarly transported. Thus, for a field wave $\mu\gg 1$ and for a space-charge wave $\mu\ll 1$. For this case,

$$\mu=\frac{(\gamma/\beta)^2}{1+(\gamma/\beta)^2}\,G(\Delta),\quad 0\leqslant G(\Delta)\leqslant 1. \tag{20}$$

Since $\gamma/\beta\ll 1$, to obtain gain, μ is quite small in this case ($\gamma/\beta\approx 0.1$). This is in contrast to the traveling-wave tube, where γ is of the order of β and, hence, μ is correspondingly larger. Thus, in this case, the matching of the input and output to the beam will be similar to that of a klystron and different from that of a traveling-wave tube wherein one matches electromagnetic fields.

Recent Telecommunication Development

Television Picture Monitor

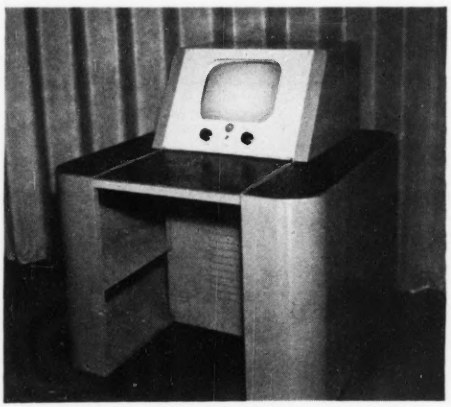

Laboratory and production testing of video-frequency amplifiers for television is expedited with a new high-quality picture monitor. It is equally useful for monitoring the output of a television transmitter and it will not reduce the resolution of the signal being checked. Its resolving power permits operation well beyond 600 horizontal lines.

The deflection circuits have been designed for stable operation and are independent of the separately driven pulse high-voltage supply. This permits the adjustment of horizontal linearity and size without concern for the effect on high voltage. A 16-kilovolt supply aids in producing a bright crisp 14-inch picture.

Designated *FTL-84A*, the monitor is a development of Federal Telecommunication Laboratories.

Periodic-Waveguide Traveling-Wave Amplifier for Medium Powers*

By G. C. DEWEY,† PHILIP PARZEN, and T. J. MARCHESE

Federal Telecommunication Laboratories, Incorporated; Nutley, New Jersey

A THEORETICAL and experimental study of singly corrugated coaxial transmission lines is given here. The properties of the structure as a transmission line are calculated and the effect of the electron beam is taken into account by a field method. Theoretical values of gain and bandwidth are obtained. The results of the experimental study are compared with the theory. An amplifier giving a 50-watt output with 20-decibel gain and 100-megacycle bandwidth at a wavelength of 6.5 centimeters has been obtained. The best power output and efficiency that have been obtained are 125 watts and 7 percent, respectively.

• • •

1. Introduction

Theoretical analyses and experimental studies of helix-type traveling-wave tubes have been carried out by Kompfner[1] and Pierce.[2] Other workers have contributed to the theoretical problem, notably Chu[3] who obtained a boundary-value solution to the problem using Pierce's ideal helical current-sheet boundary and including the effect of Pierce's electron beam by the method of Hahn and Ramo. Field[4] has investigated other types of waveguide structures.

This paper is concerned with a traveling-wave tube using a corrugated-inner-conductor coaxial transmission line with an annular electron beam between the inner and outer conductors. The first part deals with the theoretical analysis of the structure following the method of Goldstein[5] for a field solution in the absence of the electron beam and includes the electronic parameters by the method Chu used for the helix traveling-wave tube. The second part deals with an experimental study and the comparison of the results with the theory.

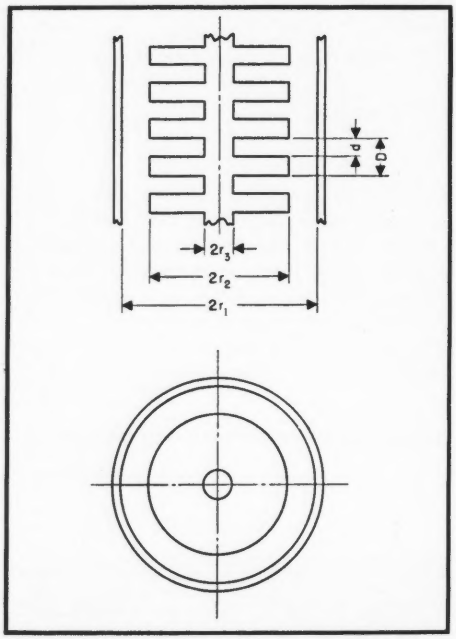

Figure 1—Singly corrugated coaxial transmission line.

* Reprinted from *Proceedings of the I.R.E.*, v. 39, pp. 153–159; February, 1951. A partial summary report under the same title was presented at the National Electronics Conference, Chicago, Illinois, November 5, 1948. This development was sponsored by Coles Laboratory, Signal Corps, United States Army.

† Now with Weapons Systems Evaluation Group, Office of the Secretary of Defense, Washington, District of Columbia.

[1] R. Kompfner, "Traveling Wave Valve," *Wireless World*, v. 52, pp. 369–372; November, 1946.

[2] J. R. Pierce, "Theory of the Beam-Type Traveling-Wave Tube," *Proceedings of the I.R.E.*, v. 35, pp. 111–123; February, 1947.

[3] L. J. Chu and J. D. Jackson, "Field Theory of Traveling-Wave Tubes," *Proceedings of the I.R.E.*, v. 36, pp. 853–862; July, 1948.

[4] L. M. Field, "Some Slow-Wave Structures for Traveling-Wave Tubes," *Proceedings of the I.R.E.*, v. 37, pp. 34–40; January, 1949.

[5] H. H. Goldstein, "Cavity Resonators and Waveguides Containing Periodic Elements," Doctoral Thesis, Massachusetts Institute of Technology; 1943.

The choice of the corrugated coaxial structure from the plethora of possible slow-waveguide structures was made after a wide investigation. The type of amplifier described by Field and the iris-loaded waveguide structure proved to have very limited bandwidth; the singly corrugated coaxial line represented a compromise between gain, power output, and bandwidth.

2. *Theoretical Study*

2.1 Calculation of the Cold Phase Velocity

The structure we are considering, which is assumed to be lossless, is shown in Figure 1. It belongs to a large class of periodic waveguides along with the linear magnetron and the iris-loaded waveguide used in linear-accelerator work. The properties of such structures are dealt with extensively by Brillouin,[6] Slater,[7] and Goldstein;[5] the latter treats in detail, but with certain approximations, the properties of our structure.

The method of solution is to obtain in the annular or "hole" region $r_1>r>r_2$ solutions satisfying Maxwell's equation and meeting the boundary conditions at $r=r_1$, and to obtain standing-wave solutions for the fields in the slots $r_2>r>r_3$, including higher-order cutoff modes. The field expansions are Fourier series, and by equating coefficients, an equation may be obtained with the required degree of approximation depending on the number of terms used.

The wave functions for circularly symmetric *TM* waves in this geometry are Bessel functions of order zero of the first and second kinds. The wave equation is easily separated and the following functions are obtained, taking into account that $E_z=0$ at $r=r_1$ and at $r=r_3$. For $r_1>r>r_2$

$$E_z=\sum_{\infty}^{\infty} A_n Z_0(\gamma_n, r, r_1)e^{ih_n z}$$
$$H_\theta=\sum_{\infty}^{\infty} \frac{ik^2 A_n}{\mu\omega\gamma_n} Z_0'(\gamma_n, r, r_1)e^{ih_n z}, \tag{1}$$

where

$$k^2=\gamma_n^2+h_n^2 \quad \text{and} \quad h_n=H_0+2\pi n/D.$$
$$Z_0(\gamma_n, r, r_1)\equiv J_0(\gamma_n r)\,Y_0(\gamma_n r_1)-J_0(\gamma_n r_1)\,Y_0(\gamma_n r),$$

where the derivatives are taken with respect to the arguments, and k is the free-space wave number.

For $r_3\leqslant r\leqslant r_2$ in the sth slot the fields can be written

$$E_z=\sum_{-\infty}^{\infty} e^{iH_0 sD}\left[a_p Z_0(k_p, r, r_3)\cos\frac{2\pi pz}{d}+b_p Z_0(K_p, r, r_3)\sin\frac{(2p+1)\pi z}{d}\right]$$
$$H_\theta=\sum_{-\infty}^{\infty} e^{iH_0 sD}\,ik^2\left[\frac{a_p}{k_p}Z_0'(k_p, r, r_3)\cos\frac{2\pi pz}{d}+\frac{b_p}{K_p}Z_0'(K_p, r, r_3)\sin\frac{(2p+1)\pi z}{d}\right], \tag{2}$$

where

$$k_p=\left[k^2-\left(\frac{2\pi p^2}{d}\right)\right]^{1/2}$$

and

$$K_p=\left[k^2-\left(\frac{(2p+1)\pi}{d}\right)^2\right]^{1/2}.$$

For one period of the structure at $r=r_2$, the longitudinal electric field must be zero for

$$\frac{D}{2}\geqslant Z\geqslant\frac{d}{2}$$

and for $|Z|\leqslant d/2$, continuity of the fields is required. By the usual manipulation of the Fourier coefficients, (3) is obtained.

$$A_n Z_0(\gamma_n, r_2, r_1)D=\sum_p\sum_q \frac{A_q}{\gamma_q}Z_0'(\gamma_q, r_2, r_3)\frac{2}{d}R_{pqn}$$

$$R_{pqn}=k_p\frac{4h_n h_q\sin\frac{h_n d}{2}\sin\frac{h_q d}{2}}{\left[\left(\frac{2\pi p}{d}\right)^2-h_n^2\right]\left[\left(\frac{2\pi p}{d}\right)^2-h_q^2\right]}\frac{Z_0(k_p, r_2, r_3)}{Z_0'(k_p, r_2, r_3)}\frac{1}{\epsilon_p}$$
$$-K_p\frac{4h_n h_q\cos\frac{h_n d}{2}\cos\frac{h_q d}{2}}{\left[\left((2p+1)\frac{\pi}{d}\right)^2-h_n^2\right]\left[\left((2p+1)\frac{\pi}{d}\right)^2-h_q^2\right]}\frac{Z_0(K_p, r_2, r_3)}{Z_0'(K_p, r_2, r_3)}, \tag{3}$$

[6] L. Brillouin, "Wave Propagation in Periodic Structures," McGraw-Hill Book Co., New York, New York; 1946.

[7] J. C. Slater, "Electromagnetic Waves in Iris-Loaded Wave-Guides," Report 48, Massachusetts Institute of Technology, Research Laboratory of Electronics, Cambridge, Massachusetts; September 19, 1947.

where

$$\epsilon_p = 1, \quad p \neq 0$$
$$\epsilon_p = 2, \quad p = 0.$$

Equation (3) is a set of n homogeneous equations in n unknowns; it is the usual type of equation obtained in these problems and can be solved in principle. Provided the guide wavelength is large compared to D, the amplitudes of the space harmonics are small and one can consider the case where $n = p = q = 0$. This amounts to taking the principal mode in the hole and the first even and odd modes in the slot. For values of $H_0 \rightarrow (\pi/D)$, the space harmonics must be included and Slater[7] has given a more general method of solution to this type of problem.

We are concerned only with geometries where $D < r_2$ and $|H_0 D/2\pi| < 1$. Under these conditions, letting $\gamma_0 = i\gamma_0$, and going to the modified Bessel functions, (3) becomes

$$\gamma_0 \frac{I_0(\gamma_0 r_2)K_0(\gamma_0 r_1) - I_0(\gamma_0 r_1)K_0(\gamma_0 r_2)}{I_1(\gamma_0 r_2)K_0(\gamma_0 r_1) + I_0(\gamma_0 r_1)K_1(\gamma_0 r_2)} = \frac{d}{D} k \frac{J_0(kr_2)Y_0(kr_3) - J_0(kr_3)Y_0(kr_2)}{J_1(kr_2)Y_0(kr_3) - J_0(kr_3)Y_1(kr_2)} \left[\frac{\sin(H_0 d/2)}{H_0 d/2}\right]^2$$
$$+ \frac{8(H_0 d)^2}{D\pi^3}\left(\cos^2 \frac{H_0 d}{2}\right) \frac{I_0\left(\frac{\pi r_2}{d}\right)K_0\left(\frac{\pi r_3}{d}\right) - I_0\left(\frac{\pi r_3}{d}\right)K_0\left(\frac{\pi r_2}{d}\right)}{I_1\left(\frac{\pi r_2}{d}\right)K_0\left(\frac{\pi r_3}{d}\right) + I_0\left(\frac{\pi r_3}{d}\right)K_1\left(\frac{\pi r_2}{d}\right)}. \quad (4)$$

It is convenient to regard (4) as an impedance equation. It can be obtained without the second term on the right by equating at $r = r_2$ the values of E_z/H_θ averaged over a period of the structure for the fields of the two regions. This latter method does not allow one to calculate the effect of the odd-slot mode, which gives an important correction to the phase velocity obtained from the simple method. A qualitative picture of the electric field is shown in Figure 2.

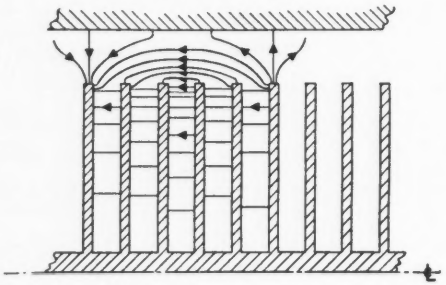

Figure 2—Qualitative picture of the electric field.

For very low frequencies, the asymptotic values of the Bessel functions for small arguments may be used in (4), except in the second term on the right, which is, for most traveling-wave tube geometries, very nearly unity. The resulting asymptotic phase velocity for low frequencies is

$$\frac{V}{C} = \frac{1}{\left[\dfrac{\dfrac{8d^2}{\pi^3 D r_2} - \dfrac{d}{D}\log\dfrac{r_2}{r_3}}{\dfrac{8d^2}{\pi^3 D r_2} - \log\dfrac{r_1}{r_2}}\right]^{1/2}} \quad (5)$$

which is independent of the frequency and always less than the velocity of light. Figure 3 shows the results of an approximate phase-velocity calculation for a typical structure. Figure 4 shows a comparison between measured results and the data computed from (3). The mean error is about four percent and cannot be much reduced without including the effect of several space harmonics.

2.2 Properties with an Electron Beam Filling the Region $r_2 \leq r \leq r_1$

We calculate here, by a small-signal approximation, the modification of the cold properties introduced by a monochromatic electron beam constrained to move axially at a velocity small compared to that of light. Under these conditions, only the z component of the electric field (always neglecting the Lorentz forces) interacts with the electron stream, and it may easily be shown[3] that the alternating-current density has only a z component, which is linearly related to the longitudinal electric field by the relation

$$J = \left[\frac{-\omega e/mJ_0}{v_0^2(\beta - H)^2}\right] E_z,$$

where $\beta = \omega/v_0$.

With this relation, the analysis of Section 2.1 may be carried out and an equation analogous to (3) obtained.

$$\frac{\gamma}{1-\frac{\alpha}{(\beta-H)^2}}P(\gamma, r_2, r_1)$$

$$=\frac{d}{D}k_0\frac{Z_0(k_0, r_2, r_3)}{Z_0'(k_0, r_2, r_3)}\left[\frac{\sin(Hd/2)}{Hd/2}\right]^2$$

$$+\left(\cos^2\frac{Hd}{2}\right)\left[\frac{8(Hd)^2}{D\pi^3}\right], \quad (6)$$

where

$$P=\frac{I_0(\gamma r_2)K_0(\gamma r_1)-I_0(\gamma r_1)K_0(\gamma r_2)}{I_1(\gamma r_2)K_0(\gamma r_1)+I_0(\gamma r_1)K_1(\gamma r_2)},$$

$$\gamma^2=(H^2-k_0^2)\left[1-\frac{\alpha}{(\beta-H)^2}\right],$$

and

$$\alpha=\frac{4\pi(e/m)\rho_0}{v_0^2}$$

$$=9.5\times10^4\frac{J_0}{V_0^{\frac{3}{2}}}\frac{\text{amperes/centimeter}^2}{\text{volts}}.$$

Equation (6) can be solved exactly numerically, but it is far easier to obtain a solution by considering the hot-propagation constant as a perturbation on the cold case. This method is in contradistinction to the method of Pierce[2] who considers the hot modes to be perturbations of the Hahn-Ramo waves traveling on the electron stream.

The propagation constant H, with the electron beam, differs from the cold constant H_0 by a small quantity δ which may be complex. One may modify (6) by expanding P in a Taylor series about $\gamma=\gamma_0$ to the first order in α and δ. Setting $H=H_0$ in the terms on the right (since the term is a correction, the error so introduced is negligible), the equation can be reduced to the following form:

$$\delta(u-\delta)^2+A=0, \quad (7)$$

where

$$u=\beta-H_0$$

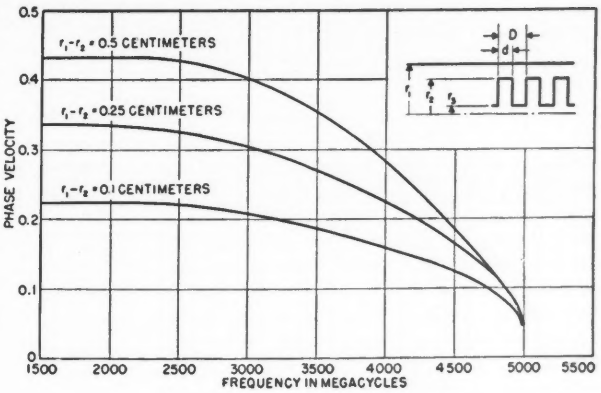

Figure 3—Approximate theoretical phase velocity for a tube in which $d/D=0.135$ and which has dimensions in centimeters of $r_2=1.2$, $r_3=0.4$, and $D=0.15$.

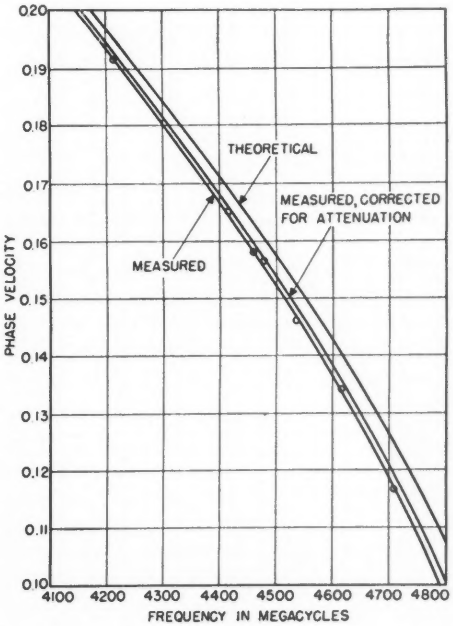

Figure 4—Comparison of the experimental phase velocity with theoretical values calculated from the complete theory.

and

$$A=\left\{\frac{\alpha\left\{\frac{d}{2}k\frac{Z_0(k,r_2,r_3)}{D\,Z_0'(k,r_2,r_3)}\left[\frac{\sin(H_0d/2)}{H_0d/2}\right]^2+\left(\cos^2\frac{H_0d}{2}\right)\left(\frac{8(H_0d)^2}{D\pi^3}\right)\right\}}{\left(P+H_0\frac{dP}{d\gamma}\right)}\right\}_{\gamma=\gamma_0}.$$

Equation (7) is a form of the usual cubic equation obtained in traveling-wave-tube theory.

The imaginary part of the complex pair of roots is the gain in nepers per centimeter. Reduced values of the imaginary part of the complex pair of roots are shown in Figure 5 and for the real part in Figure 6. For calculating the frequency dependence of the gain, one must calculate A as a function of the frequency from the cold theory and then one readily gets the gain and hot phase velocity from Figures 5 and 6 and (7).

For small values of α, i.e., low beam current, the frequency dependence of the gain is mainly determined by the rate of change of u with frequency, i.e., the cold dispersion of the structure. For large values of α, the frequency dependence of A becomes important.

Actual calculation of the performance of a given length of this structure depends on the initial boundary conditions and corrections for the presence of loss. The method in which these calculations are carried out is similar to that used for helix-type traveling-wave tubes for which extensive analyses are available in the literature.[2,3,8,9]

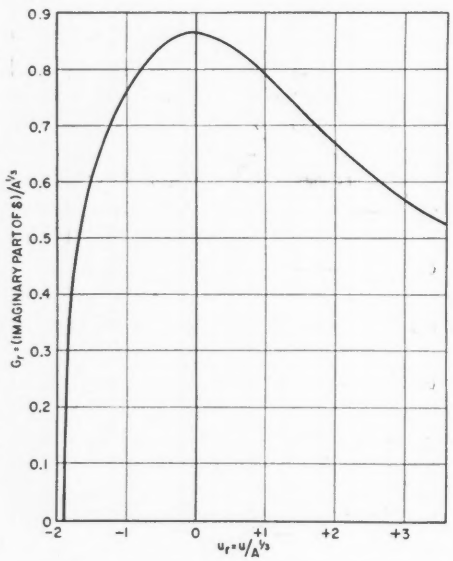

Figure 5—Reduced imaginary part of the complex pair of roots of (7).

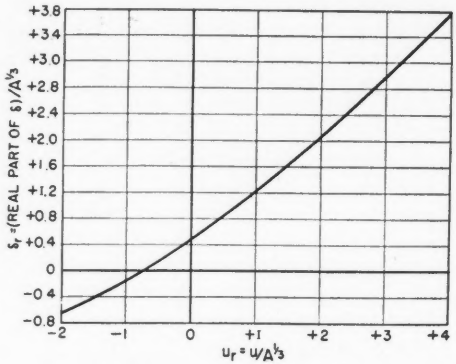

Figure 6—Reduced real part of complex pair of roots of (7)

3. *Experimental Study*

3.1 Description of the Experimental Tube

A number of different structures based on the previous calculation have been made and tested. A drawing of a typical structure is shown in Figure 7.

The corrugated inner conductor is made by assembling punched metallic disks with small metallic spacers on a refractory metallic mandrel and clamping the ends. The dimensions of the active part of the tube are, in the notation of Figure 1 in centimeters,

$r_1=1.35$	$d=0.10$
$r_2=1.20$	$D=0.125$
$r_3=0.20$	length $=l=14.2$.

[8] M. Goudet, "Les Recents Progrès des Tube Amplificateurs pour Ondes Centrimétriques," *Ann. Télécommun.*, v. 3, pp. 445–455; December, 1948.

[9] O. E. H. Rydbeck, "Theory of Traveling-Wave Tubes," Ericsson Techniques No. 46, Telefonaktiebologet L. M. Ericsson, Stockholm; 1948.

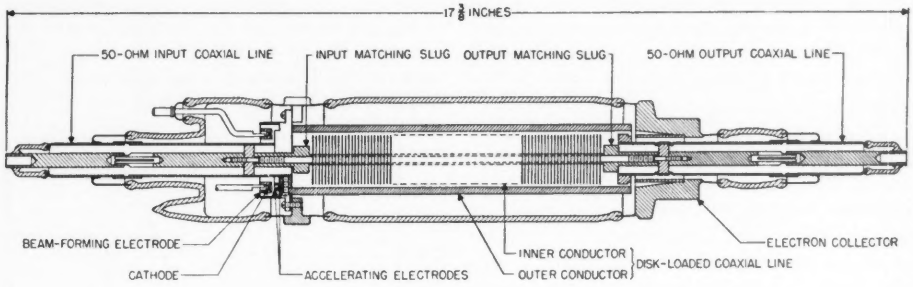

Figure 7—Experimental tube.

The input and output of the corrugated coaxial structure are matched to $\frac{5}{8}$-inch outside-diameter 50-ohm coaxial transmission line. The outer conductor has three longitudinal slots cut through it; the slots have been found to prevent propagation of an asymmetrical mode, which otherwise propagates freely and causes the amplifier to oscillate.

The annular electron beam is obtained from a pure tantalum ring emitter operated temperature limited for control of the beam current. The electrostatic and magnetic fields are so controlled that the electron orbits are very nearly rectilinear and space-charge forces, in the range of currents used, are generally small. The annular beam enters the coaxial structure through an annulus with four transverse spokes that serve to connect the outer conductors for radio-frequency currents. The beam leaves through a similar structure and is collected on a separate collector. The ratio of collected current to cathode current has varied between 0.6 and 0.8. The maximum possible beam efficiency is about 0.8 due to the part of the area of the annulus subtended by the radial spokes.

3.2 Experimental Results and Comparison with Theory

The operation of a dispersive traveling-wave tube of this type is characterized by a resonant dependence of the electronic gain and power output on frequency. The terminal impedance match is sufficiently broad-band so that the electronic properties alone determine the frequency response of the amplifier.

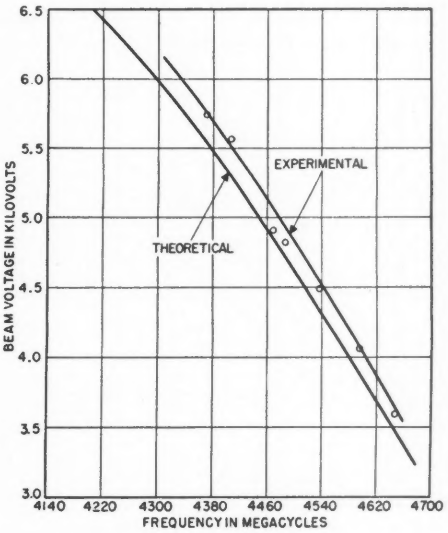

Figure 8—Experimental resonance beam voltage for very small beam currents.

Figure 8 shows the resonance voltage[10] as a function of frequency taken with very small beam currents. This curve gives a relation between beam voltage and frequency that allows one to plot the various parameters as a function of this beam voltage. Operation in a region of power saturation causes an upward shift in the resonance beam voltage, but the shift has never exceeded 10 percent.

[10] The ratio of d/D for the theoretical curve is larger than that for the experimental curve, which explains the higher experimental voltages in contrast to Figure 4.

Figure 9 shows the small-signal gain of the tube, with finite cold attenuation, as a function of beam current for various values of the beam voltage, which corresponds to the values of frequency given.

The gain of the amplifier as a function of power level exhibits the usual marked saturation effect seen in traveling-wave tubes. As the power input increases, a point is finally reached where an increase in the input power results in a decrease in the output power. The power output is then the maximum power output of the tube.

Figure 10 shows the saturation power output as a function of beam current. In the curves in Figure 10, a slight shift towards higher voltage has taken place due to saturation.

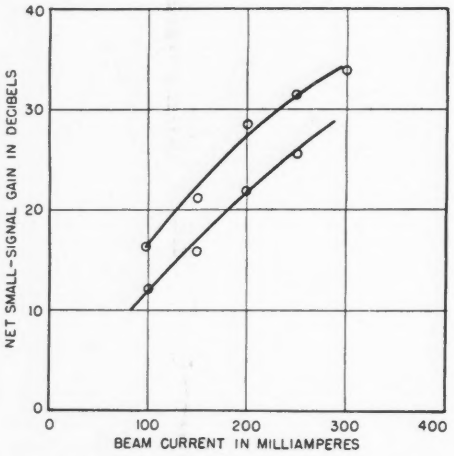

Figure 9—Small-signal gain plotted against beam current. The values of V_0 in kilovolts and frequency in megacycles for the upper curve are 3.6 and 4650 and, for the lower curve, 4.6 and 4550.

In comparing these results with the theory, it is necessary to take into account the excitation of the three forward waves at the input and the effect of the insertion loss. Excitation of the three forward waves results in a loss calculated[2,11] to be 9 decibels in the growing wave at synchronism. The value of this excitation loss can be shown by (7) to depend in a complicated fashion on the cold attenuation and the separation of the beam velocity from that for synchronism. The nature of this dependence is not sensitive and the value of excitation loss varies from 6 to 12 decibels for practical ranges of operation. The correction obtained for attenuation L, uniform along the structure, has been calculated by numerous authors[2,8] and it can be shown that (7) leads to the same conclusion, that one must subtract one-third the attenuation from the gross electronic gain for small values of attenuation. The behavior for values of attenuation comparable to the gain can be shown by (7) to require subtracting about one-half the total loss. Subject to the use of approximate values, the formula relating the net gain G_{net} to the gain per unit length G, which was calculated in Section 2, is

$$G_{net} = lG - 9 - \frac{2L}{5} \text{ decibels.} \qquad (8)$$

The values G in decibels per centimeter obtained from the experimental results by (8) are compared to the theoretical values in Figure 11.

The frequency dependence of the gain for fixed beam voltage is readily calculated from (7), and Figure 12 shows the experimental gain as a func-

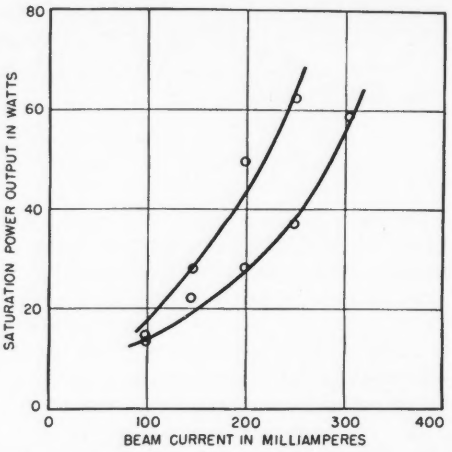

Figure 10—Saturation power output plotted against beam current. In the upper curve, $V_0 = 4.9$ kilovolts, $f = 4550$ megacycles, and the gain is 16.9 decibels. The values for the lower curve are, respectively, 4.0, 4650, and 20.

[11] J. R. Pierce, "Effect of Passive Modes in Traveling-Wave Tubes," *Proceedings of the I.R.E.*, v. 36, pp. 993–996; August, 1948.

tion of frequency compared to the theoretical value, again by means of (8). The tube was operating partly saturated when this curve was taken, which has resulted in a shift of the center

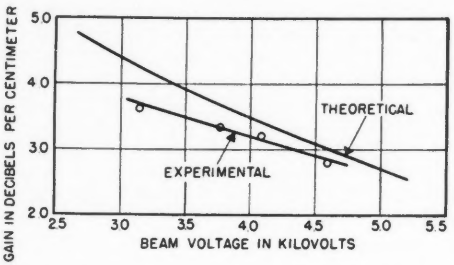

Figure 11—Gain per unit length for an experimental tube with small-signal input compared with theoretical values, for 250 milliamperes beam current.

frequency of the experimental curve towards the theoretical value.

3.3 Power Output

The power output of a traveling-wave tube cannot be calculated from the foregoing analysis due to the failure of the small-signal approximation. In general, numerical techniques are required. However, experimental studies of helix tubes and qualitative theoretical arguments indicate that the power output is in general given by

$$P_{\text{sat}} = \frac{KG\lambda_g}{8.68\pi(3)^{\frac{1}{2}}} I_0 V_0, \qquad (9)$$

where G is the electronic gain in decibels per centimeter and K is a constant that depends on a variety of factors; K is most sensitive to the uniformity and losslessness of the output section of the tube. For helix tubes, values of K as high as three have occasionally been obtained. We have been largely unable to control the magnitude of the attenuation in the output section of our tube. The values of K corresponding to the measured powers shown in Figure 10 range between 0.9 and 1.2. The best values of efficiency

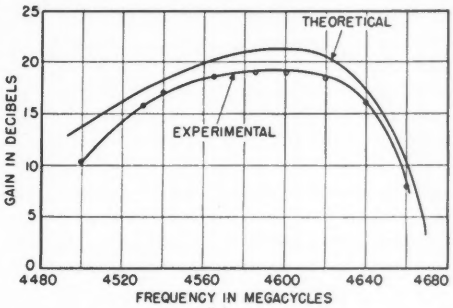

Figure 12—Experimental and theoretical gain plotted against frequency. In the experimental case, the power input was 0.50 watt. The beam values were 4 kilovolts and 200 milliamperes.

and power output that have been obtained are about 7 percent and 125 watts at about 4.5 kilovolts and 380 milliamperes beam current with a gain of about 17 decibels. In view of the work with the helix tubes and of certain theoretical arguments, it is likely that efficiencies of the order of 15 to 25 percent and power outputs in the vicinity of 500 watts are possible in this frequency range with tubes of this general type.

Effect of Hydrostatic Pressure in an Electron Beam on the Operation of Traveling-Wave Devices*

By PHILIP PARZEN and LADISLAS GOLDSTEIN

Federal Telecommunication Laboratories, Incorporated; Nutley, New Jersey

SMALL velocity spreads in an electron beam appear to cause a decrease in gain and noise figure of a traveling-wave tube. The actual decrease depends on a quantity μ, which can be interpreted physically as a measure of the ratio of the coupling of the electrons to each other via the hydrostatic pressure to the coupling of the electrons to the external waveguide circuit. Thus, physically, the effect of the velocity spread is to introduce further interactions among the electrons, in which the external circuit does not take part. This interaction may be thought of as a hydrostatic pressure similar to that in a liquid or gas.

• • •

The macroscopic properties of a gas can be calculated from the distribution function $f(x, u, t)$, where $fdxdu$ is the number of particles having their position between x and $x+dx$ and their velocity between u and $u+du$. This function can be determined from the Boltzmann transport equation which, if written in one dimension, is

$$(\partial f/\partial t)+u(\partial f/\partial x)+a\partial f/\partial u=\partial f/\partial t|_{\text{collision}}, \quad (1)$$

where a is the acceleration of a particle. Equation (1) is the mathematical statement of the conservation of the number of particles in detail along a flow line.

The mean (drift) velocity v and total particle density n are given by

$$n=\int f du, \quad (2)$$

$$v=(1/n)\int uf(u)du, \quad (3)$$

and only velocities in the x direction are considered.

As shown by Chapman and Cowling,[1] the integrals of (1), which express the conservation of matter on the whole and momentum, eliminate the collision term and also determine the variation of the total particle density and mean velocity.

These expressions are

$$(\partial n/\partial t)+\partial(nv)/\partial x=0, \quad (4)$$

$$dv/dt=a-\partial P/nm\partial x, \quad (5)$$

where m is the mass of a particle and P is the hydrostatic pressure.

The evaluation of P may be carried out in terms of an equivalent temperature T of the distribution function. Thus,

$$kT/2=(1/n)\int \tfrac{1}{2}m(u-v)^2 f du, \quad (6)$$

$$P=nkT, \quad (7)$$

k being Boltzmann's constant.

We see from (5) that the effect of the distribution on the mean velocity is to introduce an additional term in the force equation. The advantage of working with these integral expressions is that they constitute two simultaneous differential equations for n and v in those flow processes in which T is constant. This constitutes a considerable simplification in the solution of flow problems in a gas.

A, perhaps, trivial example of such a process is that of isothermal flow in a gas. The more important example of an approximately isothermal process that we wish to discuss here is that of interaction between an electron gas and an electromagnetic wave, in which the determination of n and v are of paramount importance.

* Reprinted from *Journal of Applied Physics*, v. 22, pp. 398–401; April, 1951. This work was sponsored by the Signal Corps Engineering Laboratories.

[1] Chapman and Cowling, "Mathematical Theory of Non-Uniform Gases," Cambridge University Press, London; 1939: p. 51.

It is well known that electromagnetic waves propagate in electron beams[2,3] and under certain conditions, which occur for example in the traveling-wave tube[4] and in the double-electron-beam tube,[5] there exists amplification of the electromagnetic wave. In these problems, the calculation of gain depends on the change in velocity, charge density, and current density by the perturbing electromagnetic traveling wave. The magnitude of this change will also depend on the distribution function f. We shall now calculate this for the one-dimensional case of an electron beam traveling in an electromagnetic field characterized by an electric field E in the same direction. Thus

$$E=\bar{E}\exp(j\omega t-\Gamma x), \tag{8}$$

$$a=-e\bar{E}\exp(j\omega t-\Gamma x)/m, \tag{9}$$

where the tilde indicates an alternating-current value.

The electron beam is considered as an electron gas with a direct-current distribution function $f_0(u)$ and drift velocity u_0. In accordance with the usual small-signal approximations, we assume that with the perturbing electric field

$$\left.\begin{aligned} v&=u_0+\tilde{v}\exp(j\omega t-\Gamma x)\\ n&=n_0+\tilde{n}\exp(j\omega t-\Gamma x)\\ T&=T_0+\tilde{T}\exp(j\omega t-\Gamma x)\\ J\text{ (current density)}&=J_0+\tilde{J}\exp(j\omega t-\Gamma x)\\ J_0&=-en_0u_0\\ \tilde{J}&=-e(n_0\tilde{v}+\tilde{n}u_0). \end{aligned}\right\} \tag{10}$$

Substituting these into (4), (5), and (7) and retaining only first-order terms, we have

$$\begin{aligned} &j\omega\tilde{v}-\Gamma u_0\tilde{v}\\ &\quad=-(e\bar{E}/m)+\Gamma(kT_0\tilde{n}/mn_0)+\Gamma(k\tilde{T}/m), \end{aligned} \tag{11}$$

$$j\omega\tilde{n}-\Gamma(n_0\tilde{v}+\tilde{n}u_0)=0. \tag{12}$$

We shall now assume that the process is isothermal. Thus, $\tilde{T}=0$. Under these conditions,

$$\tilde{J}=j\beta I_0\bar{E}/2V_0[(-\Gamma+j\beta)^2-\alpha\Gamma^2], \tag{13}$$

$$\tilde{v}=-u_0(j\beta-\Gamma)\bar{E}/2V_0[(j\beta-\Gamma)^2-\alpha\Gamma^2], \tag{14}$$

$$\tilde{n}=-n_0\Gamma\bar{E}/2V_0[(j\beta-\Gamma)^2-\alpha\Gamma^2], \tag{15}$$

where

$$\begin{aligned} &\beta=\omega/u_0,\\ &I_0=en_0u_0=\text{direct-current density},\\ &V_0=\text{voltage corresponding to } u_0, \text{ and}\\ &\alpha=kT_0/mu_0^2, \end{aligned} \tag{16}$$

which is a measure of the random energy to the directed energy. For $\alpha=0$, these equations reduce to those quoted elsewhere.[4,5]

To calculate the interaction between the electron beam and the electromagnetic field, it is necessary to add to these equations the circuit equations. These are obtained from Maxwell's equations and are determined by the geometry of the surrounding waveguide system. We shall now give these calculations for the traveling-wave tube, using the method of Pierce[4] to obtain the circuit equation for a filamentary electron beam.

1. Effect of Velocity Spread in a Traveling-Wave Tube with a Filamentary Electron Beam

Here n = number of electrons per unit length and $\tilde{J}$ = total current.

According to Pierce,[4] the relation between alternating current $\tilde{J}$ and the alternating electric field $\bar{E}$ on the axis is

$$\bar{E}=\tilde{J}\Gamma_0/\psi_0(\Gamma^2-\Gamma_0^2) \tag{17}$$

if only one mode is considered; Γ_0 and ψ_0 are the propagation constant and admittance, respectively, of the waveguide in the absence of the beam.

Substituting this into (13), we have the following equation for Γ:

$$\Gamma^2-\Gamma_0^2=j2\beta^3C^3\Gamma_0/(-\Gamma+j\beta)^2-\alpha\Gamma^2. \tag{18}$$

$$\begin{aligned} C&=\text{Pierce coupling coefficient}\\ &=(I_0/\psi_0\beta^24V_0)^{1/4}. \end{aligned} \tag{19}$$

---

[2] W. C. Hahn, "Small Signal Theory of Velocity Modulated Electron Beams," *General Electric Review*, v. 42, pp. 258–270; June, 1939.

[3] S. Ramo, "Electronic-Wave Theory of Velocity Modulation Tubes," *Proceedings of the I.R.E.*, v. 27, pp. 757–763; December, 1939.

[4] J. R. Pierce, "Theory of Beam Type Traveling-Wave Tube," *Proceedings of the I.R.E.*, v. 35, pp. 111–123; February, 1947: p. 114.

[5] A. V. Haeff, "Electron-Wave Tube—A Novel Method of Generation and Amplification of Microwave Energy," *Proceedings of the I.R.E.*, v. 37, pp. 4–10; January, 1949.

We shall calculate Γ for the synchronous case only. Thus,

$$\Gamma_0 = j\beta.$$

Let

$$\Gamma = j\beta - \delta; \quad \delta \ll \beta. \tag{20}$$

Thus, to first-order terms in δ, (19) becomes

$$\delta^3 + \alpha\beta^2\delta = -j\beta^3 C^3. \tag{21}$$

Now let $\delta = j\beta CX$ and $\mu = \alpha/C^2$, hence,

$$X^3 - \mu X - 1 = 0. \tag{22}$$

As is well known, an amplified wave corresponds to a complex root of (22).

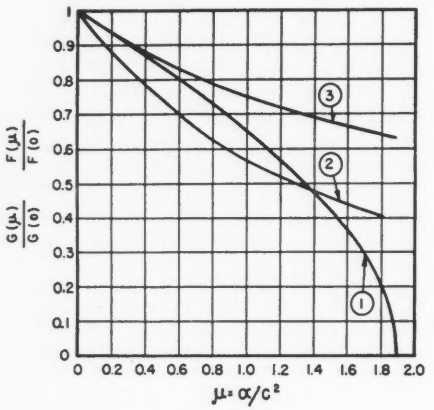

Figure 1—Reduction in gain and noise figure in a traveling-wave tube as a result of velocity spread. Plotted against μ, are relative values of (1) gain in decibels per centimeter, (2) noise figure for current-modulation fluctuations, and (3) noise figure for velocity-modulation fluctuations.

Let $G(\mu)$ = gain of the growing wave in decibels per centimeter for any μ. Hence

$$G(\mu)/G(0) = 2X_i/3^{1/2}, \tag{23}$$

X_i being the imaginary part of a root of (22).

$G(0)$ corresponds to the case of a monochromatic beam. In Figure 1, $G(\mu)/G(0)$ is plotted against μ. It is seen that the gain is reduced by the velocity spread in the beam. Let us consider the following example: $kT_0 = 0.10$ volt (corresponding to a cathode temperature ≈ 1200 degrees Kelvin),† $C = 0.015$, and $V_0 = 500$ volts. Then $\mu = 1$ and the reduction in gain is about 65 percent.

Thus, considerable reductions in gain from that given by the Pierce equation may be ascribed to a velocity spread in the electron beam.

2. *Effect of Velocity Spread on Noise Figure in Traveling-Wave Tubes*

Here, it is important to know the magnitude of the field in each mode that is excited by an initial input of electric field E, velocity modulation $\tilde{v}$, or current modulation $\tilde{J}$. From (13), (14), and (15), the initial conditions are

$$\Sigma E_i = E, \tag{24}$$

$$\Sigma (j\beta - \Gamma_i)E_i/(j\beta - \Gamma_i)^2 - \alpha\Gamma_i^2 = -2V_0\tilde{v}/u_0, \tag{25}$$

$$\Sigma [E_i/(j\beta - \Gamma_i)^2 - \alpha\Gamma_i^2] = 2V_0\tilde{J}/j\beta I_0, \tag{26}$$

for $\alpha = 0$, these are the same conditions as those of Pierce.

If α is assumed to be small, these reduce to

$$\Sigma e_i[1 - 2j\alpha(\beta/\delta_i) + \alpha(\beta/\delta_i)^2] = E, \tag{24A}$$

$$\Sigma e_i/\delta_i = -2V_0\tilde{v}/u_0, \tag{25A}$$

$$\Sigma e_i/\delta_i^2 = 2V_0\tilde{J}/j\beta I_0, \tag{26A}$$

where

$$\delta_i = j\beta - \Gamma_i \quad \text{and} \quad e_i = E_i/[1 - 2j\alpha(\beta/\delta_i) + \alpha(\beta/\delta_i)^2].$$

The gaining wave E_1 with a corresponding root X_1 of (22) is

$$E_1 = [1 - 2j\alpha(\beta/\delta_1) + \alpha(\beta/\delta_1)^2] \times \frac{E + \tilde{v}(2V_0/u_0)(\delta_2 + \delta_3 - 2j\alpha\beta) + (2V_0/j\beta I_0)(\delta_2\delta_3 - \alpha\beta^2)\tilde{J}}{(1 - \delta_2/\delta_1)(1 - \delta_3/\delta_1)}. \tag{27}$$

We shall now compute the noise figure F for the following two cases using the method of Pierce.

2.1 Case 1

Beam enters the waveguide with only current-modulation fluctuations.

† It can be shown with the aid of (40) that the direct-current process for rectilinear electron beams of small current density is essentially isothermal.

Here,

$$F(\mu)/F(0) = |\delta_2\delta_3 - \alpha\beta^2|^2/\beta^4C^4 = |1+X_1\mu|^2/|X_1|^2, \quad (28)$$

$$F(0) = 2\Gamma^2 eV_0C/kT. \quad (29)$$

In Figure 1, we have plotted $F(\mu)/F(0)$ against μ. It is seen that the noise figure is reduced by the velocity spread in the beam.

2.2 CASE 2

Beam enters the waveguide with only velocity modulation $\tilde{v}$.

Here,[6]

$$\langle v^2\rangle_{hf} = 4\eta kT_c(1-\tfrac{1}{4}\pi)\Delta f/I_0, \quad (30)$$

where $\eta = e/m$ and T_c = cathode temperature in degrees Kelvin.

$$F(\mu)/F(0) = |\delta_2+\delta_3-2j\alpha\beta|/\beta^2C^2 = |X_1|^2, \quad (31)$$

$$F(0) = 2(1-\tfrac{1}{4}\pi)T_c/TC, \quad (32)$$

where T = ambient temperature in degrees Kelvin.

In Figure 1, $F(\mu)/F(0)$ is plotted against μ. Here, too, the noise figure is reduced by velocity spread.

3. *Partial Justification of $\tilde{T}=0$*

We shall now determine under what conditions the alternating-current temperature $\tilde{T}$ may be neglected. We shall estimate this by deriving (13) by another method that deals with the distribution function f itself without regard to the concepts of pressure and temperature, which may be derived from f.

Let $f_0(u)du$ be the direct-current distribution function. Then, from the Boltzmann transport equation, neglecting collisions and making the usual small-signal approximations, the alternating-current density $d\tilde{J}$ due to the electrons whose speed lies between u and $u+du$ is given by

$$d\tilde{J} = j\omega\eta eEf_0(u)du/(j\omega-\Gamma u)^2. \quad (33)$$

This can also be obtained by a derivation similar to that of Pierce.[7] Hence,

$$\tilde{J} = j\omega\eta eE\int f_0(u)du/(j\omega-\Gamma u)^2 = j\omega\eta eEP. \quad (34)$$

[6] A. J. Rack, "Effect of Space Charge and Transit Time on the Shot Noise in Diodes," *Bell System Technical Journal*, v. 17, pp. 592–619; October, 1938.

[7] J. R. Pierce, "Possible Fluctuations in Electron Streams Due to Ions," *Journal of Applied Physics*, v. 19, pp. 231–236; March, 1948.

Now let $\Delta = u-u_0$ and assume that f_0 is such that $f_0(\Delta)\neq 0$ only for $\Delta<\Delta_0$.

Thus, we are dealing only with very small velocity spreads. Hence,

$$P = \int_{-\Delta_0}^{\Delta_0} f_0(\Delta)d\Delta/(j\omega-\Gamma u_0-\Gamma\Delta)^2. \quad (35)$$

Let us further assume that

$$|j\omega-\Gamma u_0| \gg |\Gamma\Delta_0|. \quad (36)$$

Then

$$P = \frac{1}{(j\omega-\Gamma u_0)^2} \times \int f_0(\Delta)\left[1-\frac{2\Gamma\Delta}{j\omega-\Gamma\mu_0}+\frac{3\Gamma^2\Delta^2}{(j\omega-\Gamma\mu_0)^2}\right]d\Delta, \quad (37)$$

by expanding the integrand of (35) up to terms in Δ^2. Now

$$\left.\begin{aligned} &\int f_0(\Delta)d\Delta = n_0 \\ &\int f_0(\Delta)\Delta d\Delta = 0 \\ &\int f_0(\Delta)\Delta^2 d\Delta = n_0kT_0/m \text{ by (6).} \end{aligned}\right\} \quad (38)$$

Hence,

$$\tilde{J} = [j\beta I_0\tilde{E}/2V_0(-\Gamma+j\beta)^2] \times[1+3\alpha\Gamma^2/(-\Gamma+j\beta)^2], \quad (39)$$

which is equivalent to (13) for small α/C^2 except for a factor of 3. The requirement stated in (36) is also valid for small α/C^2.

This derivation, however, is not correct, in that it neglects the effect of collisions. There are two types of collisions to be considered. The collisions of electrons with gas atoms or positive ions may be neglected if the frequency of the electromagnetic wave is much greater than the collisional frequency. This will always be true for sufficiently high frequencies and sufficiently low gas pressures. The collisions between electrons because of their coulombian law of interaction may not be neglected. It is the electron–electron interaction that will determine whether the process is isothermal.

While one may not hope to solve the Boltzmann equation with this collision term, it is possible to use a method of successive approximations[8] that depends on the fact that f is

[8] See p. 107 of reference 1.

completely determined by a knowledge of certain macroscopic quantities that are functions of position and time only. These are n, v, and T. The variation of n and v is given by (4) and (5). The equation[1] governing the variation of T, which is equivalent to the conservation of energy, is

$$dT/dt = -2T(\partial v/\partial x) - 2\partial q/kn\partial x. \quad (40)$$

The random energy flow per unit area per unit time is

$$q = m\int \tfrac{1}{2}(u-v)^3 f\,du. \quad (41)$$

In this method of successive approximations, the first approximation is one for which $q=0$ and f is essentially maxwellian. For the second approximation, which is the first to depend on the nature of the interaction or collisions among the particles,

$$q = -\lambda\partial T/\partial x, \quad (42)$$

where λ, the coefficient of thermal conductivity, is a function of the collision forces, n, and T. Thus, to this order of approximation, n, v, T may be determined from (4), (5), (40), (41), and (42). Repeating the steps of the small-signal approximation as previously gives the alternating-current density $\tilde{J}$ as

$$\tilde{J} = j\beta I_0 E/2V_0[(j\beta-\Gamma)^2 - \alpha\Gamma^2(1+2/r)], \quad (43)$$

with

$$r = 1+2\lambda\Gamma^2/kn_0(j\omega-\Gamma\mu_0), \quad (44)$$

where, in accordance with the small-signal approximations, λ is now a constant and is computed at n_0, T_0. There is a similar change in the denominator in the expressions for $\tilde{n}$ and $\tilde{v}$.

Now, for an adiabatic process, $\lambda=0$ and $r=1$; and for an isothermal process, $\lambda=\infty$ and $r=\infty$.

Thus, as λ goes from 0 to ∞, this is the equivalent of the process going from adiabatic to isothermal. Also, it is seen from (43) that the effect of an adiabatic process over that of an isothermal process is to triple the value of α. Thus, it is possible to say that, for the actual physical process, the effective α will always lie somewhere between α and 3α. It is seen in general that for $r\gg 2$, the process is essentially isothermal. Now λ can be computed for the case of electron–electron interaction from an equation given by Chapman and Cowling.[9] For $n_0=10^9$ and $T_0=1000$ degrees Kelvin, $\lambda=18$ centimeter-gram-second units. Taking the values of Γ computed previously on the assumption of an isothermal process and substituting them into r, r is given approximately by

$$r = 1+2\lambda\beta^2/kn_0\omega CX. \quad (45)$$

For practical values, $\beta>10$ and $\omega=2\pi\times5\times10^9$, $X\approx1$; $r\approx100$. Hence, in the traveling-wave tube, the process is isothermal. In general, whether the process is isothermal can be ascertained only by computing r for each process and geometry under consideration. Furthermore, it is seen that the analysis used in deriving (39) tacitly assumes an adiabatic process in that it neglects the coulombian collisions among particles.

4. Conclusions

Small velocity spreads in an electron beam appear to cause a decrease in gain and noise figure of a traveling-wave tube. The actual decrease depends on a quantity μ, which can be interpreted physically as a measure of the ratio of the coupling of the electrons to each other via the hydrostatic pressure to the coupling of the electrons to the external waveguide circuit. Thus, physically, the effect of the velocity spread is to introduce further interactions between the electrons, in which the external circuit does not take part. This interaction may be thought of as a hydrostatic pressure,[10] similar to that in a liquid or gas.

---

[9] See p. 179 of reference 1.

[10] W. C. Hahn, "Effects of Hydrostatic Pressure on Electron Flow in Diodes," *Proceedings of the I.R.E.*, v. 36, pp. 1115–1121; September, 1948.

Magneto-Optics of an Electron Gas with Guided Microwaves *

By LADISLAS GOLDSTEIN, M. A. LAMPERT, and J. F. HENEY

Federal Telecommunication Laboratories, Incorporated; Nutley, New Jersey

IN RECENT YEARS the magneto-optics of electromagnetic-wave propagation have been extended to guided propagation at microwave frequencies. In particular, Faraday-effect experiments have been made[1-4] in which the plane of maximum E field of the TE_{11} mode in a circular waveguide is rotated by propagation through a section of the guide filled with a liquid or solid dielectric and located in an axial unvarying magnetic field. In all of the published work to date, very small angles of rotation are obtained per guide wavelength, even at the gyromagnetic resonant field.

We have performed magneto-optic propagation experiments in circular waveguides in the range of frequencies from 4600 to 5500 megacycles per second employing as the dielectric the decaying plasma from a pulsed direct-current gas discharge. The main results are:

A. Very large angles of rotation, on the order of 90 degrees or more per guide wavelength, exhibiting a pronounced resonance behavior in the region where the gyromagnetic frequency of the electrons approaches the signal frequency.

B. Departure from linear polarization as resonance is approached. Polarization becomes more broadly elliptical and finally almost purely circular at resonance.

C. Demonstration of an analogue, for guided microwaves, of the crossed-Nicol-prisms experiment.

The anisotropic electron gas is produced by a pulsed direct-current discharge in a hot-cathode tube containing a rare gas, which completely fills a 5-inch-long section of guide that is enveloped by a solenoid. A signal pulse 10 microseconds wide, with variable time delay after the direct-current discharge pulse, is sampled by a probe, in a following section of guide, that can be mechanically rotated about the guide axis.

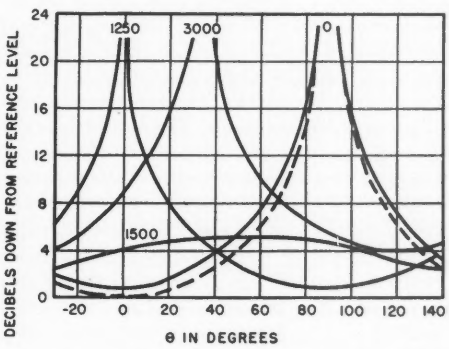

Figure 1—Relative radio-frequency field distribution over the periphery of a circular waveguide plotted as a function of angle for the four indicated magnetic field intensities H in gausses. The solid lines are with and the broken lines are without a gas discharge. The gas was a mixture of neon with 1 percent of argon at a pressure of 1 millimeter of mercury. The reference plane for θ and the reference level for the E-field values are the plane and amplitude, respectively, of the maximum E field with no discharge. The radio-frequency signal pulse was applied 50 microseconds after a 5-microsecond-duration direct-current discharge pulse having peak values of 1050 volts and 135 milliamperes.

In Figure 1, the radio-frequency electric field at the guide periphery is plotted as a function of angle for several values of magnetic field. In Figure 2, the angle of rotation of the plane of maximum E field is plotted as a function of the magnetic field. The experimental conditions are indicated on the graphs. Measurements were made at 4600, 4900, 5200, and 5500 megacycles in a guide with cutoff at 4430 megacycles over a range of gas pressures from 0.5 to 100 millimeters

* Reprinted from the *Physical Review*, v. 82, pp. 956–957; June 15, 1951. This work was sponsored by the Signal Corps Engineering Laboratories of the United States Army.

[1] P. Keck, "Der Faraday effect in Ionisierten Gases," *Annallen der Physik*, Series 5, v. 15, pp. 903–925; December, 1932.

[2] M. C. Wilson and G. F. Hull, Jr., "On the Faraday Effect At Microwave Frequencies," *Physical Review*, v. 74, p. 711; September 15, 1948.

[3] R. G. Barnes and G. F. Hull, Jr., "Microwave Faraday Effect." Presented at meeting of American Physical Society, New York, New York; February, 1951.

[4] J. Soutif-Guicherd and M. M. Lambinet, "Mise en Evidence de la polarization rotatoire Magnetique a la frequence de 3000 MHz," *Comptes Rendus*, v. 231, pp. 1460–1461; December, 1950.

of mercury, and at various pulse direct currents and voltages.

The results obtained are readily explained in terms of decomposition of the "linear" TE_{11} wave into two oppositely rotating circularly polarized waves, an "anomalous" and a "normal" wave. The anomalous wave exhibits, in the region of gyromagnetic resonance, very strong attenuation and a reversal of the sign of its phase shift with respect to propagation in vacuum. The normal wave is only slightly attenuated in this region and accounts for the circular polarization observed at gyromagnetic resonance.

The roles of anomalous and normal waves are interchanged if the sense of the magnetic field is reversed. Consequently, each of the circularly polarized waves is heavily attenuated by one or the other of two opposing magnetic fields, both at gyromagnetic resonance. This fact enabled the construction, with two independent solenoids, of a microwave analogue of crossed Nicol prisms.

The circularly polarized waves are not true propagating modes through the plasma in these experiments. Our interpretation remains, however, valid because a short section of plasma was employed. The theoretical details have been worked out for the case of the unbounded anisotropic plasma, including electron-collision effects. Further theoretical work remains for the waveguide case.

These results hold promise as a tool for the study of gas discharge phenomena. They are applicable also to switching, amplitude, phase, or frequency modulation, and polarization control in an electronically controllable medium.

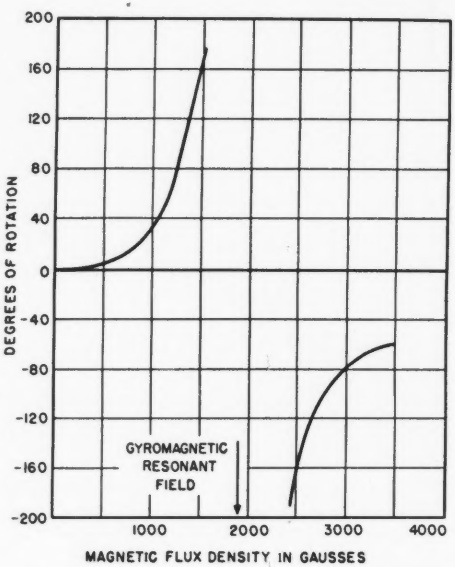

Figure 2—Rotation of the plane of the maximum E field plotted against the magnetic field intensity.

Growth and Amplification*

By HENRY BUSIGNIES

Federal Telecommunication Laboratories, Incorporated; Nutley, New Jersey

FOR CENTURIES, classical theories in the field of physics sufficed for the study of phenomena and the prediction of effects. More recently, complex and puzzling small-scale occurrences forced the development of a more penetrating set of theories. Heisenberg's uncertainty principle, the methods of statistical mechanics, modern communications theories, the laws governing certain nuclear phenomena, and even developments in cybernetics have largely revolutionized scientific thought in branches of physics, chemistry, and biology and begin to impinge on psychology.

It is already clear that, on the "micro" scale, phenomena are largely random, unpredictable, statistical in nature, and influenced by extremely minute disturbances. The "micro" phenomena then build up to, and "control" the larger-scale or "macro" effects. Thus initial uncertainty, minute influences, a definite effect, amplification of that effect, and a major result all seem parts of the same chain of events.

Modern communications engineers will therefore find much to interest and stimulate them in the following searching and inspiring guest editorial by the Technical Director of the Federal Telecommunication Laboratories, Inc., who has received the Fellow Award of The Institute of Radio Engineers and has served on a number of its Technical Committees.—*The Editor* (*Proceedings of the I.R.E.*)

THE URGE of educated man to see, feel, and analyze smaller and smaller quantities, as well as to see and communicate farther, has been satisfied with no greater brilliance than in the production of the microscope, telescope, and electronic amplifier. Actually, amplification has already reached in some fields that extreme limit where distinguishable patterns of intelligence or orderliness have disappeared in the apparent chaos of random effects.

It is at this low level of random effect that all events and all things that later become perceptible to man are born and grow. This applies to thoughts that, in the originating or some other brain, are developed intentionally or otherwise to produce a masterpiece of art or literature, an airplane crash, the tallest building, or a concept of human progress. It includes such things as the molecules that assemble into the seed that may precede by even a decade or two a mature living creature, and also the agitation of the still air that produces the tornado.

History shows that at some particular place and time and in a favorable environment a very minute pattern emerges from chaos and, supported by other forces, feedback, and correlation, attains a growth that finally produces a significant phenomenon of distinguishable proportions. Then through some such effect as saturation, growth stops and stabilization occurs, only to be succeeded by decay. Growth is not linear in most cases; it proceeds through thresholds and intermediate steps, and consumes from microseconds to years to produce an end result. At its origin and for a fraction of its early life, the magnitude of the emerging pattern is so minute that it could be influenced, shifted, modified, or destroyed by a force of the same order of magnitude. One is led to believe that, however small they may be, brain waves could influence the outcome of physical events if they were available in suitable form at just the right time, and thus by the proper application of man-made patterns of very small magnitude, beneficial control of large physical effects could be achieved.

In the superregenerative circuit of Professor Armstrong, a small electromotive force corresponding to a signal pattern just above the thermal-agitation level builds up in a fraction of a millisecond to become perceptible to the human senses: but it could have been influenced by a dissimilar, although just as minute, force applied with a timing accuracy of some microseconds.

An effect of very small relative magnitude is used by Doctor Langmuir in seeding clouds to throw out of balance a low-level threshold controlling atmospheric conditions over a large area. Similar thresholds exist in many forms and at varying levels; they represent stages of development where potential growth has momentarily stopped.

In the fields of education and propaganda, thought seeds that are properly timed produce opinions and prejudices that become strongly entrenched. Although they may encounter many thresholds and, particularly, saturations, they are very difficult to modify once they have reached a high level of acceptance.

From an engineering point of view, one marvels at the possibilities of low-level control of the growth of events and things favorable to humanity. The electronic engineer, with his knowledge and experience in amplification and control, together with his accurate notion of timing, may soon explore and harvest in this promising field of growth control.

* Reprinted from *Proceedings of the I.R.E.*, v. 38, p. 979; September, 1950.

Selenium Rectifier for Protecting Electric Contacts

CONDUCTING CONTACTS for switching electric circuits are abundant in telephone exchanges and their lives depend mostly on the transient voltage and current surges that occur

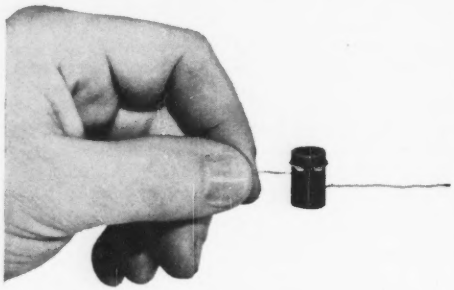

at the moment a current-carrying circuit is opened. Such surges are greatest when the circuit is highly inductive as is the case when it includes the actuating solenoid of relays, contactors, clutch magnets, and similar apparatus.

If a highly inductive winding is shunted by a device that acts like an open-circuit while the normal current is flowing through the winding but behaves like a short-circuit during the period immediately following the opening of the circuit supplying current to the coil, the inductive voltage surge will be absorbed by the shunting device and the opening contacts protected. Voltage stresses on the insulation of the windings and wiring are also reduced. A selenium rectifier is such a shunting device. Gas-filled tubes, varistors, and capacitor–resistor combinations are also used for this purpose.

The selenium rectifier shown in the photograph is small enough to be hung directly across the terminals of a relay coil. Its characteristics compare favorably with those of other devices used for this purpose. It is low in cost and takes little power while the winding is energized. This latter feature is an important difference between the selenium rectifier and the varistor, which two devices have quite similar properties in other respects. Tests involving many millions of operations of representative pairs of contacts show that their lives may be extended at least 20 times beyond that obtained with unprotected contacts.

This development was done jointly by Federal Telephone and Radio Corporation and Federal Telecommunication Laboratories.

Royal Air Force Radio Installation at Nairobi

THE NEW Royal Air Force radio station at Nairobi, Kenya, will be equipped with 19 high-frequency transmitters built by Standard Telephones and Cables, Limited. Three types of apparatus, *DS10*, *DS12*, and *DS13*, having power ratings of 4, 5, and 40 kilowatts, respectively, will be included in the total of 369 kilowatts of installed transmitters.

Each transmitter will have dual output stages permitting separate transmissions on different frequencies. Modulation methods include double-, single-, and independent-sideband transmissions and frequency-shift keying for telephony, telegraphy, and teleprinter communication. Remote control facilities are being provided by a time-sharing-multiplex equipment, type *D.P.1*, giving 48 operating channels.

The station will be in a position to handle every type of radio communication and will probably be the largest British armed forces telecommunication center outside the British Isles.

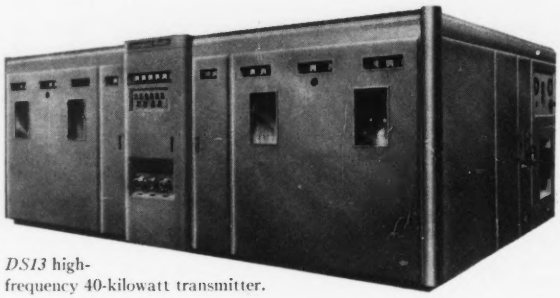

DS13 high-frequency 40-kilowatt transmitter.

Contributors to This Issue

HENRI BUSIGNIES

HENRI BUSIGNIES was born at Sceaux, France, on December 29, 1905. He received the degree of Electrical Engineer from Paris University in 1926.

On completion of his military service, he entered the Paris Laboratories of the International Telephone and Telegraph Corporation in 1928. Until about 1940, Mr. Busignies traveled to Italy, Spain, Switzerland, England, Africa, and the United States in the interests of the company. Since 1940, he has been an executive engineer and is now the Director of Federal Telecommunication Laboratories.

His first patent was issued in 1926 and has been followed by almost a hundred others. They have been dominantly in the field of automatic direction finding with particular attention to aircraft applications. He received the Lakhovsky award of the Radio Club of France in 1926.

Mr. Busignies is a Fellow of the Institute of Radio Engineers.

• • •

GORDON C. DEWEY was born at New York City in 1923. He received the B.A. and M.A. degrees in physics from Harvard University.

During the second world war, Mr. Dewey was at the Radiation Laboratory of Massachusetts Institute of Technology. From 1947 to 1949, he was associated with Federal Telecommunication Laboratories and is at present with the Weapons Systems Evaluation Group of the National Military Establishment.

Mr. Dewey is an Associate of the Institute of Radio Engineers.

• • •

LISCUM DIVEN was born at New York, New York, on September 18, 1918. He received a B.A. degree from Columbia University in 1940, majoring in physics.

He was employed by Western Electric Company until 1943, at which time he joined the engineering staff of Federal Telecommunication Laboratories. He has specialized in pulse communication systems and in selenium-rectifier development. Mr. Diven is now in the Phoenix, Arizona, laboratories of Motorola, Incorporated.

• • •

LOUIS FEIT was born at Union City, New Jersey, on May 21, 1921. From New York University in 1943, he received a B.A. degree, majoring in physics and mathematics, and an M.S. degree in 1948. He served in the United States army from June to October, 1943, following which he taught physics at the College of the City of New York.

Mr. Feit joined the engineering staff of Federal Telecommunication Laboratories in 1944. He has done development work on pulse multiplex communication systems and selenium rectifiers. He is now working on color television.

LISCUM DIVEN

He is a member of the American Physical Society, the Association for Computing Machinery, and the Institute of Radio Engineers.

• • •

LADISLAS GOLDSTEIN was born in 1906 in Hungary. He received from the University of Paris a bachelor's degree in 1924, master's in 1928, and doctor of science in 1937.

He was employed as a research physicist in the Curie Laboratory of the Institute of Radium of the University of Paris from 1928 to 1940. During the following year, he was with the Institute of Atomic Physics of the University of Lyon.

In 1941, he came to New York City where from 1942 to 1944 he was employed as a research physicist by

GORDON C. DEWEY

LOUIS FEIT

LADISLAS GOLDSTEIN

the Canadian Radium and Uranium Corporation. Since 1945, he has been with Federal Telecommunication Laboratories and is a senior project engineer.

Dr. Goldstein is a member of the American Physical Society.

• • •

JOHN F. HENEY was born on September 29, 1925, at Englewood, New Jersey. After four years in the army during the second world war, he attended Rensselaer Polytechnic Institute and received a B.S. degree in electrical engineering in 1949.

On graduation, he joined Federal Telecommunication Laboratories and has been working on gas counter tubes and gas microwave tubes.

• • •

JOHN F. HENEY

MURRAY A. LAMPERT was born at New York City in 1921. He received the B.A. and M.A. degrees from Harvard University.

During the second world war, he taught in the Army–Navy Officers Electronics Training School at Harvard for two years and spent another year doing optical design work for the Harvard Observatory optical research project.

After the war, he worked for three years at the radiation laboratory of the University of California at Berkeley on the interaction of high-energy particles with nuclei.

Since 1949, Mr. Lampert has been in the vacuum tube department of Federal Telecommunication Laboratories, where he has worked on microwave amplifiers and microwave propagation through electron gases.

• • •

LEONARD LEWIN. A biography of Mr. Lewin appears on page 158 of the June, 1951, issue.

• • •

THEODORE J. MARCHESE was born on October 17, 1912 at Carlstadt, New Jersey. He received the B.S. degree in electrical engineering from the evening school of Newark College of Engineering in 1948.

He was employed by Federal Telegraph Company in 1932 as a technician and was transferred in 1941 to the engineering department of Federal Telephone and Radio Corporation as an engineer on large vacuum tubes. He was transferred again, in 1947, to Federal Telecommunication Laboratories, where he is doing development work on microwave power generators, negative grid tubes, and traveling-wave tubes.

Mr. Marchese is a Senior Member of the Institute of Radio Engineers.

• • •

SIDNEY MOSKOWITZ was born at Brooklyn, New York, on February 23, 1919. In 1940, he received the B.E.E. degree from the College of the City of New York. From 1941 to 1945, he was a

MURRAY A. LAMPERT

member of the evening-session staff at that College.

While teaching evenings, he was also engaged in the development of electronic apparatus for the Industrial Scientific Corporation in New York. In 1943 Mr. Moskowitz joined the Federal Telecommunication Laboratories, where he has been active in the design and development of pulse-time-modulation systems.

He is a coauthor with J. Racker of a recently published book on "Pulse Techniques".

Mr. Moskowitz is a Member of the Institute of Radio Engineers and a member of Tau Beta Pi.

• • •

M. C. B. NEYT was born on January 23, 1900, at Brussels, Belgium. He

THEODORE J. MARCHESE

SIDNEY MOSKOWITZ

graduated as a mining engineer from the Faculté Polytechnique of the University of Brussels in 1923.

He joined Bell Telephone Manufacturing Company in 1924. After serving in the circuits division until 1932, he was placed in charge of the development of routine tests for rotary telephone switching systems. In 1946, he was assigned to the extension of general telephone switching in Belgium with particular attention to the further development of automatic subscriber toll switching with its required identification and ticketing processes.

Mr. Neyt served in the engineering corps of the Belgian army as an officer during 1939.

• • •

M. C. B. NEYT

L. J. G. NIJS was born at Perwez, Belgium, on August 4, 1902. He was graduated as a mining engineer from the University of Liege in 1925.

After three years as an engineer in the Belgium coal mines, he joined the Bell Telephone Manufacturing Company in 1928. From 1930 to 1937, he was in charge of raw materials, metallurgical, and chemical studies in the manufacturing division. He was then transferred to the apparatus division, becoming its head in 1950.

Mr. Nijs served as an officer in the corps of engineers of the Belgian army for a year starting in September, 1939.

• • •

L. J. G. NIJS

PHILIP PARZEN was born on June 28, 1916, in Poland. He received the B.S. degree in physics from the College of the City of New York in 1939 and the M.S. degree in physics from New York University in 1946.

During the second world war, he was employed at the Westinghouse Research Laboratories. Since 1947, he has been with Federal Telecommunication Laboratories and has worked on microwave tubes and electromagnetic-wave propagation.

Mr. Parzen is a member of the American Physical Society.

• • •

S. SCHEUER was born in March of 1882 at Brussels, Belgium.

He joined the Belgian Post Office in 1901 and served in various branches of that administration. At present, he is General Inspector attached to the staff of the Prime Minister of Belgium.

During his long career, he handled many problems for the postal organization, giving considerable attention to mechanization to reduce some of the drudgery and unhealthy aspects of mail sorting. The collaboration with Bell Telephone Manufacturing Company in this field continues.

PHILIP PARZEN

• • •

T. R. SCOTT was educated at Heriot Watt College and Edinburgh University, receiving the B.Sc. degree.

He joined the Standard organization in 1921, working in the cable engineering department, high-voltage laboratories, and the I.T.&T. Laboratories.

S. SCHEUER

T. R. SCOTT

Later, he went to the power cable division of which he was chief engineer until 1942.

During the second world war, he was chairman of the War Emergency Technical Committee, working with the cable planning organization of the Minister of Supply.

After the war, he initiated the company's Central Laboratories for development of materials and is now assistant director of research of Standard Telecommunication Laboratories.

Mr. Scott was awarded the Distinguished Flying Cross for his services during the first world war. He is a member of the Institution of Electrical Engineers, has served on its council, and has acted twice as chairman of its transmission section.

• • •

A. T. STARR

A. T. STARR received both M.A. and Ph.D. degrees. He served as a lecturer at Faraday House Training and Testing Institution and as a consultant to Callander's Cable Company from 1931 to 1938. The following two years were spent with Marconi's Wireless Telegraph Company. From 1940 to 1945, he was with Telecommunications Research Establishment working on microwave and miniaturised radar and pulse telephony.

In 1945, he joined Standard Telecommunication Laboratories in London. He is interested in miniaturisation, television, centimeter waves, application of high-voltage particles to new types of X-ray tubes, industrial control, and electronics.

Dr. Starr is the author of a number of books including "Electric Currents, Wave Filters" and "Generation, Transmission, and Utilisation of Electric Power," and has contributed widely to the technical press.

INTERNATIONAL TELEPHONE AND TELEGRAPH CORPORATION

Associate Manufacturing and Sales Companies

United States of America

International Standard Electric Corporation, New York, New York

Federal Telephone and Radio Corporation, Clifton, New Jersey

International Standard Trading Corporation, New York, New York

Capehart-Farnsworth Corporation, Fort Wayne, Indiana

The Coolerator Company, Duluth, Minnesota

Flora Cabinet Company, Inc., Flora, Indiana

Thomasville Furniture Corporation, Thomasville, North Carolina

Great Britain and Dominions

Standard Telephones and Cables, Limited, London, England

Creed and Company, Limited, Croydon, England

International Marine Radio Company Limited, Croydon, England

Kolster-Brandes Limited, Sidcup, England

Standard Telephones and Cables Pty. Limited, Sydney, Australia

Silovac Electrical Products Pty. Limited, Sydney, Australia

Austral Standard Cables Pty. Limited, Melbourne, Australia

New Zealand Electric Totalisators Limited, Wellington, New Zealand

Federal Electric Manufacturing Company, Ltd., Montreal, Canada

South America

Compañía Standard Electric Argentina, Sociedad Anónima, Industrial y Comercial, Buenos Aires, Argentina

Standard Electrica, S.A., Rio de Janeiro, Brazil

Compañía Standard Electric, S.A.C., Santiago, Chile

Europe and Far East

Vereinigte Telephon- und Telegraphenfabriks Aktiengesellschaft Czeija, Nissl & Co., Vienna, Austria

Bell Telephone Manufacturing Company, Antwerp, Belgium

Standard Electric Aktieselskab, Copenhagen, Denmark

Compagnie Générale de Constructions Téléphoniques, Paris, France

Le Matériel Téléphonique, Paris, France

Les Téléimprimeurs, Paris, France

C. Lorenz, A.G. and Subsidiaries, Stuttgart, Germany

Mix & Genest Aktiengesellschaft and Subsidiaries, Stuttgart, Germany

Süddeutsche Apparatefabrik Gesellschaft m.b.H., Nuremberg, Germany

Nederlandsche Standard Electric Maatschappij N.V., The Hague, Netherlands

Fabbrica Apparecchiature per Comunicazioni Elettriche, Milan, Italy

Standard Telefon og Kabelfabrik A/S, Oslo, Norway

Standard Electrica, Lisbon, Portugal

Compañía Radio Aérea Marítima Española, Madrid, Spain

Standard Electrica, S.A., Madrid, Spain

Aktiebolaget Standard Radiofabrik, Stockholm, Sweden

Standard Telephone et Radio S.A., Zurich, Switzerland

Telephone Operating Systems

Compañía Telefónica Argentina, Buenos Aires, Argentina

Compañía Telegráfico-Telefónica Comercial, Buenos Aires, Argentina

Compañía Telegráfico-Telefónica del Plata, Buenos Aires, Argentina

Companhia Telefônica Nacional, Porto Alegre, Brazil

Compañía de Teléfonos de Chile, Santiago, Chile

Compañia Telefónica de Magallanes S.A., Punta Arenas, Chile

Cuban American Telephone and Telegraph Company, Havana, Cuba

Cuban Telephone Company, Havana, Cuba

Compañía Peruana de Teléfonos Limitada, Lima, Peru

Porto Rico Telephone Company, San Juan, Puerto Rico

Radiotelephone and Radiotelegraph Operating Companies

Compañía Internacional de Radio, Buenos Aires, Argentina

Compañía Internacional de Radio Boliviana, La Paz, Bolivia

Companhia Radio Internacional do Brasil, Rio de Janeiro, Brazil

Compañía Internacional de Radio, S.A., Santiago, Chile

Radio Corporation of Cuba, Havana, Cuba

Radio Corporation of Porto Rico, San Juan, Puerto Rico

Cable and Radiotelegraph Operating Companies

(Controlled by American Cable & Radio Corporation, New York, New York)

The Commercial Cable Company, New York, New York[1]

Mackay Radio and Telegraph Company, New York, New York[2]

All America Cables and Radio, Inc., New York, New York[3]

Sociedad Anónima Radio Argentina, Buenos Aires, Argentina[4]

[1]Cable service. [2]International and marine radiotelegraph services.
[3]Cable and radiotelegraph services. [4]Radiotelegraph service.

Laboratories

Federal Telecommunication Laboratories, Inc., Nutley, New Jersey

International Telecommunication Laboratories, Inc., New York, New York

Laboratoire Central de Télécommunications, Paris, France

Standard Telecommunication Laboratories, Limited, London, England

Printed in U.S.A.
LANCASTER PRESS, INC., LANCASTER, PA.